Fitted Numerical Methods for Two-Parameter Singularly Perturbed Problems

Mekashaw Ali Mohye

A Ph.D. Dissertation Submitted to the Department of Applied Mathematics, School of Applied Natural Science

Presented in Partial Fulfillment of the Requirement for the Degree of Doctor of Philosophy in Mathematics (Numerical Analysis)

Office of Graduate Studies

Adama Science and Technology University

May, 2024

Adama, Ethiopia

Fitted Numerical Methods for Two-Parameter Singularly Perturbed Problems

Mekashaw Ali Mohye

Supervisor: Justin B. Munyakazi (Ph.D, Prof.)

Co-Supervisor: Tekle Gemechu Dinka (Ph.D, Asso. Prof.)

A Ph.D Dissertation Submitted to the Department of Applied Mathematics, School of Applied Natural Science

Presented in Partial Fulfillment of the Requirement for the Degree of Doctor of Philosophy in Mathematics (Numerical Analysis)

Office of Graduate Studies

Adama Science and Technology University

May, 2024

Adama, Ethiopia

DECLARATION

I hereby declare that this dissertation entitled "**Fitted Numerical Methods for Two-Parameter Singularly Perturbed Problems**" is my work. It has not been submitted to any university for a similar purpose. Proper citations have been used to duly recognize the references and sources of the materials utilized in this research.

Name of student	Signature	Date

RECOMMENDATION

We, the supervisors of this dissertation, hereby certify that have closely supervised the student while doing this dissertation by reading and revising the dissertation entitled "**Fitted Numerical Methods for Two-Parameter Singularly Perturbed Problems**" prepared under our guidance by **Mekashaw Ali Mohye** submitted in Partial Fulfillment of the Requirement for the Degree of Doctor of Philosophy in Mathematics (Numerical Analysis). Therefore, we recommend the submission of the dissertation to the department for further review and defense.

_____	_____	_____
Name of major Supervisor	Signature	Date
_____	_____	_____
Name of co-supervisor	Signature	Date

APPROVAL PAGE

We hereby certify that the recommendation and suggestion given by the board of examiners are appropriately incorporated into the final version of the dissertation entitled "**Fitted Numerical Methods for Two-Parameter Singularly Perturbed Problems**" by **Mekashaw Ali Mohye**.

Name of major Supervisor	Signature	Date
Name of co-supervisor	Signature	Date

We, the undersigned, members of the Board of Examiners of the dissertation open defense by **Mekashaw Ali Mohye** have read and evaluated the dissertation entitled "**Fitted Numerical Methods for Two-Parameter Singularly Perturbed Problems**" and examined the candidate during an open defense. This is, therefore, to certify that the dissertation is accepted for partial fulfillment of the requirement for the degree of Doctor of Philosophy in Mathematics (Numerical Analysis).

Chairperson	Signature	Date
Internal Examiner 1	Signature	Date
Internal Examiner 2	Signature	Date
External Examiner 1	Signature	Date
External Examiner 2	Signature	Date

Finally, approval and acceptance of the dissertation are contingent upon submission of its final copy to the Office of Postgraduate Studies (OPGS) through the candidate's Department Graduate Council (DGC) and School Graduate Committee (SGC).

Department Head	Signature	Date
School Dean	Signature	Date
Office of Postgraduate Study, Dean	Signature	Date

ACKNOWLEDGMENT

First and foremost, I express my sincere gratitude to Almighty God (Allah) for guiding and assisting me throughout this work. Next to this, I am delighted and honored to convey my profound gratitude to my primary supervisor, Prof. Justin Munyakazi, and my co-supervisor, Dr. Tekle Gemechu. I am immensely thankful for their invaluable support, unwavering assistance, insightful recommendations, and meticulous guidance during my dissertation research.

I would like to extend my sincere appreciation to all members of the doctoral committee for their invaluable constructive evaluation of the progress reports. I am truly grateful to the Editors and Reviewers for providing valuable feedback on the manuscripts submitted to journals for publication. Furthermore, I wish to express my gratitude to the Examiners for their insightful comments and suggestions, which greatly contributed to the finalization of this dissertation and the advancement of this research. Also, I would like to thank my fellow postgraduate students for their constant encouragement and unwavering support throughout this journey.

I express my genuine and heartfelt gratitude to my family members, specifically my beloved wife, Hanan Asfaw, my supportive brother, Abdulaziz Ali, and my esteemed father, Ali Mohye. Their unwavering support, invaluable assistance, and remarkable patience have been crucial to my accomplishments. Their tireless aid, encouragement, and understanding have played a pivotal role in enabling me to reach this significant milestone. I am truly grateful for their presence in my life.

Lastly, I would like to take this opportunity to give my deep appreciation to Adama Science and Technology University for the generous financial support towards the completion of this dissertation. Additionally, I am grateful to Wolkite University for sponsoring my Ph.D. scholarship. I would also like to extend my thanks to all the dedicated staff members of the Applied Mathematics departments in both institutions for their committed cooperation, support, and encouragement throughout this endeavor.

TABLE OF CONTENTS

DECLARATION i
RECOMMENDATION ii
APPROVAL PAGE iii
ACKNOWLEDGMENT iv
LIST OF ACRONYMS AND ABBREVIATIONS xi
LIST OF SYMBOLS xii
ABSTRACT xiii
CHAPTER 1: INTRODUCTION **1**
1.1 Singular perturbation problems 1
1.1.1 Convection-diffusion problem 4
1.1.2 Reaction-diffusion equation 4
1.1.3 Turning point problems 5
1.1.4 Boundary layers 6
1.1.5 Delay differential equations 6
1.1.6 Fitted mesh finite difference methods 8
1.1.7 Fitted operator finite difference methods 9
1.2 Statement of the problem 9
1.3 Objectives of the study 10
1.3.1 General objective of the study 10
1.3.2 Specific objectives of the study 10
1.4 Significance of the study 11
1.5 Scope of the study 11
1.6 Mathematical preliminaries 12
1.7 Organization of the study 13
CHAPTER 2: LITERATURE REVIEW **15**
2.1 Singularly perturbed problems 15
2.2 Singularly perturbed problems with time delay 16
2.3 Two-parameter singularly perturbed problems 19
2.4 Nonlinear singularly perturbed problems 23
CHAPTER 3: RESEARCH METHODOLOGY **26**
3.1 Study area and period 26
3.2 Study design 26
3.3 Source of information 26
3.4 Development of the numerical method 26

3.5 Mathematical procedures 27
CHAPTER 4: A FITTED OPERATOR FINITE DIFFERENCE METHOD FOR TWO-PARAMETER SINGULARLY PERTURBED TIME-DELAY PROBLEMS **28**
4.1 The governing problem 28
4.2 Properties of the continuous problem 29
4.3 Derivation of the numerical scheme 31
4.3.1 Semi-discrete scheme using temporal discretization 31
4.3.2 Full-discrete scheme using spatial discretization 35
4.4 Discrete stability and uniform convergence analysis 37
4.5 Numerical results and discussion 41
4.6 Summary 46
CHAPTER 5: ALMOST SECOND ORDER NUMERICAL METHOD FOR TWO-PARAMETER SINGULARLY PERTURBED TIME-DELAY PARABOLIC PROBLEMS **47**
5.1 The governing problem 47
5.2 Qualitative properties of the continuous problem 48
5.3 Derivation of the numerical scheme 48
5.4 Boundedness of discrete solution and error analysis 53
5.4.1 Error analysis 54
5.5 Numerical results and discussion 57
5.6 Summary 71
CHAPTER 6: A FITTED PARAMETER CONVERGENT FINITE DIFFERENCE SCHEME FOR TWO-PARAMETER SINGULARLY PERTURBED PARABOLIC DIFFERENTIAL EQUATIONS **72**
6.1 The governing problem 72
6.2 Some qualitative properties of the continuous problem 73
6.3 Derivation of the numerical scheme 74
6.3.1 Temporal discretization 74
6.3.2 Spatial discretization for full-discrete scheme 77
6.4 The convergence analysis of the numerical scheme 78
6.5 Numerical implementations and discussions 79
6.6 Summary 88
CHAPTER 7: A STABLE NUMERICAL TECHNIQUE FOR SOLVING NON-LINEAR TWO-PARAMETER SINGULARLY PERTURBED PDEs **89**
7.1 The governing problem 89
7.1.1 Properties of the continuous problem 89
7.2 Construction of the numerical scheme 94

7.2.1 Time discretization 94
7.2.2 Analysis of the semi-discrete scheme 95
7.2.3 Quasilinearization 98
7.2.4 Full-discrete scheme 100
7.3 Analysis of the developed numerical scheme 101
7.4 Numerical examples and discussions 104
7.5 Summary 111
REFERENCES **114**
CHAPTER A: LIST OF PUBLISHED AND SUBMITTED PAPERS **122**
CHAPTER B: MATLAB AND PYTHON PROGRAMS **123**

LIST OF TABLES

Table 4.1 Maximum absolute errors, $Err_{\varepsilon,\mu}^{N,M}$ and rates of convergence, $Roc^{N,M}$ using scheme (4.9) for Example 4.1 with $\mu = 10^{-3}$ and different values of ε 42

Table 4.2 Maximum absolute errors, $Err_{\varepsilon,\mu}^{N,M}$ and rates of convergence, $Roc^{N,M}$ using scheme (4.9) for Example 4.1 with $\varepsilon = 10^{-3}$ and different values of μ 43

Table 4.3 Maximum absolute errors, $Err_{\varepsilon,\mu}^{N,M}$ and rates of convergence, $Roc^{N,M}$ using scheme (4.9) for Example 4.1 with $\mu = 10^{-3}$ and different values of ε. 44

Table 4.4 Comparison of $Err_{\varepsilon,\mu}^{N,M}$ of our scheme in (4.9) with an existing schemes in Kumar et al. (2020) using Example (4.1) 45

Table 5.1 Maximum absolute errors, $Err_{\varepsilon,\mu}^{N,M}$ and rates of convergence, $Roc_{\varepsilon,\mu}^{N,M}$ using scheme (5.7) for Example 5.1 with $\mu = 10^{-3}$ and different values of ε. 59

Table 5.2 Maximum absolute errors, $Err_{\varepsilon,\mu}^{N,M}$ and rates of convergence, $Roc_{\varepsilon,\mu}^{N,M}$ using scheme (5.7) for Example 5.1 with $\varepsilon = 10^{-3}$ and different values of μ. 60

Table 5.3 Maximum absolute errors, $Err_{\varepsilon,\mu}^{N,M}$ and rates of convergence, $Roc_{\varepsilon,\mu}^{N,M}$ using scheme (5.7) for Example 5.2 with $\mu = 10^{-3}$ and different values of ε. 61

Table 5.4 Maximum v errors, $Err_{\varepsilon,\mu}^{N,M}$ and rates of convergence, $Roc_{\varepsilon,\mu}^{N,M}$ using scheme (5.7) for Example 5.2 with $\varepsilon = 10^{-3}$ and different values of μ. . . . 63

Table 5.5 Comparison of the proposed scheme in (5.7) with an existing schemes in Kumar et al. (2020) using Example 5.1 63

Table 5.6 Maximum absolute errors, $Err_{\varepsilon,\mu}^{N,M}$ and rates of convergence, $Roc_{\varepsilon,\mu}^{N,M}$ using scheme (5.7) for Example 5.3 with $\mu = 10^{-3}$ and different values of ε. 64

Table 5.7 Maximum absolute errors, $Err_{\varepsilon,\mu}^{N,M}$ and rates of convergence, $Roc_{\varepsilon,\mu}^{N,M}$ using scheme (5.7) for Example 5.3 with $\varepsilon = 10^{-3}$ and different values of μ. 65

Table 5.8 Maximum absolute errors, $Err_{\varepsilon,\mu}^{N,M}$ and rates of convergence, $Roc_{\varepsilon,\mu}^{N,M}$ using scheme (5.7) for Example 5.4 with $\mu = 10^{-3}$ and different values of ε. 66

Table 5.9 Maximum absolute errors, $Err_{\varepsilon,\mu}^{N,M}$ and rates of convergence, $Roc_{\varepsilon,\mu}^{N,M}$ using scheme (5.7) for Example 5.4 with $\varepsilon = 10^{-3}$ and different values of μ. 67

Table 6.1 Maximum absolute errors, $Err_{\varepsilon,\mu}^{N,M}$ and rates of convergence, $Roc_{\varepsilon,\mu}^{N,M}$ using scheme (6.10) for Example 6.1 with $\mu = 2^{-3}$ and different values of ε. 81

Table 6.2 Maximum absolute errors, $Err_{\varepsilon,\mu}^{N,M}$ and rates of convergence, $Roc_{\varepsilon,\mu}^{N,M}$ using scheme (6.10) for Example 6.1 with $\varepsilon = 10^{-3}$ and different values of μ. 82

Table 6.3 Maximum absolute errors, $Err_{\varepsilon,\mu}^{N,M}$ and rates of convergence, $Roc_{\varepsilon,\mu}^{N,M}$ using scheme (6.10) for Example 6.1 with $\mu = 10^{-3}$ and different values of ε. 83

Table 6.4 Maximum absolute errors, $Err_{\varepsilon,\mu}^{N,M}$ and rates of convergence, $Roc_{\varepsilon,\mu}^{N,M}$ using scheme (6.10) for Example 6.1 with $\mu = 10^{-3}$ and different values of μ. 84
Table 6.5 Comparison of $Err_{\varepsilon,\mu}^{N,M}$ of our scheme in (6.10) with an existing schemes in Munyakazi (2015) using Example 6.1 84
Table 6.6 Maximum absolute errors, $Err_{\varepsilon,\mu}^{N,M}$ and rates of convergence, $Roc_{\varepsilon,\mu}^{N,M}$ using scheme (6.10) for Example 6.2 with $\mu = 10^{-2}$ and different values of ε. 85
Table 6.7 Maximum absolute errors, $Err_{\varepsilon,\mu}^{N,M}$ and rates of convergence, $Roc_{\varepsilon,\mu}^{N,M}$ using scheme (6.10) for Example 6.2 with $\varepsilon = 10^{-2}$ and different values of μ. 85
Table 6.8 Maximum absolute errors, $Err_{\varepsilon,\mu}^{N,M}$ and rates of convergence, $Roc_{\varepsilon,\mu}^{N,M}$ using scheme (6.10) for Example 6.2 with $\mu = 10^{-3}$ and different values of ε. 86
Table 6.9 Comparison of $Err_{\varepsilon,\mu}^{N,M}$ of our scheme in (6.10) with an existing schemes in Das and Mehrmann (2016) using Example 6.2 86

Table 7.1 $Err_{\varepsilon,\mu}^{N,M}$ and $Roc_{\varepsilon,\mu}^{N,M}$ using scheme (7.37) for Example 7.1 with $\mu = 10^{-5}$ and different values of ε. 107
Table 7.2 $Err_{\varepsilon,\mu}^{N,M}$ and $Roc_{\varepsilon,\mu}^{N,M}$ using scheme (7.37) for Example 7.1 with $\mu = 10^{-10}$ and different values of ε. 108
Table 7.3 $Err_{\varepsilon,\mu}^{N,M}$ and $Roc_{\varepsilon,\mu}^{N,M}$ using scheme (7.37) for Example 7.2 with $\mu = 10^{-5}$ and different values of ε. 109
Table 7.4 $Err_{\varepsilon,\mu}^{N,M}$ and $Roc_{\varepsilon,\mu}^{N,M}$ using scheme (7.37) for Example 7.2 with $\mu = 10^{-10}$ and different values of ε. 110

LIST OF FIGURES

Figure 1.1 The profile of a viscous flow for Euler and Navier-Stokes models (Miller et al., 1996) 2

Figure 4.1 Numerical solution of Example 4.1 for (a) $\mu = 10^{-10}$, $\varepsilon = 10^{-3}$ taking $N = 128$ and $M = 64$, (b) $\mu = 10^{-3}$, $\varepsilon = 10^{-10}$ taking $N = 128$ and $M = 64$ 45
Figure 4.2 Log-Log plot of N vs maximum absolute errors for Example 4.1 . . 46

Figure 5.1 Surface plot for Example 5.1 using scheme in (5.7) with $N = M = 64$ and (a) $\varepsilon = 10^{-8}, \mu = 10^{-4}$, (b) $\varepsilon = 10^{-4}, \mu = 10^{-8}$ 62
Figure 5.2 Surface plot for Example 5.2 using scheme in (5.7) with $N = M = 64$ and (a) $\varepsilon = 10^{-8}, \mu = 10^{-4}$, (b) $\varepsilon = 10^{-4}, \mu = 10^{-8}$ 62
Figure 5.3 Surface plot for Example 5.3 using scheme in (5.7) with $N = M = 64$ and (a) $\varepsilon = 10^{-8}, \mu = 10^{-4}$, (b) $\varepsilon = 10^{-4}, \mu = 10^{-8}$ 68
Figure 5.4 Surface plot for Example 5.4 using scheme in (5.7) with $N = M = 64$ and (a) $\varepsilon = 10^{-8}, \mu = 10^{-4}$, (b) $\varepsilon = 10^{-4}, \mu = 10^{-8}$ 68
Figure 5.5 Log-Log plot of N vs maximum absolute error for Example 5.1. . . 69
Figure 5.6 Log-Log plot of N vs maximum absolute error for Example 5.2. . . 69
Figure 5.7 Log-Log plot of N vs maximum absolute error, for Example, 5.3. . . 70
Figure 5.8 Log-Log plot of N vs maximum absolute error, for Example, 5.4. . 70

Figure 6.1 Numerical results of Example 6.1 using scheme (6.10) (a) for $N = M = 64$, $\varepsilon = 2^{-20}$, $\mu = 2^{-3}$ and (b) for $N = M = 64, \varepsilon = 2^{-20}, \mu = 1$ . . . 80
Figure 6.2 Numerical results of Example 6.1 using scheme (6.10) (a) for $N = M = 64$, $\varepsilon = 1 = \mu$ and (b) for $N = 128, M = 64, \varepsilon = 1, \mu = 2^{-40}$ 87
Figure 6.3 Numerical results of Example 6.2 using scheme (6.10) (a) for $N = 128 = M$, $\varepsilon = \mu = 2^{-2}$ and (b) for $N = 128 = M, \varepsilon = \mu = 2^{-12}$ 87
Figure 6.4 Log-Log plots of (a) Example 6.1 and (b) Example 6.2 87

Figure 7.1 Numerical results of Example 4.1 using scheme (7.37) (a) for $N = 320, M = 160$, $\varepsilon = 10^{-12}$, $\mu = 10^{-2}$ and (b) for $N = 320, M = 160, \varepsilon = 10^{-2}, \mu = 10^{-12}$ 105
Figure 7.2 Log-Log plots for Example 7.1 using scheme (7.37) 106
Figure 7.3 Log-Log plots for Example 7.2 using scheme (7.37) 106

LIST OF ACRONYMS AND ABBREVIATIONS

SPPs	Singularly Perturbed Problems
RPPs	Regularly Perturbed Problems
ODE	Ordinary Differential Equation
PDE	Partial Differential Equation
CDE	Convection Dispersion Equation
DDEs	Delay Differential Equations
SPDDEs	Singularly Perturbed Delay Differential Equations
DPDEs	Delay Partial Differential Equations
FDMs	Finite Difference Methods
FMFDMs	Fitted Mesh Finite Difference Methods
FOFDMs	Fitted Operator Finite Difference Methods
NSFDMs	Nonstandard Finite Difference Methods
FEM	Fitted Element Methods
FVM	Fitted Volume Methods
BEM	Boundary Mlement Methods

LIST OF SYMBOLS

Ω & $\bar{\Omega}$	Open domain and closed domain respectively
$C^k(\Omega)$	k times continuously differentiable functions in the respective domain
r & σ	Mesh parameters
N & M	Spatial and temporal mesh numbers, respectively
τ	Mesh transition parameter
γ	Delay parameter
D^+, D^0, δ^2	Forward, backward, and central difference operators, respectively
u, u_ε	Solution of the continuous problem
$U_i, U^{N,M}$	Solutions of the discrete problem
x, x_i, t, t_i	Independent variables
C	Generic positive constant independent of ε, N, M
ε	Perturbation parameter
$\mathbb{R}$	The set of real numbers
D & $\bar{D}$	Open domain and closed domain, respectively
D_x & $\bar{D}_x$	Open and closed spatial domain, respectively
D_t & $\bar{D}_t$	Open and closed temporal domain, respectively
D^N & $\bar{D^M}$	Discrete domain
L	Differential operator
L^N, L^M	Difference operators
∂D	Boundary of the domain D
$Err^{N,M}$	Maximum absolute error
$Roc^{N,M}$	Rate of convergence

ABSTRACT

This dissertation focuses on a class of second-order two-parameter singularly perturbed parabolic problems, with and without time delay. These problems exhibit narrow boundary layers near the domain boundaries due to the presence of the perturbation parameters, as well as an interior layer because of the presence of discontinuous data in the convection term and/or source term. The rapid changes observed within these layer regions make analytical solutions challenging to obtain, while standard numerical methods often fail to capture the layer behaviors effectively. Consequently, the development of parameter-uniform numerical schemes for such singularly perturbed problems has become a prominent research area. Based on our literature review, we have encountered two major difficulties regarding the solutions to singularly perturbed problems. These difficulties include standard numerical methods failing to capture the behavior of the problem's solution, as well as the need for improvement in the accuracy of the solution obtained using existing numerical schemes. Therefore, in order to address these challenges, the main objective of this dissertation is to formulate and analyze fitted numerical schemes that exhibit convergence independent of the parameters. Two effective approaches are explored: the fitted operator finite difference method and the fitted mesh finite difference method. The fitted operator numerical methods are obtained by replacing the perturbation parameter with positive functions. Alternatively, in fitted mesh numerical methods, the successful approach of formulating a parameter-uniform numerical scheme involves employing standard finite difference operators on a specialized piece-wise uniform mesh condensed around the layer regions. These approaches yield uniformly convergent numerical results, overcoming the limitations of standard numerical methods. In this dissertation work, five uniformly convergent numerical schemes are formulated. Again, the stability estimate of each scheme is established and the parameter-uniform convergence of the schemes are investigated and proved. Various numerical experiments are conducted to demonstrate the validity and applicability of the formulated numerical schemes, and numerical results using Python and/or MATLAB tools are presented in tables and graphs. The theoretical and numerical results confirm that the formulated schemes are more accurate and uniformly convergent as compared to other existing literature.

Keywords: Delay differential equations, Two-parameter singularly perturbed problems, Turning point problems, Boundary or interior layer, Fitted operator finite difference methods, fitted operator finite difference method, and Uniform convergence analysis.

CHAPTER 1

INTRODUCTION

In this section, we provide a comprehensive overview of singular perturbation problems and present various models of singularly perturbed partial differential equations. We state the specific problem that will be addressed in this dissertation work and outline the statement of the problem, objectives, significance, and scope of the study.

1.1 Singular perturbation problems

The idea of singular perturbation problems (SPPs) was initially introduced by Prandtl (1904), a German physicist and engineer, during his presentation on fluid motion with small friction at the 3^{rd} International Congress of Mathematicians in Heidelberg. At this time, he demonstrated that fluid flow over a body can be divided into two regions, a boundary layer region, and an outer layer region. However, the term singular perturbations was first used by Friedrichs and Wasow (1946) in a paper presented at a seminar on nonlinear vibrations at New York University.

Fluid and gas dynamics are described by Navier-Stokes equations (Miller et al., 1996). In two dimensions, these are made of the following system of three nonlinear partial differential equations for the conservation of mass, momentum, and energy

$$\begin{aligned}
&\frac{\partial \rho}{\partial t}+\frac{\partial \rho u}{\partial x}+\frac{\partial \rho v}{\partial y}=0,\\
&\frac{\partial \rho v}{\partial t}+\frac{\partial(\rho uv)}{\partial x}+\frac{\partial\left(\rho v^2+p\right)}{\partial y}-\mu\left(\frac{\partial \tau_{yx}}{\partial x}+\frac{\partial \tau_{yy}}{\partial y}\right)=0,\\
&\frac{\partial \rho e}{\partial t}+\frac{\partial}{\partial x}\left(\rho u\left(e+\frac{p}{\rho}\right)\right)+\frac{\partial}{\partial y}\left(\rho v\left(e+\frac{p}{\rho}\right)\right)\\
&-\mu\left(\frac{\partial}{\partial x}\left(u\tau_{xx}+v\tau_{xy}\right)+\frac{\partial}{\partial y}\left(u\tau_{yx}+v\tau_{yy}\right)\right)-k\left(\frac{\partial^2 T}{\partial x^2}+\frac{\partial^2 T}{\partial y^2}\right)=0,
\end{aligned}$$

where ρ, u, v, and e are the dependent variables; ρ is the density of the material (fluid), u and v are the components of the velocity of the fluid, and e is the internal energy. The coefficients μ and k are respectively the inverse of the Reynolds number Re and that of the Prandtl number Pr. The components $\tau_{xx}, \tau_{xy}, \tau_{yx}$, and τ_{yy} of the viscous stress tensor τ are expressed in terms of the rate of change in space of the velocities by the relations:

$$\tau_{xx}=\frac{4}{3}\frac{\partial u}{\partial x}-\frac{2}{3}\frac{\partial v}{\partial y};\quad \tau_{yy}=-\frac{2}{3}\frac{\partial u}{\partial x}+\frac{4}{3}\frac{\partial v}{\partial y};\quad \tau_{xy}=\tau_{yx}=\frac{\partial v}{\partial x}+\frac{\partial u}{\partial y}.$$

Notice that the last three of the above-mentioned Navier-Stokes equations are of second order. The order of these equations drops to the first order when setting $\mu = 0$ and $k = 0$. The equations thus obtained are the Euler equations. The solutions of the Navier-Stokes equations contain more integration parameters than those of the Euler equations, and consequently, more boundary conditions are required to specify the solution of the Navier-Stokes equations. For instance, the imposition of a condition of zero velocity (the 'no-slip' condition) at the surface of the plate in the case of steady, incompressible laminar flow over an infinite flat plate is allowed for the Navier-Stokes equations but not for the Euler equations. In this case, the 'no-slip' condition creates a layer near the surface of the infinite flat plate.

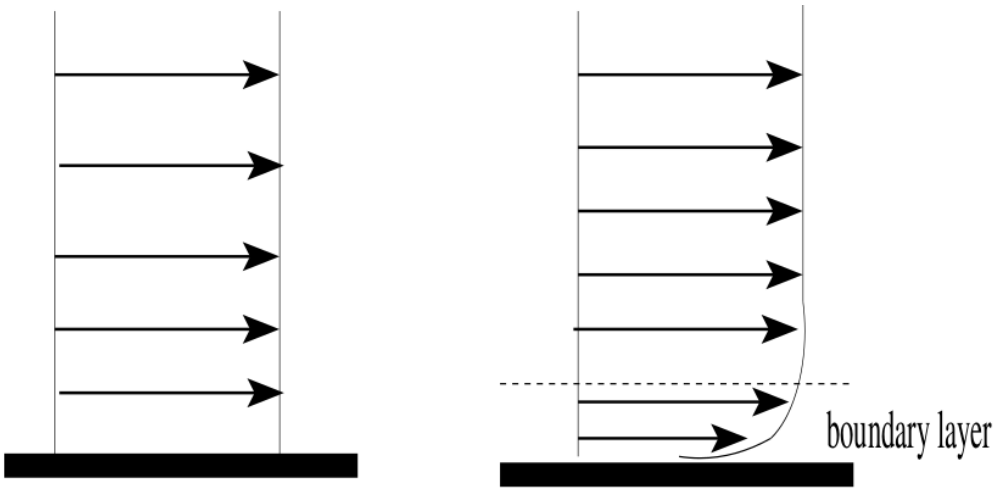

Figure 1.1: The profile of a viscous flow for Euler and Navier-Stokes models (Miller et al., 1996)

Differential equations (ODEs or PDEs) whose highest derivative terms are multiplied by a small parameter, ε, are said to be singularly perturbed. As ε approaches zero, the problem shows a singularity or a rapid change solution behavior. This singularity can make it difficult to analyze and solve analytically.

Many real-life problems are modeled by parameter-dependent differential equations whose solution behavior depends on the magnitude of the parameter. Depending on the location of the perturbation parameter it contains, perturbation problems can be classified into two categories. These categories are singular perturbation problems and regular perturbation problems.

In a perturbation problem, if the solution can be approximated by setting the value of the perturbation parameter equal to zero (i.e., $\varepsilon = 0$), then the problem is called a Regularly Perturbed Problem (RPP). Otherwise, it is called a Singular Perturbation Problem (SPP). In other words, a singularly perturbed differential equation is one in which the highest-order derivative term is attached to a small positive parameter. Otherwise, if the parameter is

attached to either of the terms other than the highest-order derivative term, it is called a regular perturbed differential equation. Singularly Perturbed Problems (SPPs) arise in the modeling of fluid dynamics, elasticity, quantum mechanics, reaction-diffusion processes, chemical-reactor theory, plasma dynamics, meteorology, diffraction theory, aerodynamics, the modeling of semi-conductors, hydrodynamics, and many other applied areas (Kevorkian and Cole, 1981). These problems also frequently occur in applications including geophysical fluid dynamics, oceanic and atmospheric circulation, chemical reactions, and optimal control (O'malley et al., 1991). Singularly perturbed problems appear in various branches of applied mathematics and physics, such as fluid mechanics, quantum mechanics, elasticity, plasticity, semiconductor device physics, geophysics, optimal control theory, aerodynamics, oceanography, and mathematical models of chemical reactions (Nayfeh, 2000) and also in engineering, biology, and lubrication theory (Verhulst, 2005). The numerical solution of singularly perturbed differential equations exhibits multi-scale behavior. That means there is a thin layer(s) of the domain where the solution changes rapidly or jumps suddenly, forming a boundary or interior layer, while away from the layer(s), the solution behaves regularly or changes slowly in the outer region. As a result, such problems are also called boundary layer problems.

To determine the solution of singularly perturbed problems (boundary layer problems), there are two approaches: numerical approaches and asymptotic approaches. The asymptotic approach helps us gain insight into the qualitative behavior of the problem and gives only semi-quantitative information, whereas the numerical approach provides quantitative information about the particular member of the family of solutions. Asymptotic methods require the problem solver to have some knowledge of the behavior of the expected solution and treat a comparatively restricted class of problems. Few researchers combined both of the above approaches to yield better results, for example, (Kadalbajoo and Reddy, 1989; Cengizci et al., 2019; Salama and Al-Amery, 2015).

The classification of singularly perturbed problems as linear or nonlinear depends on the form of the underlying equations. Linear singularly perturbed problems exhibit equations that are linear in the dependent variables or their derivatives, while nonlinear singularly perturbed problems involve equations that are nonlinear in the dependent variables or their derivatives. Solving linear singularly perturbed problems can be challenging due to the presence of a specific parameter that leads to singularity within the solution region. Additionally, the complexity of analyzing and solving nonlinear singularly perturbed problems is significantly influenced by the existence of nonlinearity in the given equations, as nonlinear cases often exhibit more intricate behavior, requiring the application of specialized techniques for analysis.

1.1.1 Convection-diffusion problem

The convection-diffusion problem is a problem in differential equation form that combines the effects of convection and diffusion in a physical system. It describes the transport and distribution of a scalar quantity, such as temperature, concentration, or fluid velocity, in a medium. Convection represents the transport of the scalar quantity due to the bulk movement of the medium, whereas diffusion refers to the spreading or dispersal of the scalar quantity due to molecular motion. The convection-diffusion equation combines these two processes and mathematically describes how the scalar quantity changes with time and space. The convection-diffusion equation finds applications in various fields, including fluid dynamics, heat transfer, mass transfer, and chemical engineering. Solving this equation allows for the analysis and prediction of the behavior and distribution of the scalar quantity in a given system, considering the combined effects of convection and diffusion. The Convection-Dispersion Equation (CDE) in one-dimensional has the following form:

$$D\frac{\partial^2 u}{\partial x^2} - v\frac{\partial u}{\partial x} = \frac{\partial u}{\partial t} \tag{1.1}$$

where D is dispersion, v is velocity, and u is concentration. The CDE in (1.1) is referred to as the Convection- Diffusion equation with diffusion D. The concentration $u(x,t)$ is a function of space and time. Thus, we assume that D and v are real, scalar constants. From (1.1), the dispersion term is $D \cdot \partial^2 u/\partial x^2$ and the convection term is $v \cdot \partial u/dx$. In this model, when the dispersion term is much larger than the convection term, the CDE behaves like the heat conduction equation, which is a parabolic Partial Differential Equation (PDE). Again, if the dispersion term is much smaller than the convection term, the CDE behaves like a first-order hyperbolic PDE. The mathematical models which describe the CDE correspond to several physical phenomena. For example, for modeling fluid flow the CDE equation can be used to examine two important classes of PDEs (parabolic and hyperbolic).

1.1.2 Reaction-diffusion equation

The reaction-diffusion problem is a problem in differential equation form that combines the effects of diffusion and chemical reactions in a system. It describes how the concentration of one or more chemical species changes over time and space due to both diffusion and chemical reactions occurring within the system. Diffusion represents the spreading or dispersion of chemical species due to molecular motion, whereas chemical reactions involve the transformation of one or more chemical species into different species. It finds applications in various fields, including chemistry, biology, ecology, and pattern formation.

A reaction-diffusion equation in one dimension is an equation of the form:

$$u_t = D\Delta u + f(u) \tag{1.2}$$

where $u = u(x,t)$. Then, (1.2) comprises a diffusion term and a reaction term, $D\Delta u$ and $f(u)$, respectively. Thus, the first term, $D\Delta u$ on the right-hand side describes the diffusion with the diffusion coefficient (D) and second term, $f(u)$ is a smooth function and describes changes in the processes. That means $f(u)$ is the reaction part. Both reaction-diffusion and convection-diffusion equations appear in the form of singularly perturbed problems, and the following examples are some model examples of convection-diffusion SPP and reaction-diffusion RPP, which appear in the form of differential equations (ODEs or PDEs).

1.1.3 Turning point problems

Singularly perturbed problems, in which the convection coefficient vanishes at some points in the domain of the problem, are called singularly perturbed turning point problems (SPTPPs), and zeros of the convection coefficient are said to be turning points. Consider the following two-point Dirichlet boundary-value problem:

$$Ly = -\varepsilon y_{xx}(x) - p(x)y_x(x) + q(x)y(x) = f(x) \quad \text{for } x \in (-1,1), \tag{1.3}$$

with the boundary data

$$y(-1) = d_1, \quad y(1) = d_2, \tag{1.4}$$

where $0 < \varepsilon \leq 1$ is a constant and $p(x)$ is assumed to be in $C^2[-1,1], q$ and f are required to be in $C^1[-1,1]$, and d_1 and d_2 are given constants. In addition, we assumed that $p(x) \geq \alpha > 0$, $q(x) \geq \beta$ to obtain a unique solution for the given problem in (1.3)-(1.4). But, in our assumption, if $p(x) \equiv 0$, then the given problem depending on the sign of q(x). If q(x)¡0, for all x, then the problem is oscillatory. If q(x)¿0 the solution would have a boundary layer.

The given problem has a turning point depending on the zeros of the smooth function $p(x)$. Let the function $p(x)$ has a finite number of zeros located at points $x_1, x_2 \ldots, x_j$ in $(-1,1)$. Again, we assume that these zeros of p are single simple zeros in $(-1,1)$, and $p(-1)p(1)$ must not vanish(*i.e.* $p(-1)p(1) \neq 0$). Then, the points x_j are called turning points of the problem in (1.3) - (1.4). Again, bounds on the behavior near a given turning point x_j depend specifically on ε and on the constant β_j where, $\beta_j = \dfrac{q(x_j)}{p_x(x_j)}$ (Berger et al., 1984). If $\beta_j < 0$, it will be shown that $y(x)$ is smooth (no interior layer) near $x = x_j$; on the other hand if $\beta_j > 0$, then there is an "interior layer" at $x = x_j$.

In particular, the hypotheses

$$\left.\begin{array}{lll} (1) & p(0)=0, & p'(0)>0, \\ (2) & q(x)\geq q(0)>0, & x\in[-1,1], \\ (3) & |p'(x)|\geq \dfrac{|p'(0)|}{2}, & x\in[-1,1]. \end{array}\right\}. \tag{1.5}$$

guarantee the presence of an interior layer at x=0.

Two-parameter singularly perturbed boundary-value problems are applied in different fields (such as in chemistry as chemical reactor Zahra and Mhlawy (2013)), in biological phenomena. For example, population ecology, control theory, viscous elasticity, and materials with thermal memory, hybrid optical systems, models for physiological processes, red blood cell systems, predator-prey models, and so on (Duressa, 2021).

1.1.4 Boundary layers

Definition 1.1.1. *(Miller et al., 1996) A boundary layer is defined as a region of the independent variable where the dependent variable rapidly changes to satisfy the given boundary conditions. On the other hand, the outer region is a region in which the solution behaves regularly and varies slowly*

Again, in singularly perturbed problems, if the data given in the source term or the coefficient term is non-smooth (has discontinuity), then the solution of the problems forms the layers and these layers are called interior layers.

1.1.5 Delay differential equations

Definition 1.1.2. *Delay Differential Equations (DDEs) are a type of differential equation in which the derivative of the unknown function at a certain time is given in terms of the values of the function at previous times. The n^{th} order DDE is given by*

$$\begin{aligned} &F\left(t,u(t),u\left(t-\gamma_1\right),\ldots,u\left(t-\gamma_k\right),u'(t),u'\left(t-\gamma_1\right),\ldots,u'\left(t-\gamma_k\right),\ldots,\right. \\ &\left.u^{(n)}(t),u^{(n)}\left(t-\gamma_1\right),\ldots,u^{(n)}\left(t-\gamma_k\right)\right)=0, \end{aligned}$$

where F is a given functional and $\gamma_i,\forall i=1,2,\ldots,k$ are given fixed positive numbers called the delay parameters.

In general, a Singularly Perturbed Delay Differential Equation (SPDDE) is a differential equation where the highest order derivative term is multiplied by a small parameter and involves the inclusion of at least one delay term either at the space variable, time variable, or both.

In many application areas the models that describe the response of the system depend on the history or delay of the system in a more complicated way. That is the inclusion of time delay terms in the differential equations involves a small delay parameter. In most applications in the life sciences, a delay is introduced when there are some hidden variables and processes that are not well understood but are known to cause a time lag. Delay differential equations have different applications in a variety of fields, for example in the bio-science of population dynamics and epidemiology, where the delay is due to gestation or maturation period, in engineering and numerical control, where the delay arises from the processing in the controller feedback loop, in which the time evolution depends not only on present states but also on states at or near a given time in the past. Singularly perturbed parabolic differential equations with delay in time are more practical as the time delay represents the time-lag or after effect (Wang, 1963). These types of models cannot be modeled by conventional differential equations, and hence make the delay parabolic equations more peculiar and have numerous applications in science and engineering, especially in biological, chemical, electronic, and transportation systems. Some of these include simulation of oil extraction from underground reservoirs (Ewing, 1983), chemical processes (Adomian and Rach, 1983), fluid flows, water quality problems in river networks (Roos et al., 1996), mechanical systems (Baranowski, 2010), control theory (Van Harten and Schumacher, 1978). To explain the motivation of the time-delay parabolic partial differential equation, in a more precise way, we present some singularly perturbed models with time delay that describe some real-world problems.

i. The Britton-model

$$\frac{\partial u(x,t)}{\partial t} = \varepsilon \Delta u + u(1 - g \star u) \quad \text{with} \quad g \star u = \int_{t-\tau}^{t} \int_{\Omega} g(x-y, t-s) u(y,s) ds$$

here, $u(x,t)$ denotes a population density, which evolves through random migration and reproduction (Ansari et al., 2007). A wide range of Delay Partial Differential Equation (DPDE) models can be found in (Murray, 2002).

ii. A mathematical model for singularly perturbed parabolic DPDE of the overall control system is represented by the equation

$$\frac{\partial u(x,t)}{\partial t} = \varepsilon \frac{\partial^2 u(x,t)}{\partial x^2} + v g[u(x,t-\tau)] \left(\frac{\partial u(x,t)}{\partial x} \right) + c f[u(x,t-\tau)] - u(x,t)$$

defined on a one-dimensional spatial domain $x \in (0,1)$, where v is the instantaneous material strip velocity depending on a prescribed spatial average of the time-delayed temperature distribution $u(x,t-\tau)$, and f represents a distributed temperature source function depending on $u(x,t-\tau)$. For more details, readers may refer to (Wang, 1963).

iii. Hutchinson's equation

$$\frac{\partial u(x,t)}{\partial t} = \varepsilon \frac{\partial^2 u(x,t)}{\partial x^2} + \lambda(1 - u(x,t-\tau)),$$

which arises as a rough model for the evolution of a population in mathematical ecology with density (Kumar et al., 2018)

To numerically solve singularly perturbed problems when analytical solutions are unavailable or more complex, various methods can be employed, such as finite difference methods, finite element methods, spline approximation methods, and others. However, the standard methods may not be able to accurately resolve the layers within the problem unless very fine grids are utilized. Consequently, these methods may fail to provide a convergent solution over the entire domain. Two non-classical Finite Difference Methods (FDMs) commonly employed in solving SPPs are the Fitted Mesh Finite Difference Methods (FMFDMs) and the Fitted Operator Finite Difference Methods (FOFDMs). Because standard finite difference methods do not provide stable solutions in the boundary layer region, in this dissertation work, we use these two fitted numerical methods (FMFDM and FOFDM) to solve both linear and nonlinear SPPs.

1.1.6 Fitted mesh finite difference methods

FMFDMs are numerical techniques used to solve singularly perturbed problems by discretizing the domain with a non-uniform mesh that is specifically designed to capture the features of the problem, such as boundary layers or rapid transitions in the solution. These methods are applied when there is a sharp transition or boundary layer in the solution of a differential equation. The fitted mesh method is particularly suitable for handling such problems because it allows for the discretization of the computational domain in a way that aligns with the well-suited structure of the solution. In FMFDMs, the computational domain is divided into a set of grid points or nodes. However, instead of using a uniform grid, the nodes are placed in a non-uniform manner to capture the features of the solution more effectively. Typically, the fining of nodes is done near the regions where the solution exhibits rapid changes or boundary layers.

Fitted meshes through the redistribution of mesh points encompasses several approaches, wherein the meshes are non-uniform within the given domain. Examples of such adaptive/-fitted mesh techniques include Shishkin mesh, Bakhvalov mesh, Vulanović mesh, and Gartland moving mesh. To develop meshes for FMFDMs, we use the mesh generation strategy using the boundary layer function.

1.1.7 Fitted operator finite difference methods

The aim of FOFDMs is to replace the perturbation parameter with positive functions. The key idea in FOFDMs is to design finite difference approximations that are accurate and stable for the given DE. Generally, FOFDMs are classified into two categories. The first category is Exponentially Fitted Finite Difference Methods (EFFDMs) and in this method, the perturbation parameter is replaced by a positive exponential function to stabilize the singular perturbation problem. The second category is the Non-Standard Finite Difference Method (NSFDM). The basic idea of the non-standard finite-difference (NSFD) scheme was first introduced by Mickens in his papers, (Mickens, 1994). Later, there is an important reference book Mickens (2005) to the non-standard finite-difference (NSFD) scheme. Mickens believed that important benefits can be found with the use of appropriate 'non-local' terms. In these FOFDMs, denominator functions of the classical derivatives are replaced by positive functions derived in such a way that they capture some notable properties of the governing differential equation.

1.2 Statement of the problem

Two-parameter singularly perturbed parabolic differential equations with time delay have many applications in different fields, for example, in engineering like the drift-diffusion equation of semiconductor modeling (Polak et al., 1987), chemical reactor model (Chen and O'Malley, 1974), and fluid dynamics (Schlichting and Kestin, 1961).

The nature of the singularly perturbed two-parameter problems changes depending on the values of the perturbation parameters ε and μ. Specifically, when $\mu = 1$, the problem represents a convection-diffusion equation, and a boundary layer of width $O(\varepsilon)$ appears in the neighborhood of the edge $x = 0$. On the other hand, when $\mu = 0$, the problem corresponds to a parabolic reaction-diffusion equation, and thin boundary layers of width $O(\sqrt{\varepsilon})$ emerge in the neighborhoods of both $x = 0$ and $x = 1$. The behavior of these singularly perturbed problems is influenced by the ratio of μ^2 to ε. O'Malley (1967) introduced these two-parameter problems and studied asymptotic expansions for their solutions. He noted that the choice of the ratio μ^2/ε significantly affects the nature of these problems. When ε/μ^2 tends to zero as μ approaches zero, the solution exhibits dissipative behavior. Conversely, when μ^2/ε tends to zero as ε approaches zero, the solution displays dispersive behavior.

Various methods have been developed to enhance the accuracy of the asymptotic methods proposed by O'Malley (1967) and other researchers for the numerical solution of two-parameter singularly perturbed problems. In Patidar (2008) and Munyakazi (2015), nonstandard finite difference methods have been employed for both stationary and time-dependent

cases to effectively solve two-parameter singularly perturbed problems. In addition to non-standard finite difference methods, several other numerical techniques have been employed for the numerical solution of two-parameter singularly perturbed ordinary differential equations with smooth data. These techniques include higher-order methods, adaptive methods, and exponential fitting methods. Works such as Das and Natesan (2013a); Das (2015); Das and Natesan (2012,0,0); Dehghan (2004); Gracia et al. (2006); Kadalbajoo and Jha (2012); Kaushik (2008); Kellogg and Tsan (1978); Linss (2010); O'Riordan et al. (2003); Vulanović (2001) have utilized these techniques. Moreover, research has also been conducted for non-smooth data, as seen in Chandru et al. (2017); Shanthi et al. (2006).

Asymptotic methods can be used to give qualitative information about the solutions, for example, to know the width and the location of layers. Numerical methods are used when analytical solutions of singularly perturbed problems are not available. These numerical methods can be used for linear or non-linear singularly perturbed problems with turning point(s) or without turning point(s). The methods are finite difference methods, finite elements methods, spline approximation methods, and so on. However, standard methods fail to resolve the layer(s) for all values of the parameter ε unless a very fine grid is considered, which unfortunately raises the computational complexities. Again, in our literature review, existing numerical methods show a lack of accuracy and simplicity of solutions for two-parameter singularly perturbed problems. Therefore, in this work, we have formulated fitted numerical schemes to improve the accuracy and minimize the computational complexity of the existing schemes for both linear and nonlinear two-parameter singularly perturbed problems.

1.3 Objectives of the study

1.3.1 General objective of the study

The general objective of this study is to develop fitted numerical methods for linear and nonlinear two-parameter singularly perturbed problems with and without delay.

1.3.2 Specific objectives of the study

The specific objectives of this study are to:

- develop fitted numerical schemes for a class of linear two-parameter singularly perturbed problems with and without delay.
- formulate fitted numerical schemes for a class of nonlinear two-parameter singularly perturbed problems.

- establish the stability estimate of the developed numerical methods.
- analyze the parameter-uniform convergence of the proposed schemes.

1.4 Significance of the study

The result obtained from this study will contribute convergent theoretical and computational results for the class of linear and nonlinear singularly perturbed two-parameter time-delay parabolic problems. Furthermore, the developed numerical schemes are simple, easy to implement, and provide more accurate results. They have the potential to serve as an alternative approach to solving similar problems. The results of this study also contribute to the body of knowledge, inspire many mathematics graduate students, and assist them in understanding research and scientific procedures in this research area.

1.5 Scope of the study

This research study is concerned with the class of linear and nonlinear two-parameter singularly perturbed problems with and without time-delay on a rectangular domain. In this study, we consider the following problems.

Governing problem I

Consider a two-parameter singularly perturbed time delay initial boundary value convection-reaction diffusion problem as

$$\begin{aligned}\mathfrak{L}u(x,t) \equiv \varepsilon u_{xx}(x,t) + \mu a(x,t)u_x(x,t) - b(x,t)u(x,t) - u_t(x,t) = -c(x,t)u(x,t-\gamma) \\ +f(x,t)\ (x,t) \in D = (0,1)\times(0,T]\end{aligned} \tag{1.6}$$

subject to

$$\begin{aligned}u(x,t) &= \Phi_d(x,t), \quad \text{for } (x,t) \in [0,1]\times[-\gamma,0] \\ u(0,t) &= \Phi_l(x,t), \quad u(1,t) = \Phi_r(x,t), \quad \text{for } t \in [0,T]\end{aligned} \tag{1.7}$$

where $0 < \varepsilon \leq 1$ and $0 \leq \mu \leq 1$ are perturbation parameters, and $\gamma > \varepsilon$ is a delay parameter.

Governing problem II

The second model problem is considered as

$$\begin{aligned} L_{\varepsilon,\mu}u(x,t) &= \varepsilon u_{xx}(x,t) + \mu a(x,t)u_x(x,t) - b(x,t)u_t(x,t) - c(x,t)u(x,t) = f(x,t), \ \ (x,t) \in D \\ u(x,0) &= u_0(x), \quad x \in \bar{D}_x = [0,1] \\ u(0,t) &= \Phi_0(t), \quad u(1,t) = \Phi_1(t), \quad t \in \bar{D}_t = [0,T] \end{aligned} \tag{1.8}$$

such that $D = D_x \times D_t = (0,1) \times (0,T]$ and ε and μ are small positive parameters where $0 < \varepsilon \leq 1$ and $0 \leq \mu \leq 1$.

Governing problem III

A second-order two-parameter nonlinear singularly perturbed problem in the domain $D = (0,1) \times (0,T]$ is considered for our third research study in the following form:

$$\begin{cases} Lu(x,t) + u_t(x,t) = f(x,t), \ (x,t) \in D \\ u(x,0) = g(x), \ \ x \in D_x = (0,1), \\ u(0,t) = s(t), \ \ u(1,t) = m(t), \ \ t \in D_t = [0,T], \end{cases} \tag{1.9}$$

where $Lu(x,t) \equiv -\varepsilon u_{xx}(x,t) + \mu a(x,t)u(x,t)u_x(x,t) - b(x,t)(u(x,t))^2$, $0 < \varepsilon \leq 1$ and $0 \leq \mu \leq 1$ are perturbation parameters. In Chapter 7, we propose a numerical method for this model problem, along with its corresponding analysis.

1.6 Mathematical preliminaries

Definition 1.6.1. *An M-matrix has non-negative diagonal entries and non-positive off-diagonal entries. Specifically, an M-matrix is a matrix that satisfies the following conditions:*

1. *All of its diagonal entries are non-negative.*

2. *All of its off-diagonal entries are non-positive.*

It is also known as a monotone square matrix with certain properties that make it useful in various mathematical applications.

Definition 1.6.2. *Finite difference approximations are numerical methods used to approximate the derivatives of a function at a given point. The basic idea behind finite difference approximations is to replace the derivative of a function with a difference quotient involving*

function evaluations at nearby points. The most commonly used finite difference approximations include the forward difference, backward difference, and central difference approximations, and such approximations are derived using Taylor's series expansion for any mesh function u_i at a mesh point x_i with mesh size $h = x_{i+1} - x_i$. The notations for the most commonly used finite difference approximations are given below.

$$D^+u_i = \frac{u_{i+1} - u_i}{h} + O(h)$$
$$D^-u_i = \frac{u_i - u_{i-1}}{h} + O(h)$$
$$D^0u_i = \frac{u_{i+1} - u_{i-1}}{2h} + O(h^2)$$
$$\delta^2u_i = D^+D^-u_i = \frac{u_i - 2u_i + u_{i-1}}{h^2} + O(h^2)$$

Definition 1.6.3. *(Miller et al. (2012)) Let P_ε be a family of mathematical problems which are singularly perturbed and parameterized by a singular perturbation parameter ε, where ε lies in the semi-open interval $0 < \varepsilon \leq 1$. Again, assume u_ε be the exact solution of P_ε and $U^{N,M}$ is the approximate sequence of numerical solutions, defined on meshes $D^{N,M}$, where N and M are the time discretization parameter and space discretization parameter respectively. Then, the numerical solutions $U^{N,M}$ are said to converge ε-uniformly to the exact solution u_ε, if there exists a positive integer N_0, and positive numbers C, p and q, all independent of N and ε, such that, for all $N \geq N_0$ and $M \geq M_0$,*

$$\sup_{0<\varepsilon\leq 1}\left[\max_{0\leq i\leq N, 0\leq j\leq M}\left|U^{N,M} - u_\varepsilon\right|_{D^{N,M}}\right] \leq C(N^{-p} + M^{-q})$$

Thus, p and q are called the ε-uniform rate of convergences, and C is called the ε uniform error constant.

1.7 Organization of the study

This dissertation research is composed of seven chapters, and each chapter includes descriptions of our study's work. In Chapter 1, we discuss the introduction of singularly perturbed problems. This chapter also covers a statement of the problem, study objectives, the scope of the study, the significance of the study, and the scope of the study. This chapter also incorporates various mathematical preliminaries that are widely used throughout this research work. In Chapter 2, we review recent related works on various forms of singularly perturbed problems. In our review of the literature, we examined the methods used and identified gaps. Chapter 3 of the dissertation covers the study area and period, study design, sources of information, and study procedure. We will discuss the key findings of the dissertation works from

Chapters 4-7. These chapters mainly focus on three main governing problems. Chapters 4 and 5 deal with the governing problem I and the formulation of a FOFDM and a FMFDM, along with their respective analyses of the problems. In this chapter, we develop the FOFDM for the considered problem. In Chapter 6, we formulate a nonstandard numerical method for solving the governing problem II. Chapter 7 deals with the governing problem III, which is a nonlinear problem.

CHAPTER 2

LITERATURE REVIEW

This chapter provides an overview of the relevant literature in the field of singularly perturbed problems, specifically focusing on the development of numerical methods to solve such problems.

2.1 Singularly perturbed problems

Several authors have developed uniformly convergent numerical methods for singularly perturbed time-dependent delay differential equations. For singularly perturbed problems, numerous books or monographs have been seen as publications that are focused on either the asymptotic approach or the numerical methods, such as Van Dyke (1975); O'malley et al. (1991); Farrell et al. (2000); Holmes (2007); Nayfeh and Balachandran (2008); Roos (2008); Shishkin and Shishkina (2008); Linß (2009); Miller et al. (1996). Again, there are some surveys that are focused on such problems, for instance, Kadalbajoo and Reddy (1989); Kumar et al. (2007); Kadalbajoo and Gupta (2010); Roos (2012); Duressa et al. (2023), which are published in this area.

Furthermore, there have been several published studies on recently developed uniformly convergent numerical methods for singularly perturbed problems. For example, Munyakazi and Patidar (2014) formulated a fitted operator finite difference method for singularly perturbed turning point problems of the form

$$Lu = \varepsilon u'' + a(x)u' - b(x)u(x) = f(x), \quad x \in \Omega = (-1,1), \tag{2.1}$$

$$u(-1) = A, \quad u(1) = B, \tag{2.2}$$

where A and B are given real constants and $\varepsilon \in (0,1]$, and the coefficients $a(x)$, $b(x)$, and $f(x)$ are sufficiently smooth functions in Ω. The suggested method is robust with respect to the singular perturbation parameter ε and is of order almost one. However, the authors improve the accuracy of the methods by employing Richardson extrapolation.

Bullo et al. (2021a) considered the singularly perturbed parabolic reaction-diffusion IBVP as

$$\left(\varepsilon \frac{\partial^2 u}{\partial x^2} - bu - \frac{\partial u}{\partial t}\right)(x,t) = f(x,t), \ \forall x \in \Omega = (0,1) \times (0,1), \tag{2.3}$$

subject to the initial and boundary conditions

$$\begin{cases} u(x,0) = s(x), \ \forall x \in [0,1], \\ u(0,t) = q_0(t), \ u(1,t) = q_1(t), \ \forall t \in [0,1], \end{cases} \tag{2.4}$$

where ε is perturbation parameter that satisfies $0 < \varepsilon \leq 1$ and assume that the coefficient function $b(x,t) \geq \beta > 0$ is sufficiently smooth. The authors proposed a fitted operator finite difference method to solve problems whose solution exhibits twin boundary layers. The Richardson extrapolation technique was used to accelerate the rate of convergence.

2.2 Singularly perturbed problems with time delay

Singularly perturbed problems with time delays are mathematical problems that combine differential equations with a singular perturbation parameter, ε, and a time delay parameter. These problems incorporate time delays, which introduce complexities by including memory effects and feedback dynamics in the system. The presence of time delay can lead to stability problems, oscillations, or the emergence of complex dynamics (Zak et al., 2003). The literature contains various numerical methods that have been developed specifically for addressing these types of problems. These methods aim to accurately capture the dynamics of systems with time delay, enabling the analysis and prediction of their behavior with improved precision and reliability. For example, Ansari et al. (2007) investigated a singularly perturbed delay parabolic equation with Dirichlet boundary conditions on $\Gamma = \Gamma_1 \cup \Gamma_b \cup \Gamma_r$, where $\Gamma_l = \{0\} \cup (0,T]$, $\Gamma_r = \{1\} \cup (0,T]$, $\Gamma_b = (0,1) \cup (-\tau,0]$, and $D = (0,1) \times (0,T]$ of the form

$$\begin{aligned} Lu_\varepsilon(x,t) \equiv \left(\frac{\partial u_\varepsilon}{\partial t} - \varepsilon \frac{\partial^2 u_\varepsilon}{\partial x^2} + a u_\varepsilon \right)(x,t) &= -b(x,t) u_\varepsilon(x,t-\tau) + f(x,t), \quad (x,t) \in D, \\ u_\varepsilon(x,t) = \phi_1(t), \quad (x,t) \in \Gamma_1, \quad u_\varepsilon(x,t) &= \phi_r(t), \quad (x,t) \in \Gamma_r, \\ u_\varepsilon(x,t) = \phi_b(x,t), \quad (x,t) &\in \Gamma_b, \end{aligned}$$

where $0 < \varepsilon \leqslant 1$ and $\tau > 0$ (note that $T = k\tau$ for some integer $k > 1$) and the coefficients, $a(x,t), b(x,t), f(x,t), (x,t) \in \bar{D}$, and $\phi_1(t), \phi_b(x,t)$ and $\phi_r(t), (x,t) \in \Gamma$, are sufficiently smooth and bounded functions that satisfy

$$a(x,t) \geqslant 0, \quad b(x,t) \geqslant \beta \geqslant 0, \quad (x,t) \in \bar{D}.$$

The authors employed a numerical method that utilized a standard finite difference operator (centered in space and implicit in time) on a rectangular piecewise uniform fitted mesh consisting of $N_x \times N_t$ elements (where N_x represents the number of spatial mesh elements and N_t

denotes the number of temporal mesh elements). This method was particularly effective in capturing boundary layer phenomena and demonstrated robustness with respect to the small parameter. The numerical solutions obtained using this method exhibited uniform convergence in the maximum norm to the exact solution across the entire range of parameter values in the half-open interval $(0,1]$. Specifically, it was established that the errors were bounded in the maximum norm by $O\left(N_x^{-2}\ln^2 N_x + N_t^{-1}\right)$.

Bashier and Patidar (2011) consider a singularly perturbed delay parabolic partial differential equation of the form

$$Lu(x,t) \equiv \left(\frac{\partial u}{\partial t} - \varepsilon\frac{\partial^2 u}{\partial x^2} + au\right)(x,t) = f(x,t) - b(x,t)u(x,t-\tau), \quad (x,t) \in \bar{\Omega} \tag{2.5}$$

with the initial data

$$\begin{aligned} u(x,t) &= \theta(x,t), \quad (x,t) \in [0,1]\times[-\tau,0], \\ u(0,t) &= \Gamma_l(t), \\ u(1,t) &= \Gamma_r(t), \end{aligned} \tag{2.6}$$

where $0 < \varepsilon \leqslant 1$ is the singular perturbation parameter and $\tau > 0$ represents the delay parameter. The coefficients $f(x,t), a(x,t), b(x,t)$, and $\theta(x,t) \in \bar{\Omega}$ are sufficiently smooth and bounded functions that satisfy

$$a(x,t) \geqslant 0, \quad b(x,t) \geqslant \beta \geqslant 0, \quad (x,t) \in \bar{\Omega}.$$

The authors suggested a fitted operator finite difference method to obtain the numerical solution. The developed method is unconditionally stable and convergent with the order $O(k+h^2)$, where k and h are respectively the time and space step-sizes, which is better than the one obtained by (Ansari et al., 2007). Within this year, the authors also developed a second-order robust fitted operator finite difference method for singularly perturbed time-delay parabolic partial differential equations of the convection-diffusion type. The method is constructed by replacing the classical differential operator with a fitted operator based on Crank-Nicolson's discretization. The proposed method is analyzed for stability and convergence, and it is found that this method is unconditionally stable and is convergent with order $\mathscr{O}\left(k^2+h^2\right)$, where k and h are respectively the time and space step sizes.

Singh et al. (2018) designed a domain decomposition method for solving singularly perturbed parabolic reaction-diffusion problems with time delay by discretizing the problem using the backward Euler scheme in the time direction and the piece-wise uniform mesh of

Shishkin type in the spatial direction. The researchers considered the problem as

$$Lu(x,t)+b(x,t)u(x,t-\tau)=f(x,t), \quad (x,t)\in D \tag{2.7}$$

with

$$u(x,t)=\phi_\ell(t), \quad (x,t)\in\Gamma_\ell=\{0\}\times(0,T], \tag{2.8}$$
$$u(x,t)=\phi_r(t), \quad (x,t)\in\Gamma_r=\{1\}\times(0,T], \tag{2.9}$$
$$u(x,t)=\phi_b(x,t), \quad (x,t)\in\Gamma_b=[0,1]\times[-\tau,0], \tag{2.10}$$

where

$$Lu(x,t):=u_t(x,t)-\varepsilon u_{xx}(x,t)+a(x,t)u(x,t)$$

and

$$D:=\Omega\times(0,T]=(0,1)\times(0,T]$$

where $0<\varepsilon\ll 1,\tau>0$ and $b\leq 0, a+b\geq\alpha>0$ on $\bar{D}$. Thus, the proposed the method is shown to be uniformly convergent, having almost second order in space and first order in time.

Woldaregay et al. (2023) considered a singularly perturbed parabolic delay differential equation on the domain $D=\Omega_x\times\Omega_t=(0,1)\times(0,T]$ with the boundary $\partial D=\bar{D}\backslash D$, where $\bar{D}=\bar{\Omega}_x\times\bar{\Omega}_t=[0,1]\times[0,T]$, which is given by

$$\begin{aligned}
&u_t-\varepsilon u_{xx}+a(x)u_x+b(x,t)u(x,t)=-c(x,t)u(x,t-\tau)+f(x,t),(x,t)\in D,\\
&u(x,t)=\phi_b(x,t),(x,t)\in[0,1]\times[-\tau,0],\\
&u(0,t)=\phi_l(t),t\in\Omega_t,\\
&u(1,t)=\phi_r(t),t\in\Omega_t
\end{aligned} \tag{2.11}$$

where $\varepsilon\in(0,1]$ is a perturbation parameter and $\tau>0$ is the delay parameter. The terminal time T is assumed to satisfy the condition $T=k\tau$ for some positive integer k. The functions $a(x),b(x,t),c(x,t)$, $f(x,t)$ and $\phi_l(t),\phi_b(x,t),\phi_r(t)$ are assumed to be sufficiently smooth, bounded and satisfy $a(x)\geq\alpha>0, b(x,t)\geq\zeta>0, c(x,t)\geq\kappa>0,(x,t)\in\bar{D}$. The authors designed a fitted exact difference method for solutions of a singularly perturbed time delay parabolic PDE, by utilizing the Crank-Nicolson method for temporal discretization and fitted mesh exact finite difference method for spatial discretization.

2.3 Two-parameter singularly perturbed problems

Two-parameter singularly perturbed parabolic differential equations with time delay find numerous applications across various fields. For instance, in engineering, they are employed in modeling phenomena such as drift-diffusion in semiconductors Polak et al. (1987), chemical reactor behavior Chen and O'Malley (1974), and fluid dynamics Schlichting and Kestin (1961).

In various studies, different researchers have contributed to the development of such numerical methods, ensuring their convergence and reliability. These methods enable the accurate and efficient computation of solutions for two-parameter singularly perturbed parabolic differential equations with a time delay. Some of such studies were found in O'Malley (1967); Chen and O'Malley (1974); O'Malley (1979); Vulanović (2001); Roos and Uzelac (2003); Gracia et al. (2006); O'Riordan et al. (2006); Patidar (2008); Kadalbajoo and Yadaw (2012); Kadalbajoo and Jha (2012); Zahra and Mhlawy (2013); Munyakazi (2015); Chandru et al. (2017,0); Govindarao et al. (2019); Sumit et al. (2020); Bullo et al. (2021b); Roy and Jha (2022); Negero et al. (2023).

Patidar (2008) consider the singularly perturbed differential equation of the form

$$L_{\varepsilon,\mu}u \equiv \varepsilon u''(x) + \mu a(x)u'(x) - b(x)u(x) = f(x), x \in \Omega = (0,1), \tag{2.12}$$

$$u(0) = \alpha_0, \quad u(1) = \alpha_1, \tag{2.13}$$

where $0 < \varepsilon$ and $\mu \leq 1$ are two small parameters and the functions $a(x), b(x), f(x)$ are sufficiently smooth with $a(x) \geq \alpha > 0$ and $b(x) \geq \beta > 0; \alpha, \beta \in \mathbb{R}$. In their work, the author derived FOFDMs for a class of singularly perturbed two-point BVPs with two small parameters multiplying the derivatives. These methods are referred to as nonstandard finite difference methods (named NSFDM-I, II and III) and computed solutions with them for purposes of comparison. The only difference between these schemes is the denominator functions.

Kadalbajoo and Jha (2012) considered the singularly perturbed convection-diffusion problem as

$$Ly \equiv -\varepsilon y'' - \mu a(x)y' + b(x)y = f(x) \quad x \in \Omega = (0,1) \tag{2.14}$$

$$y(0) = y_0, \quad y(1) = y_1, \tag{2.15}$$

with two small parameters ε and μ satisfying $0 < \varepsilon \ll 1$ and $0 < \mu \ll 1$. The functions $a(x), b(x)$ and $f(x)$ are assumed to be sufficiently smooth with $a(x) \geq \alpha > 0, b(x) \geq \beta >$

$0, b(x)/a(x) \geq \delta > 0, \alpha, \beta, \delta \in \mathbb{R}$ for $x \in [0,1]$. The researchers used cubic splines to develop an exponentially fitted difference scheme for a singularly perturbed ordinary differential equation with two small parameters affecting convection and diffusion terms. They demonstrated that the solution to the considered problem has a boundary layer on the left side of the domain and determined the bounds of the solution's derivatives. Their approach is also uniformly convergent at the first order.

Kadalbajoo and Yadaw (2012) consider a singularly perturbed two-parameter parabolic reaction-diffusion boundary value problem defined on the domain $D = \Omega \times (0,T]$ with $\Omega = (0,1)$.

$$\varepsilon \frac{\partial^2 u}{\partial x^2} + \mu a(x) \frac{\partial u}{\partial x} - b(x)u(x) - \frac{\partial u}{\partial t} = f(x,t), \quad (x,t) \in D, \tag{2.16}$$

$$u(x,0) = u_0(x), \quad x \in \bar{\Omega}, \tag{2.17}$$

$$u(0,t) = 0, \quad u(1,t) = 0 \quad t \in [0,T] \tag{2.18}$$

with two small parameters $0 < \varepsilon \ll 1$ and $0 < \mu \ll 1$, such that $\mu^2/\varepsilon \to 0$ as $\varepsilon \to 0$. The method combines a standard implicit finite difference scheme applied to discretize the temporal direction on a uniform mesh using Rothe's method with a finite element method employed in the spatial direction on a piecewise uniform mesh of Shishkin type. It has been demonstrated that the method is unconditionally stable and achieves an accuracy of order $O(N^{-2}(\ln N)^2 + \triangle t)$, where N represents the number of spatial grid points and $\triangle t$ denotes the time step size.

Zahra and Mhlawy (2013) considered two-parameter singularly perturbed semi-linear boundary value problem has the following form

$$Ly(x) \equiv -\varepsilon_d y'' + \varepsilon_c p(x) y' + f(x,y) = 0, \quad x \in (0,1) \tag{2.19}$$

where the boundary conditions are: $y(0) = \mu_1, \quad y(1) = \mu_2$, with two small parameters $0 < \varepsilon_c << 1, 0 < \varepsilon_d << 1$, where $p(x)$ and $f(x,y)$ are sufficiently smooth functions and $p(x) \geqslant \tilde{p} > 0$, for $x \in [0,1]$, assuming that $f_y(x,y) > 0$. The authors solved the problem by employing an exponential spline on a Shishkin mesh.

Munyakazi (2015) considered a class of time-dependent singularly perturbed convection-diffusion problems with two parameters affecting the diffusion and the convection terms on $Q = \Omega \times (0,T], \Omega = (0,1)$,

$$L_{x,t}u \equiv \varepsilon \frac{\partial^2 u}{\partial x^2} + \mu a(x) \frac{\partial u}{\partial x} - b(x)u(x) - \frac{\partial u}{\partial t} = f(x,t), \ (x,t) \in \Omega, \tag{2.20}$$

subject to the initial and boundary conditions

$$u(x,0) = u_0(x), x \in \bar{\Omega}, \tag{2.21}$$

$$u(0,t) = u(1,t) = 0, t \in [0,T], \tag{2.22}$$

with two small parameters $0 < \varepsilon, \mu \leq 1$. The functions $a(x), b(x)$ and $f(x,t)$ are sufficiently smooth and satisfy $a(x) \geq \alpha > 0$ and $b(x) \geq \beta > 0$, α and β are real numbers. The author employed the classical backward Euler method to discretize the time variable and utilized the nonstandard methodology introduced by Mickens on a uniform mesh to discretize the space variable.

A numerical method was designed for two-parameter singularly perturbed parabolic convection-diffusion problems with non-smooth data by Chandru et al. (2017). In this work, the authors considered the two-parameter parabolic initial-boundary value problem (IBVP) on the domain $\bar{\Gamma} = \bar{\Omega}_x \times \Omega_t$, which combines the reaction-diffusion and convection-diffusion terms as

$$L_{\varepsilon,\mu} y(x,t) \equiv (\varepsilon y_{xx} + \mu a y_x - by - cy_t)(x,t) = f(x,t), \quad (x,t) \in \left(\Gamma^- \cup \Gamma^+\right), \tag{2.23}$$

$$y(x,t) = p(x,t), (x,t) \in \Gamma_c, y(x,t) = q(x,t), (x,t) \in \Gamma_l, y(x,t) = r(x,t), (x,t) \in \Gamma_r. \tag{2.24}$$

where, $0 < \varepsilon \ll 1, 0 \leq \mu \leq 1$ are two singular perturbation parameters. The coefficient functions $b(x,t), c(x,t)$ are assumed to be sufficiently smooth functions on Γ such that $b(x,t) \geq \beta > 0, c(x,t) \geq v > 0$. In addition, we assume $a(x,t), f(x,t)$ are sufficiently smooth on $(\Gamma^- \cup \Gamma^+)$ such that

$$a(x,t) \leq -\alpha_1 < 0, (x,t) \in \Gamma^- \quad \text{and} \quad a(x,t) \geq \alpha_2 > 0, (x,t) \in \Gamma^+. \tag{3}$$

In this research, α_1, α_2 are positive constants with $\alpha = \min\{\alpha_1, \alpha_2\}$. In addition, the authors assumed the jumps of $a(x,t)$ and $f(x,t)$ at (d,t) satisfy $|[a](d,t)| \leq C, |[f](d,t)| \leq C$, where the jump of ω at (d,t) is defined as $[\omega](d,t) = \omega(d+,t) - \omega(d-,t)$. Again, in the research, the presence of discontinuity in $a(x,t)$ and $f(x,t)$ leads to an interior layer in the neighborhood of the point of discontinuity of $y(x,t)$ in addition to the boundary layer phenomena due to the presence of perturbation parameters.

Govindarao et al. (2019) considered the two-parameter singularly perturbed delay parabolic initial boundary value problem (IBVP) with Dirichlet boundary condition:

$$\begin{aligned}\left(\frac{\partial}{\partial t}+L_{\varepsilon,\mu}\right)u(x,t) &= -c(x,t)u(x,t-\tau)+f(x,t), \quad x\in\Omega=(0,1)\times(0,T],\\ u(x,t) &= u_0(x,t),(x,t)\in\Gamma_b,\\ u(0,t) &= \phi_1(x,t), \text{ on } \quad \Gamma_1=\{(0,t)\mid 0\le t\le T\},\\ u(1,t) &= \phi_{\mathrm{r}}(x,t), \text{ on } \quad \Gamma_{\mathrm{r}}=\{(1,t)\mid 0\le t\le T\}\end{aligned} \tag{2.25}$$

where $L_{\varepsilon,\mu}=-\varepsilon u_{xx}(x,t)-\mu a(x)u_x(x,t)+b(x,t)u(x,t)$, $\Omega=(0,1), G=\Omega\times(0,T]$, $\Gamma=\Gamma_1\cup\Gamma_b\cup\Gamma_{\mathrm{r}}$, Γ_1 and Γ_{r} are the left and the right sides of the rectangular domain G corresponding to $x=0$ and $x=1$, respectively. $\Gamma_b=[0,1]\times[-\tau,0], 0<\varepsilon,\mu\ll 1$ and $\tau>0$ are given constants. The functions $a(x),b(x,t),c(x,t),f(x,t)$ on G and $u_0(x,t),\phi_1(t),\phi_{\mathrm{r}}(t)$ on Γ, are sufficiently smooth and bounded functions that satisfy, $a(x)\ge\alpha>0, b(x,t)>0$, $c(x,t)\ge\beta>0$ on $\bar{G}=[0,1]\times[0,T]$. Under these assumptions, the authors of this work used the implicit Euler scheme on a uniform mesh for time variable discretization and the upwind difference scheme on the Shishkin-type meshes (standard Shishkin mesh, Bakhvalov-Shishkin mesh) for spatial variable discretization to develop the numerical scheme. Additionally, they proved that the proposed method is uniformly convergent, parameter independent, and achieves first-order convergence.

In the work of Sumit et al. (2020), the authors considered singularly perturbed delay initial-boundary value problem in one space dimension with two small parameters on $\bar{G}=G\cup\partial G$, where $G=(0,1)\times(0,T]$ and $\partial G=\Gamma_b\cup\Gamma_r\cup\Gamma_l$ with $\Gamma_b=[0,1]\times[-\tau,0], \Gamma_l=\{0\}\times(0,T]$, and $\Gamma_r=\{1\}\times(0,T]$ as

$$\begin{aligned}Lu\equiv L_{\varepsilon,\mu}u-u_t &= -cu(x,t-\tau)+f(x,t) \text{ in } G,\\ u|_{\Gamma_b} &= \varphi_b(x,t),\\ u|_{\Gamma_l} &= \varphi_l(t),\\ u|_{\Gamma_r} &= \varphi_r(t)\end{aligned} \tag{2.26}$$

where $L_{\varepsilon,\mu}u:=\varepsilon u_{xx}+\mu a u_x-bu$ with parameters ε and μ such that $0<\varepsilon\le 1, 0\le\mu\le 1$. The coefficients are such that

$$0<\alpha\le a(x,t), \quad 0<\beta\le b(x,t), \quad 0<\gamma\le c(x,t), \quad (x,t)\in\bar{G}.$$

The numerical method is constructed using a hybrid monotone finite difference scheme on a rectangular mesh. The difference operator incorporates an implicit Euler method for time and a hybrid scheme for space, which comprises central difference, upwind, and midpoint operators. The method is demonstrated to be almost second-order convergent in space vari-

ables and first-order convergent in time variables, regardless of the perturbation parameters.

Bullo et al. (2021b) proposed a robust finite difference method for solving two-parameter parabolic convection-diffusion problems that are singularly perturbed. They then used Micken's type of discretization on a uniform mesh to discretize the solution domain using the fitted operator approach. Their method is first-order convergent, and Richardson extrapolation accelerates it.

A parameter uniform method for two-parameter singularly perturbed boundary value problems with discontinuous data was developed by Roy and Jha (2022) using an appropriately defined Shishkin-Bakhvalov mesh type and the upwind scheme. Their scheme is first-order parameter uniform convergent.

Negero et al. (2023) proposed fitted operator finite difference methods are presented for two-parameter singularly perturbed one-dimensional parabolic partial differential equations with a delay in the time variable. The authors considered the following two-parameter singularly perturbed time-delay parabolic boundary value problem on the domain $D = \Omega_x \times (0,T], \Omega_x = (0,1)$ as

$$\pounds_{\varepsilon,\mu} u(x,t) \equiv u_t - \varepsilon u_{xx} - \mu a(x,t) u_x + b(x,t)u = g(x,t),\ x \in D \tag{2.27}$$

with initial and boundary condition

$$\begin{aligned} u(x,t) &= \Psi_b(x,t), (x,t) \in \Gamma_b = [0,1] \times [-\tau, 0], \\ u(0,t) &= \Psi_l(t), \Gamma_l = \{(0,t) : 0 \le t \le T\}, \\ u(1,t) &= \Psi_r(t), \Gamma_r = \{(1,t) : 0 \le t \le T\}, \end{aligned} \tag{2.28}$$

where $g(x,t) = -c(x,t)u(x,t-\tau) + f(x,t), (x,t) \in D,\ 0 < \varepsilon \le 1,\ 0 \le \mu \le 1$ and $\tau > 0$ represents the delay parameter. The functions $a(x,t), b(x,t),\ c(x,t), f(x,t), \Psi_b(x,t), \Psi_l(t)$ and $\Psi_r(t)$ are sufficiently smooth, bounded functions independent of ε and μ that satisfy $a(x,t) \ge \alpha > 0, b(x,t) \ge \beta > 0, c(x,t) \ge \vartheta > 0, \forall (x,t) \in \bar{D} = [0,T] \times [0,1]$. To approximate the solution to the problem, the researchers applied the Crank-Nicolson method for time discretization, while the non-standard scheme was used for space discretization on uniform meshes.

2.4 Nonlinear singularly perturbed problems

Nonlinear singularly perturbed problems are mathematical problems that involve nonlinear differential equations with a small parameter. These problems often arise in various fields,

such as physics, engineering, and biology, where the presence of a small parameter that affects the dynamics or the boundary conditions of the system O'malley et al. (1991); Wineman (2007); Nayfeh and Balachandran (2008).

Numerical methods have been developed to solve the singularly perturbed Burgers-Huxley equation, a nonlinear partial differential equation that combines the Burgers equation and the Huxley equation, for instance, Ismail et al. (2004); Kadalbajoo et al. (2005); Batiha et al. (2008); Zibaei et al. (2016); İnan (2017); Appadu et al. (2019,0); Li-Bin et al. (2020); Derzie et al. (2022,0). These methods address the challenges posed by the small parameter in the equation, providing accurate and efficient solutions by discretizing the equation and employing techniques such as finite difference, finite element, and spectral methods.

Derzie et al. (2022) considered singularly perturbed time-dependent Burgers-Huxley equation on the domain $D \equiv \Omega \times (0,T] \equiv (0,1) \times (0,T]$ as the form

$$\begin{cases} \dfrac{\partial u}{\partial t} + L_\varepsilon u(x,t) = 0, (x,t) \quad \in D, \\ u(x,0) = f(x), \quad x \in \Omega, \\ u(0,t) = h_0(t), u(1,t) = h_1(t), \quad t \in [0,T], \end{cases} \tag{2.29}$$

where

$$L_\varepsilon u(x,t) \equiv -\varepsilon u_{xx} + \alpha u u_x - \beta(1-u)(u-\gamma)u$$

$0 < \varepsilon \ll 1, \alpha \geq 0, \beta \geq 0, \gamma \in (0,1)$ are real parameters, and the prescribed functions $h_0(t), h_1(t)$ and $f(x)$ are sufficiently smooth and satisfy the compatibility conditions $h_0(0) = f(0)$ and $h_1(0) = f(1)$. The authors have developed a robust numerical scheme that exhibits uniform convergence for the singularly perturbed time-dependent Burgers-Huxley partial differential equation. The authors first discretize the time derivative of the equation using the Crank-Nicolson finite difference method, and they obtained semi-discretized nonlinear ordinary differential equations.

A robust analytical approach to the generalized Burgers-Fisher equation with fractional derivatives including singular and non-singular kernels is developed by (Prajapati and Meher, 2022). The proposed method is based on the η-homotopy analysis method with a new integral transform, and a well-proven algorithm that quickly provides approximate solutions and maintains excellent accuracy. Sawangtong et al. (2023) formulated an approximate analytic solution for the multidimensional fractional-order time and space Burger equation-based on Caputo-Katugampola derivative using the generalized Laplace homotopy perturbation method.

Standard numerical methods fail to capture the behavior of the solution for singularly perturbed problems due to the presence of certain parameters. Furthermore, the existing numerical schemes discussed in the literature do not provide the desired level of accuracy for the obtained solution. Consequently, there is a need to formulate new numerical methods that can deliver improved accuracy. Within this dissertation, we have developed uniformly convergent numerical schemes that exhibit better accuracy when compared to the existing schemes.

CHAPTER 3

RESEARCH METHODOLOGY

3.1 Study area and period

This study was conducted in Applied Mathematics, focusing on a class of time-delayed two-parameter singularly perturbed problems. The solutions to the problems considered in this study require accurate, stable, and uniformly convergent numerical schemes. The study primarily focuses on exploring fitted numerical methods for both linear and nonlinear singularly perturbed parabolic partial differential equations, with and without time delay. The study was conducted from September 2020 to June 2024.

3.2 Study design

In this study both theoretical and experimental designs were used. The numerical experimentation was conducted using MATLAB software and Python software, and the results are given in the form of tables and plots.

3.3 Source of information

The relevant sources of information for this dissertation encompass a variety of books, previously published articles, and related studies accessible through Google Scholar. Additionally, experimental results are obtained by writing and implementing computer programs for the developed numerical schemes using the Matlab and Python software packages.

3.4 Development of the numerical method

This dissertation focuses on the development of numerical methods for solving linear and nonlinear SPPs. Two methods, namely the FOFDM and the FMFDM are proposed. These methods utilize finite difference techniques on either uniform or piecewise uniform grids. The fitted operator finite difference method is employed on uniform grids. It replaces the standard finite difference operator with a modified operator that captures the layer behavior of the problem. On the other hand, the fitted mesh finite difference method is utilized on piecewise uniform grids. This method involves modifying the mesh to adapt to the singular perturbation problems, ensuring accurate solutions.

3.5 Mathematical procedures

To achieve the stated objectives, the following general procedures are employed:

1. Describing the model problem.
2. Describing the analytical properties of the continuous solution.
3. Develop numerical schemes for the considered problem.
4. Establishing the stability and convergence of the proposed numerical schemes.
5. Developing an algorithm based on the proposed scheme and writing MATLAB and/or Python codes for it.
6. Testing the accuracy of the proposed scheme using numerical examples.
7. Presenting the computed results using tables and plots.
8. Comparing the obtained results with other existing schemes in the literature.
9. Concluding the proposed methods.

CHAPTER 4

A FITTED OPERATOR FINITE DIFFERENCE METHOD FOR TWO-PARAMETER SINGULARLY PERTURBED TIME-DELAY PROBLEMS

This chapter discusses parabolic convection-reaction-diffusion time-delay SPPs with two small perturbation parameters. The solutions to SPPs exhibit boundary layers, which occur near the boundaries of the domain. These layers are characterized by steep gradients or sharp variations in the solution, leading to complex analytical solutions. To solve SPPs numerically (when analytical solutions are more complicated), one can use finite difference methods, finite element methods, spline approximation methods, and others. But, unless very fine grids are used, standard finite difference methods can not resolve the layers(s) and may not provide a uniformly convergent solution throughout the given domain. The two fitted methods used for solving SPPs are Fitted Operator Finite Difference Methods (FOFDMs) and Fitted Mesh Finite Difference Methods (FMFDMs). In this chapter, we develop the FOFDM for time-delay parabolic two-parameter SPPs. A parameter-uniform convergent scheme is formulated on a uniform mesh following the methodology of Mickens (1994).

4.1 The governing problem

Consider the time-delay parabolic two-parameter SPP on the domain $\bar{D} = D \cup \partial D$, where $D = (0,1) \times (0,T]$ and $\partial D = L_l \cup L_d \cup L_r$ with $L_d = [0,1] \times [-\gamma, 0]$ (delay interval), $L_l = \{0\} \times (0,T]$ (left side boundary) and $L_r = \{1\} \times (0,T]$ (right side boundary) described as

$$Lu(x,t) - u_t(x,t) = -c(x,t)u(x,t-\gamma) + f(x,t),\ (x,t) \in D, \tag{4.1}$$

with initial boundary data

$$\begin{aligned} u(x,t) &= \Phi_d(x,t),\ \ (x,t) \in L_d, \\ u(0,t) &= \Phi_l(t),\ \ u(1,t) = \Phi_r(t),\ \ t \in [0,T], \end{aligned} \tag{4.2}$$

where $Lu(x,t) = \varepsilon u_{xx}(x,t) + \mu a(x,t)u_x(x,t) - b(x,t)u(x,t)$, $0 < \varepsilon \leq 1$ and $0 \leq \mu \leq 1$ are perturbation parameters, and γ is a delay parameter. For the problem (4.1)-(4.2), we assume that the coefficient $a(x,t)$, $b(x,t)$, $c(x,t)$, $f(x,t)$ and initial-boundary functions $\Phi_l(t)$, $\Phi_r(t)$, $\Phi_d(x,t)$ are sufficiently smooth on $\bar{D}$. Additionally, we assume the boundedness of these

coefficient functions as $a(x,t) \geq \alpha > 0$, $b(x,t) \geq \beta > 0$, and $c(x,t) \geq \Upsilon > 0$, where α, β, and Υ are constants independent of the perturbation parameters. At the corners of the domain, the regularity and compatibility conditions are as follows.

$$u(0,0) = \Phi_l(0), \quad u(1,0) = \Phi_r(0), \quad u(0,-\gamma) = \Phi_l(-\gamma), \quad u(1,-\gamma) = \Phi_r(-\gamma)$$

Additionally, at the corner $(0,0)$, the following condition holds.

$$\begin{aligned}\varepsilon(\Phi_d)_{xx}(0,0) + \mu a(0,0)(\Phi_d)_x(0,0) - b(0,0)(\Phi_d)(0,0) - (\Phi_b)_t(0,0) \\ = -c(0,0)(\Phi_d)(0,-\gamma) + f(0,0)\end{aligned}$$

Similarly, at the corner $(1,0)$, the condition is:

$$\begin{aligned}\varepsilon(\Phi_d)_{xx}(1,0) + \mu a(1,0)(\Phi_d)_x(1,0) - b(1,0)(\Phi_d)(1,0) - (\Phi_d)_t(1,0) \\ = -c(1,0)(\Phi_d)(1,-\gamma) + f(1,0)\end{aligned}$$

These conditions ensure that the initial boundary data $\Phi_d(x,t)$ satisfies the appropriate compatibility criteria at the corners $(0,0)$ and $(1,0)$. Based on the provided assumptions, it can be concluded that the given problem in (4.1)- (4.2) possesses a unique solution within the considered domain.

4.2 Properties of the continuous problem

In this section, we focus on the analytical properties of the governing problem (4.1)-(4.2) in one spatial dimension within the defined domain $\bar{D}$. We begin by stating and proving the minimum principle and providing derivative bounds for the solution.

Lemma 4.2.1 (Minimum principle)**.** *(Kumar et al., 2020). Let $\varphi(x,t) \in C^{2,1}(\bar{D})$. If $\varphi|_{\partial D} \geq 0$ and $\left(L_{\varepsilon,\mu} - \frac{\partial}{\partial t}\right)\varphi|_D \leq 0$, then $\varphi|_{\bar{D}} \geq 0$.*

Proof. The proof starts by assuming that there exists an arbitrary point (x^*,t^*) in the domain $\bar{D} = (0,1)\times(0,T)$ where the function $\varphi(x^*,t^*)$ achieves the minimum value among all points in $\bar{D}$, i.e., $\varphi(x^*,t^*) = \min\{\varphi(x,t)\}_{(x,t)\in\bar{D}}$. Then assumes that $\varphi(x^*,t^*) < 0$. Since $(x^*,t^*) \notin \{0,1\}\times\{0,T\}$ (the boundary points of $\bar{D}$), the proof applies the first and second derivative tests for multi-variable functions. These tests allow us to conclude that at the point (x^*,t^*), the second partial derivative with respect to x, $\varphi_{xx}(x^*,t^*)$, is non-negative, and the gradients with respect to x and t are both zero, i.e., $\nabla_x\varphi(x^*,t^*) = 0$ and $\nabla_t\varphi(x^*,t^*) = 0$. Next, the

proof considers the operator $\left(L_{\varepsilon,\mu} - \frac{\partial}{\partial t}\right)\varphi|_D$ and evaluates it at (x^*,t^*), and it becomes

$$\left(L_{\varepsilon,\mu} - \frac{\partial}{\partial t}\right)\varphi|_D = \underbrace{\varepsilon\varphi_{xx}(x^*,\,t^*)}_{\geq 0} + \underbrace{\mu a(x^*,\,t^*)\nabla_x\varphi(x^*,t^*)}_{=0} \underbrace{-b(x^*,t^*)\varphi(x^*,\,t^*)}_{\geq 0} \underbrace{-\nabla_t\varphi(x^*,t^*)}_{=0} \geq 0$$

By substituting the values of the derivatives and applying the given coefficients, the expression simplifies to $\varepsilon\varphi_{xx}(x^*,t^*) - b(x^*,t^*)\varphi(x^*,t^*)$. Since $\varphi_{xx}(x^*,t^*) \geq 0$ and $b(x^*,t^*) \geq 0$, the term $\varepsilon\varphi_{xx}(x^*,t^*) - b(x^*,t^*)\varphi(x^*,t^*) \geq 0$. However, this contradicts the assumption that $\left(L_{\varepsilon,\mu} - \frac{\partial}{\partial t}\right)\varphi|_D \leq 0$ for all points in D. Therefore, the initial assumption that $\varphi(x^*,t^*) < 0$ must be incorrect. It follows that $\varphi(x^*,t^*) \geq 0$ for all $(x^*,t^*) \in \bar{D}$. Since (x^*,t^*) was chosen arbitrarily, this implies that $\varphi(x,t) \geq 0$ for all $(x,t) \in \bar{D}$. ■

Lemma 4.2.2. *(Kumar et al., 2020). The solution u of problem (4.1)- (4.2) satisfies the bound*

$$\|u\| \leq C. \tag{4.3}$$

Proof. The proof starts by considering the function $r(x,t)$ defined as $r(x,t) = u(x,t) - \phi_b(x,0)$ for $0 \leq t \leq T$ and $r(x,t) = u(x,t) - \phi_b(x,t)$ for $-\gamma \leq t \leq 0$, where $\phi_b(x,0)$ is a smooth function and $t = 1$. The function r satisfies the equation $\mathfrak{L}_{\varepsilon,\mu}r - r_t = s$ in Ω, where $s(x,t)$ is defined as:

$$s(x,t) = -c(x,t)u(x,t-\gamma) + f(x,t) - \left(\mathfrak{L}_{\varepsilon,\mu} - \frac{\partial}{\partial t}\right)\Phi_b(x,0) = f - \varepsilon\Phi_{xx}(x,t) + \mu a(x,t)\Phi_x(x,t)$$
$$-b(x,t)\Phi(x,t) - c(x,t)\Phi(x,t-\gamma)$$

with boundary conditions $r|_{\Gamma_b} = 0$, $r|_{\Gamma_l} = \Phi_l(t) - \Phi_b(0,0)$, and $r|_{\Gamma_r} = \Phi_r(t) - \Phi_b(1,0)$. To proceed with the proof, a barrier function $q(x,t)$ is introduced. The barrier function is defined as $q(x,t) = Ct$ for $t \in [0,T]$ and $q(x,t) = 0$ for $t \in [-\gamma,0]$. It satisfies the equation:

$$\left(\mathfrak{L}_{\varepsilon,\mu} - \frac{\partial}{\partial t}\right)q = -C(1+bt)$$

with boundary conditions $q|_{\Gamma_b} = 0$ and $q|_{\Gamma_l} = q|_{\Gamma_r} = 0$. By comparing the absolute value of $\left(\mathfrak{L}_{\varepsilon,\mu} - \frac{\partial}{\partial t}\right)r$ with $\left(\mathfrak{L}_{\varepsilon,\mu} - \frac{\partial}{\partial t}\right)q$ in Ω and considering the inequality $|r(x,t)| \leq q(x,t)$ on $\partial\Omega$, it is shown that $|r(x,t)| \leq q(x,t)$ holds in the closure $\bar{\Omega}$. Then, by setting $\phi_b(x,0) = 0$ and $t = 1$, it follows that $|u(x,t) - \phi_b(x,0)| \leq Ct$ in $\bar{\Omega}$. Since $\phi_b(x,0)$ is a smooth function and $t \in (0,T]$ in $\bar{\Omega}$, the desired result $\|u\| \leq C$ is obtained. For more detailed calculations and arguments, please refer to the proof provided in the referenced paper Kumar et al. (2020). ■

Lemma 4.2.3. *(Kumar et al. (2020)) The derivatives of the solution u of problem (4.1)- (4.2)*

satisfy the bounds for all non- negative integers i, j, *such that* $0 \leq i+2j \leq 4$ *are given by*

$$\left\| \frac{\partial^{i+j} u}{\partial x^i \partial t^j} \right\| \leq \begin{cases} C \dfrac{1}{(\sqrt{\varepsilon})^i}, & \text{when } \alpha\mu^2 \leq \eta\varepsilon \\ C \left(\dfrac{\mu}{\varepsilon}\right)^i \left(\dfrac{\mu^2}{\varepsilon}\right)^j, & \text{when } \alpha\mu^2 \geq \eta\varepsilon \end{cases}$$

Proof. The proof of this Lemma involves transforming the problem using stretching variables and applying the methods of steps to obtain bounds on the derivatives of the solution u. The lemma provides bounds for the derivatives of u in terms of the parameters ε, μ, α, and η. The proof considers two cases: $\alpha\mu^2 \leq \eta\varepsilon$ and $\alpha\mu^2 \geq \eta\varepsilon$. In each case, a suitable stretching variable transformation is applied to the problem to obtain a transformed problem in a new domain. The methods of steps are then used to derive bounds on the derivatives of the transformed solution.

In the first case, where $\alpha\mu^2 \leq \eta\varepsilon$, the stretching variable $\hat{x} = x/\sqrt{\varepsilon}$ is introduced. The transformed problem is analyzed using the methods of steps, and it is shown that for $i, j \in \mathbb{N}_0$ with $0 \leq i+2j \leq 4$, the derivatives of $\hat{u}$ satisfy the bound $\left\| \dfrac{\partial^{i+j}\hat{u}}{\partial \hat{x}^i \partial t^j} \right\| \leq C \dfrac{1}{(\sqrt{\varepsilon})^i}$. Finally, by returning to the original variables, the desired bounds on the derivatives of u are obtained.

In the second case, where $\alpha\mu^2 \geq \eta\varepsilon$, stretching variables $\bar{x} = \mu x/\varepsilon$ and $\tilde{t} = \mu^2 t/\varepsilon$ are used. The transformed problem is analyzed similarly, and for $i, j \in \mathbb{N}_0$ with $0 \leq i+2j \leq 4$, the derivatives of $\tilde{u}$ satisfy the bound $\left\| \dfrac{\partial^{i+j}\tilde{u}}{\partial \tilde{x}^i \partial \tilde{t}^j} \right\| \leq C \left(\dfrac{\mu}{\varepsilon}\right)^i \left(\dfrac{\mu^2}{\varepsilon}\right)^j$. Again, by transforming back to the original variables, bounds on the derivatives of u are obtained. The details of the proof can be found in Kumar et al. (2020). ■

4.3 Derivation of the numerical scheme

In this section, we develop a numerical scheme for discretizing the temporal and spatial domains, as well as the given singularly perturbed problem described in equations (4.1)-(4.2).

4.3.1 Semi-discrete scheme using temporal discretization

In this section, we will discretize the temporal domain by dividing the given time interval $[0,T]$ into a uniform mesh, and we choose a parameter γ such that $T = k\gamma$, where $k > 1$. Again, we define two sets of mesh points: D^M, which consists of all mesh points in $[0,T]$, and D_γ^m, which contains all mesh points in $[-\gamma, 0]$. Specifically, we have:

$D^M = \{t_j = j\Delta t, j = 0,1,2,...,M, t_M = T, \Delta t = \dfrac{T}{M}\}$, and

$D_\gamma^m = \{t_j = j\Delta t, j = 0,1,2,...,m, t_m = \gamma, \Delta t = \dfrac{\gamma}{m}\}$.

Here, M represents the number of mesh points in the time interval $[0,T]$, and m represents the number of mesh points in $[-\gamma,0]$. To semi-discretize the continuous problem, we employ the Crank-Nicolson finite difference method in the temporal direction. The derivation of the Crank-Nicolson scheme for $U_t(x,t_j)$ at the $(x,j+1/2)$ time step involves utilizing Taylor's series expansion for U^{j+1} and U^j, the procedure is as follow.

$$U^{j+1}(x) = U^{j+1/2}(x) + \frac{\Delta t}{2}\frac{\partial U^{j+1/2}(x)}{\partial t} + \left(\frac{\Delta t}{2}\right)^2 \frac{1}{2!}\frac{\partial^2 U^{j+1/2}(x)}{\partial t^2} + \left(\frac{\Delta t}{2}\right)^3 \frac{1}{3!}\frac{\partial^3 U^{j+1/2}(x)}{\partial t^3} + \ldots \tag{4.4}$$

$$U^{j}(x) = U^{j+1/2}(x) - \frac{\Delta t}{2}\frac{\partial U^{j+1/2}(x)}{\partial t} + \left(\frac{\Delta t}{2}\right)^2 \frac{1}{2!}\frac{\partial^2 U^{j+1/2}(x)}{\partial t^2} - \left(\frac{\Delta t}{2}\right)^3 \frac{1}{3!}\frac{\partial^3 U^{j+1/2}(x)}{\partial t^3} + \ldots \tag{4.5}$$

By subtracting equation (4.5) from equation (4.4), we eliminate the term $U^{j+1/2}(x)$ and by simplifying the result, we get

$$\frac{U^{j+1}(x) - U^{j}(x)}{\Delta t} = \frac{\partial U^{j+1/2}(x)}{\partial t} + O((\Delta t)^3),$$

and the local truncation error $T^{j+1/2}(x)$ of this discretization is given by:

$$T^{j+1/2}(x) = \frac{(\Delta t)^3}{24}\frac{\partial^3 U^{j+1/2}(x)}{\partial t^3} + \text{H.O.Ts (higher-order terms)}.$$

By rearranging the problem in (4.1) using the aforementioned discretizations, we can express the semi-discretized scheme as follows:

$$\begin{aligned}
&\frac{u(x,t_{j+1}) - u(x,t_j)}{\Delta t} = \varepsilon u_{xx}(x,t_{j+1/2}) + \mu a(x,t_{j+1/2})u_x(x,t_{j+1/2}) \\
&-b(x,t_{j+1/2})u(x,t_{j+1/2}) - f(x,t_{j+1/2}) + O((\Delta t)^3) \\
&+ \begin{cases} -c(x,t_{j+1/2})\Phi_d(x) \\ \text{for } j = 0,1,\cdots,m \\ -c(x,t_{j+1/2})u(x,t_{j+1/2-m}) \\ \text{for } j = m+1,\cdots,M-1 \end{cases}
\end{aligned} \tag{4.6}$$

where

$$u(x,t_{j+1/2}) = \frac{u(x,t_{j+1}) + u(x,t_j)}{2} + O((\Delta t)^3), \quad \text{and} \quad f(x,t_{j+1/2}) = \frac{f(x,t_{j+1}) + f(x,t_j)}{2}$$

Lemma 4.3.1 (Semi-discrete minimum principle)**.** *Assume that* $\left[L^M U^{j+1}(x)\right]$ *is the discrete operator given in (4.6) and* $\varphi^{j+1}(x)$ *is any mesh function satisfying* $\varphi^{j+1}(x)\big|_{\partial D} \geq 0$ *and* $\left[L^M \varphi^{j+1}(x)\right]\big|_D \leq 0$ *for* $0 \leq j \leq M$*, then* $\varphi^{j+1}(x)\big|_{\bar{D}} \geq 0$

Proof. Let $s^* \in D$ be any arbitrary point such that $\varphi^{j+1}(s^*) = \min_{x\in D} \varphi^{j+1}(x)$. We show that $\varphi^{j+1}(x) \geq 0$ for all $x \in \bar{D}$. For the sake of contradiction, we supposed that there exists a point $s^* \in D$ such that $\varphi^{j+1}(s^*) < 0$. Since $\varphi^{j+1}(x)$ is a mesh function, it can only take values at the mesh points but not the boundary points. That means $(s^*, t_{j+1}) \notin \{(0,t_{j+1}),(1,t_{j+1})\}$. Again, by applying first and second derivative tests, we have

$$\frac{d}{dx}\left(\varphi^{j+1}(s^*)\right) = 0 \text{ and } \frac{d^2}{dx^2}\left(\varphi^{j+1}(s^*)\right) \geq 0$$

and hence

$$L^M_{\varepsilon,\mu}\varphi^{j+1}(s^*)\,|_D = \underbrace{\varepsilon\varphi_{xx}(s^*,t_{j+1/2})}_{\geq 0} + \underbrace{\mu a(s^*,t_{j+1/2})\varphi_x(s^*,t_{j+1/2})}_{=0} - \underbrace{\left(b(s^*,t_{j+1/2})\varphi(s^*,t_{j+1/2})\right)}_{<0}$$
$$> 0$$

which is a contradiction to the given hypothesis, so that the assumption is wrong. Therefore the assumption $\varphi^{j+1}(s^*) < 0$ is wrong. Hence, we conclude that $\varphi^{j+1}(s^*)|_D \geq 0$. Since s^* is chosen arbitrarily $\varphi^{j+1}(x) \geq 0$ for all $x \in \bar{D}$. ■

Lemma 4.3.2. *(Estimate of local error). Suppose that* $\|\frac{\partial^k u(x,t)}{\partial t^k}\| \leq C, (x,t) \in \overline{D}, k = 0,1,2.$ *The error estimate in temporal direction* $e_{j+1} = U^{j+1}(x) - u(x,t_{j+1})$ *for sufficiently large constant* C *is*

$$\left\|e_{j+1}\right\| \leq C(\Delta t)^3.$$

Proof. From the Crank-Nicholson finite difference method of temporal discretization, the fourth-order Taylor's series expansion, we have

$$\frac{U^{j+1}(x) - U^j(x)}{\Delta t} = \frac{\partial U^{j+1/2}(x)}{\partial t} + O((\Delta t)^3). \tag{4.7}$$

Using (4.7) into (4.1)-(4.2) , we get

$$L_{\varepsilon,\mu}u^{j+1}(x) = u_t^{j+1}(x) + O((\Delta t)^3)$$

Again, we apply the semi-discrete minimum operator for e_{k+1}, and then we have

$$L^M_{\varepsilon,\mu}e^{j+1}(x) = O((\Delta t)^3)$$

Then, by Lemma 4.3.1 the local error is bounded and given as

$$\left\|e_{j+1}\right\| \leq C(\Delta t)^3$$

■

Lemma 4.3.3. *(Estimate of global error). The global error, $E_j = U^j(x) - u(x,t_j$ of the time discretization satisfies*

$$\|E_j\| \leq C(\Delta t)^2.$$

where C is a constant independent of ε, μ and Δt.

Proof. By using the estimation of local errors, the global error at $j+1$ nodal points is given as

$$\|E_{j+1}\| = \left\| \sum_{\iota=1}^{j} e_\iota \right\|, j(\Delta t) \leq T$$

$$\begin{aligned}
&= \|e_1 + e_2 + e_3 + e_4 + \ldots + e_j\| \\
&\leq \|e_1\| + \|e_2\| + \|e_3\| + \|e_4\| + \ldots + \|e_j\| \\
&\leq C_1(\Delta t)^3 + C_2(\Delta t)^3 + C_3(\Delta t)^3 + C_4(\Delta t)^3 + \ldots + C_j(\Delta t)^3 \\
&\leq C'(j)(\Delta t)^3 \\
&\leq C'\frac{T}{\Delta t}(\Delta t)^3 = C'T(\Delta t)^2, \ \ because \ \ j \leq \frac{T}{\Delta t} \\
&\leq C(\Delta t)^2, \quad where, \ \ C = C'T
\end{aligned}$$

Thus, the semi-discrete scheme is convergent of order two in time. ■

Lemma 4.3.4. *Let $U^j(x)$ be the semi-discrete solution of (4.1)-(4.2). For a certain order of derivative q that depends on the smoothness of data $U^j(x)$, it satisfies the following bound:*

$$\left| \frac{d^\xi U^j(x)}{dx^\xi} \right| \leq C\left(1 + \Theta_1^\xi e^{-p\Theta_1 x} + \Theta_2^\xi e^{-p\Theta_2(1-x)}\right), \quad for\ 0 \leq \xi \leq q,$$

where p is any real constant such that $0 < p < 1$.

Proof. To prove the bound for the derivatives of $U^j(x)$, we use the smoothness properties of the semi-discrete solution and the exponential decay estimates for the coefficients Θ_1 and Θ_2. Let us consider a specific derivative order ξ with $0 \leq \xi \leq q$. We need to show that

$$\left| \frac{d^\xi U^j(x)}{dx^\xi} \right| \leq C\left(1 + \Theta_1^\xi e^{-p\Theta_1 x} + \Theta_2^\xi e^{-p\Theta_2(1-x)}\right),$$

holds for some constant C. From the semi-discrete solution $U^j(x)$, we know that it satisfies the system of equations (4.1)-(4.2). By differentiating these equations ξ times with respect to x, we obtain a system of equations involving the derivatives of $U^j(x)$ up to order ξ. Using the exponential decay estimates for the coefficients Θ_1 and Θ_2, there exist positive constants

a_1, a_2, and p (where $0 < p < 1$) such that:

$$\Theta_1 \leq a_1 e^{-p\Theta_1 x}, \ \Theta_2 \leq a_2 e^{-p\Theta_2(1-x)},$$

for all $x \in [0,1]$. These estimates indicate that Θ_1 and Θ_2 decay exponentially as x approaches the boundaries of the interval $[0,1]$. The constants a_1 and a_2 control the rate of decay, while p determines the speed of exponential decay. we can estimate each term in the system of equations. Specifically, we have:

$$\begin{aligned}\left|\frac{d^{\xi}U^{j}(x)}{dx^{\xi}}\right| &\leq C\left(|1| + |\Theta_1^{\xi} e^{-p\Theta_1 x}| + |\Theta_2^{\xi} e^{-p\Theta_2(1-x)}|\right) \\ &= C\left(1 + \Theta_1^{\xi} e^{-p\Theta_1 x} + \Theta_2^{\xi} e^{-p\Theta_2(1-x)}\right),\end{aligned}$$

where C is a constant that depends on the smoothness of the solution and the coefficients of the system. Therefore, we have shown that for each derivative order ξ with $0 \leq \xi \leq q$, the bound holds:

$$\left|\frac{d^{\xi}U^{j}(x)}{dx^{\xi}}\right| \leq C\left(1 + \Theta_1^{\xi} e^{-p\Theta_1 x} + \Theta_2^{\xi} e^{-p\Theta_2(1-x)}\right).$$

This completes the proof of the Lemma. ■

4.3.2 Full-discrete scheme using spatial discretization

To discretize the spatial domain, we consider $\bar{D}^N$, that denotes the interval $[0,1]$, and then divide it into N sub-intervals such that

$$x_0 = 0, \ x_1 = x_0 + h, \ x_2 = x_1 + h = x_0 + 2h, x_3 = x_2 + h = x_0 + 3h, \ \cdots \ , x_N = x_{N-1} + h = x_0 + Nh = 1$$

Then, the discretization of the rectangular domain is $\bar{D}^{N,M} = (\bar{D}^N \times \bar{D}^M) \cup (\bar{D}^N \times \bar{D}^m)$, and also the discretization of the boundary data and boundary conditions is $\partial D^{N,M} = L_d^{\mathrm{N,M}} \cup L_l^{\mathrm{N,M}} \cup L_r^{\mathrm{N,M}}$, where $L_d^{\mathrm{N,M}} = \bar{D}^N \times \bar{D}^m, L_l^{N,M} = \bar{D}^N \cap L_l, \quad L_r^{\mathrm{N,M}} = \bar{D}^N \cap L_r$. And $\bar{D}^m$ denotes the uniform temporal meshes in $[-\gamma, 0]$. Again, using the space discretization, we can rewrite the semi-discrete scheme as

$$\begin{aligned}\left[L^{N,M}U\right]_i^j \equiv \frac{u\left(x_i,t_{j+1}\right)-u\left(x_i,t_j\right)}{\Delta t} &= \varepsilon u_{xx}\left(x_i,t_{j+1/2}\right)+\mu a(x_i,t_{j+1/2})u_x\left(x_i,t_{j+1/2}\right)\\ -b\left(x_i,t_{j+1/2}\right)u\left(x_i,t_{j+1/2}\right)-f\left(x_i,t_{j+1/2}\right)+O\left((\Delta t)^3\right)\}&\\ +\begin{cases} -c\left(x_i,t_{j+1/2}\right)\Phi_d(x_i) & \\ \text{for} \quad i=0,1,\cdots,N,\ j=0,1,\cdots,m & \\ -c\left(x_i,t_{j+1/2}\right)u\left(x_i,t_{j+1/2-m}\right) & \\ \text{for} \quad i=0,1,\cdots,N,\quad j=m+1,\cdots,M-1 & \end{cases}&\end{aligned} \tag{4.8}$$

Next, the the resulting discretized equation in (4.8) can be rearranged using a nonstandard fitted operator finite difference method following the steps in Mickens (1994).

$$\begin{aligned}\left[L^{N,M}U\right]_i^j \equiv \frac{1}{2}\left[\varepsilon\delta_x^2U_i^{j+1}+\mu a_i{}^{j+1}D_x^+U_i^{j+1}-b_i^{j+1}U_i^{j+1}+\varepsilon\delta_x^2U_i^j+\mu a_i{}^jD_x^+U_i^j-b_i^jU_i^j\right]-D_tU_i^{j+1/2}&\\ =F_i^j\quad i=0,1,2,\cdots,N-1,\quad j=0,1,2,\cdots,M-1&\end{aligned} \tag{4.9}$$

where

$$D_x^+U_i^j=\frac{U_{i+1}^j-U_i^j}{h_x},\quad D_tU_i^{j+1/2}=\frac{U_i^{j+1}-U_i^j}{\Delta t}\qquad \delta_x^2U_i^j=\left(\frac{U_{i+1}^j-2U_i^j+u_{i-1}^j}{\phi_i^2}\right)$$

$$D_x^+U_i^{j+1}=\frac{U_{i+1}^{j+1}-U_i^{j+1}}{h_x},\quad \delta_x^2U_i^{j+1}=\left(\frac{U_{i+1}^{j+1}-2U_i^{j+1}+u_{i-1}^{j+1}}{\phi_i^2}\right)$$

and

$$F_i^j=\begin{cases}\frac{1}{2}\left[-c_i^{j+1}\Phi_{di}{}^{j+1}-c_i^j\Phi_{di}{}^j+f_i^{j+1}+f_i^j\right],\ \ for\ \ j=0,1,\cdots,m\\ \frac{1}{2}\left[-c_i^{j+1}U_i^{j-m+1}-c_i^jU_i^{j-m}+f_i^{j+1}+f_i^j\right],\ \text{for}\ j=m+1,\cdots,M-1\end{cases} \tag{4.10}$$

where the denominator function ϕ_i^2 is given by

$$\phi_i^2(h,\varepsilon,\mu)\equiv\phi_i^2=\frac{h\varepsilon}{\mu a\left(x_i\right)}\left(\exp\left(\frac{\mu a\left(x_i\right)h}{\varepsilon}\right)-1\right)$$

Eq. (4.9) can be written in compact form as

$$\left[L^{N,M}U_i^{j+1}\right]\equiv\delta^+U_{i+1}^{j+1}+\delta^cU_i^{j+1}+\delta^-U_{i-1}^{j+1}=F_i^j-\delta_1^+U_{i+1}^j-\delta_1^cU_i^j-\delta_1^-U_{i-1}^j \tag{4.11}$$

where

$$\delta^+ = \left(\frac{\varepsilon}{2\phi(i)^2} + \frac{\mu a_i^{j+1}}{2h}\right),\ \delta_1^+ = \left(\frac{\varepsilon}{2\phi(i)^2} + \frac{\mu a_i^{j}}{2h}\right),\ \delta^c = \left(\frac{-\varepsilon}{\phi(i)^2} - \frac{\mu a_i^{j+1}}{2h} - \frac{b_i^{j+1}}{2} - \frac{1}{\Delta_t}\right)$$

$$\delta_1^c = \left(\frac{-\varepsilon}{\phi(i)^2} - \frac{\mu a_i^{j}}{2h} - \frac{b_i^{j}}{2} - \frac{1}{\Delta_t}\right),\quad \delta^- = \delta_1^- = \frac{\varepsilon}{2\phi(i)^2}$$

The idea for the derivation of the denominator function consists of taking a homogeneous form of the given equation with constant coefficients, and then forming an exact scheme for it following the steps in (Patidar, 2008).

4.4 Discrete stability and uniform convergence analysis

In this section, we will examine the stability and uniform convergence of the proposed scheme.

Lemma 4.4.1 (Discrete minimum principle)**.** *Assume that* $\left[L^{N,M}U_i^{j+1}\right]$ *is the discrete operator given in (4.11) and* φ_i^{j+1} *is any mesh function satisfying* $\varphi_i^{j+1}\Big|_{\partial D^{N,M}} \geq 0$ *and* $\left[L^{N,M}\varphi_i^{j+1}\right]\Big|_{D^{N,M}} \leq 0$ *for* $0 \leq i \leq N, 0 \leq j \leq M$, *then* $\varphi_i^{j+1}\Big|_{\bar{D}^{N,M}} \geq 0$

Proof. Assume that $\varphi_s^{l+1} = \min_{(i,j)} \varphi_i^{j+1}$ for $\varphi_i^{j+1} \in \bar{D}^{N,M}$, where s and l are indices. To create a contradiction, let us assume that $\varphi_s^{l+1} < 0$. It is clear that $(s,l) \notin \{0,N\} \times \{0,M\}$ because $\varphi_s^{l+1} \geq 0$. From the assumption $\varphi_s^{l+1} < 0$, we have $\varphi_{s+1}^{l+1} - \varphi_s^{l+1} > 0$ and $\varphi_s^{l+1} - \varphi_{s-1}^{l+1} < 0$. We consider the expression $L^{N,M}\varphi_s^{l+1}$:

$$\begin{aligned} L^{N,M}\varphi_s^{l+1} =& \varepsilon\left(\frac{\varphi_{s+1}^{l+1} - 2\varphi_s^{l+1} + \varphi_{s-1}^{l+1}}{\phi_s^2}\right) + \mu a_s^{l+1}\left(\frac{\varphi_{s+1}^{l} + \varphi_s^{l+1}}{h_s}\right) - b_s^{l+1}\varphi_s^{l+1} \\ =& \varepsilon\left(\frac{\varphi_{s+1}^{l+1} - \varphi_s^{l+1} + \varphi_{s-1}^{l+1} - \varphi_{s+1}^{l+1}}{\frac{h\varepsilon}{\mu a(x_s)}\left(\exp\left(\frac{\mu a(x_s)h}{\varepsilon}\right) - 1\right)}\right) + \mu a_s^{l+1}\left(\frac{\varphi_{s+1}^{l+1} + \varphi_s^{l+1}}{h_s}\right) - b_s^{l+1}\varphi_s^{l+1} > 0 \end{aligned}$$

The above inequality contradicts the assumption that $L^{N,M}\varphi_s^{l+1} \leq 0$. Therefore, we conclude that $\varphi_s^{l+1} \geq 0$. Since the indices s and l were chosen arbitrarily, we can conclude that $\varphi_i^{j+1} \geq 0$ for all $(i,j) \in \bar{D}^{N,M}$. ■

The above Lemma states the discrete minimum principle and proves that the mesh function is always non-negative.

Lemma 4.4.2 (Uniform stability estimate)**.** *At any time level t_j, if Z_i^{j+1} is any mesh function such that $Z_0^{j+1} = Z_N^{j+1} = 0$, then*

$$\left|Z_i^{j+1}\right| \leq \frac{1}{\wp} \max_{1\leq i\leq N-1} \left|L^{N,M} Z_i^{j+1}\right|, \text{ for } 0 < j < M.$$

Proof. To prove this lemma, the concept of barrier functions $(\varphi^{\pm})_i^j$ and the discrete minimum principle are utilized. Two barrier functions are defined as follows:

$$\left(\varphi^{\pm}\right)_i^{j+1} = R \pm Z_i^{j+1},$$

where

$$R = \frac{1}{\wp} \max_{1\leq i\leq N-1} \left|L^{N,M} Z_i^{j+1}\right|.$$

Consider the expressions $L^{N,M}\left(\varphi^{\pm}\right)_0^{j+1}$ and $L^{N,M}\left(\varphi^{\pm}\right)_N^{j+1}$:

$$L^{N,M}\left(\varphi^{\pm}\right)_0^{j+1} = \frac{1}{\wp} \max_{1\leq i\leq N-1} \left|\left(\varepsilon\delta_x^2 U_i^{j+1} + \mu a_i{}^{j+1} D_x^+ U_i^{+1} - b_i^{j+1} U_i^{j+1}\right)\right|, 1 \leq j \leq M-1$$
$$L^{N,M}\left(\varphi^{\pm}\right)_N^{j+1} = \frac{1}{\wp} \max_{1\leq i\leq N-1} \left|\left(\varepsilon\delta_x^2 U_i^{j+1} + \mu a_i{}^{j+1} D_x^- U_i^{j+1} - b_i^{j+1} U_i^{j+1}\right)\right|, 1 \leq j \leq M-1$$

Using the properties of the barrier functions and the fact that $Z_0^{j+1} = Z_N^{j+1} = 0$, we can simplify the above expressions and obtain:

$$L^{N,M}\left(\varphi^{\pm}\right)_0^{j+1} \geq 0, \quad L^{N,M}\left(\varphi^{\pm}\right)_N^{j+1} \geq 0$$

This is because $a(x,t) \geq \alpha > 0$ and $b(x,t) \geq \beta > 0$ for all x and t. By applying the discrete minimum principle (Lemma 7) to the expressions $L^{N,M}(\varphi^{\pm})_i^{j+1}$, we conclude that $(\varphi^{\pm})_i^{j+1} \geq 0$ for all i. Thus, we have:

$$\pm Z_i^{j+1} \leq R \quad \text{or} \quad -R \leq Z_i^{j+1} \leq R,$$

which implies:

$$\left|Z_i^{j+1}\right| \leq R = \frac{1}{\wp} \max_{1\leq i\leq N-1} \left|L^{N,M} Z_i^{j+1}\right|.$$

Therefore, the lemma holds. ■

This lemma shows the uniform stability of the operator $L^{N,M}$. In the following two lemmas, we analyze the convergence of the scheme in (4.9) using the bounds of the truncation error in both variables.

Theorem 4.4.1 (Error estimate in the spatial discretization)**.** *Let $U^{j+1}(x_i)$ and U_i^{j+1} are the solutions of (4.6) and (4.9), respectively. If N and C are mesh numbers and sufficiently large constants, then the following error bound holds.*

$$\left|L_{\varepsilon,\mu}^{N,M}\left(U^{j+1}(x_i)-U_i^{j+1}\right)\right| \leq \frac{C}{N}. \tag{4.12}$$

Proof. To prove this theorem, we use the differential and difference equations and then define the error as follows:

$$\begin{aligned}
&L_{\varepsilon,\mu}^{N,M}\left(U(x_i,t_{j+1})-U_i^{j+1}\right) = L_{\varepsilon,\mu}^{N,M}\left(U(x_i,t_{j+1})\right) - L_{\varepsilon,\mu}^{N,M}\left(U_i^{j+1}\right)\\
=&\varepsilon\frac{d^2U^{j+1}(x_i)}{dx^2}+\mu a^{j+1}(x_i)\frac{dU^{j+1}(x_i)}{dx}-b^{j+1}(x_i)-\left[\varepsilon\delta_x^2+\mu a^{j+1}(x_i)D_x^+-b^{j+1}(x_i)\right]\\
=&\varepsilon\frac{d^2U^{j+1}(x_i)}{dx^2}+\mu a^{j+1}(x_i)\frac{dU^{j+1}(x_i)}{dx}-b^{j+1}(x_i)\\
&-\left[\frac{\varepsilon}{\phi_i^2}\left(U_{i+1}^{j+1}-2U_i^{j+1}+u_{i-1}^{j+1}\right)+\frac{\mu a^{j+1}(x_i)}{h}\left(U_{i+1}^{j+1}-U_I^{j+1}\right)-b^{j+1}(x_i)\right]
\end{aligned} \tag{4.13}$$

Now, the Taylor's series expansion of U_{i+1}^{j+1}, U_{i-1}^{j+1} and $\dfrac{1}{\phi_i^2}$ are:

$$U_{i+1}^{j+1} = U_i^{j+1}+h\frac{dU^{j+1}(x_i)}{dx}+\frac{h^2}{2!}\frac{d^2U^{j+1}(x_i)}{dx^2}+\frac{h^3}{3!}\frac{d^3U^{j+1}(x_i)}{dx^3}+\frac{h^4}{4!}\frac{d^4U^{j+1}(\xi_i)}{dx^4}, \xi\in(x_{i-1},x_{i+1})$$

$$\begin{aligned}
U_{i-1}^{j+1} =& U_i^{j+1}-h\frac{dU^{j+1}(x_i)}{dx}+\frac{h^2}{2!}\frac{d^2U^{j+1}(x_i)}{dx^2}-\frac{h^3}{3!}\frac{d^3U^{j+1}(x_i)}{dx^3}+\frac{h^4}{4!}\frac{d^4U^{j+1}(\xi_i)}{dx^4}, \xi\in(x_{i-1},x_{i+1})\\
\frac{1}{\phi_i^2} =& \frac{1}{\frac{h\varepsilon}{\mu a(x_i)}\left(\exp\left(\frac{\mu a(x_i)h}{\varepsilon}\right)-1\right)} = \frac{1}{h^2}-\frac{\mu a^{j+1}(x_i)}{2\varepsilon h}+\frac{(\mu a^{j+1}(x_i))^2}{12\varepsilon^2}
\end{aligned}$$

Using these substitutions in (4.13) and applying some simplification gives:

$$\begin{aligned}
&\left(\mu a^{j+1}(x_i)\frac{d^2U^{j+1}(x_i)}{dx^2}-\frac{\mu a^{j+1}(x_i)}{2}\frac{d^2U^{j+1}(x_i)}{dx^2}\right)h+\\
&\left(\frac{(\mu a^{j+1}(x_i))^2}{12\varepsilon^2}\frac{d^2U^{j+1}(x_i)}{dx^2}-\frac{\mu a^{j+1}(x_i)}{6}\frac{d^3U^{j+1}(x_i)}{dx^3}\right)h^2+O(h^3)
\end{aligned} \tag{4.14}$$

Again, using the bounds of the derivatives in the Lemma 4.2.3, we can describe the bound of the error below.

$$\begin{aligned}
\left|L_{\varepsilon,\mu}^{N,M}\left(U(x_i,t_{j+1})-U_i^{j+1}\right)\right| &= \left|L_{\varepsilon,\mu}^{N,M}\left(U(x_i,t_{j+1})\right)-L_{\varepsilon,\mu}^{N,M}\left(U_i^{j+1}\right)\right|\\
&\leq C_1h+C_2h^2+\ldots\\
&\leq Ch=\frac{C}{N}
\end{aligned} \tag{4.15}$$

■

Remark 4.4.1. *The problem in (4.1)- (4.2) exhibits two boundary layers with different widths depending on the relation between the two parameters ε and μ.*

1. *if $\mu^2 \leq \varepsilon$ i.e $\mu^2/\varepsilon \to 0$ as $\varepsilon \to 0$, then boundary layers of width $O(\sqrt{\varepsilon})$ is expected in both neighborhood of $x = 0$ and $x = 1$.*
2. *if $\mu^2 > \varepsilon$ i.e $\varepsilon/\mu^2 \to 0$ as $\mu \to 0$, a boundary layer of width $O\left(\frac{\varepsilon}{\mu}\right)$ is predictable in a left neighborhood of $x = 0$, and a boundary layer of width $O(\mu)$ is expected in a right neighborhood of $x = 1$.*

Combining Lemma 4.3.3 and Theorem 4.4.1, we can state the following theorem as the main result.

Theorem 4.4.2. ***(The main result)*** *Let $u(x,t)$ be the solution of (4.1)- (4.2) and U_i^{j+1} is its numerical approximation obtained using (4.9). Then there exists a constant C independent of ε, μ, h and Δt such that*

$$\sup_{0<\varepsilon\leq 1, 0\leq\mu\leq 1} \left[\max_{0\leq i\leq N, 0\leq j\leq M} \left| u(x_i, t_{j+1}) - U_i^{j+1} \right| \right] \leq C((\Delta t)^2 + h). \tag{4.16}$$

Proof. To prove this Theorem, we take the left side of (4.16), then apply triangular inequality by using the semi-discrete solution, $U^{j+1}(x_i)$ as follows

$$\begin{aligned} \max_{0\leq i\leq N, 0\leq j\leq M} \left| u(x_i, t_{j+1}) - U_i^{j+1} \right| &= \max_{0\leq i\leq N, 0\leq j\leq M} \left| u(x_i, t_{j+1}) - U^{j+1}(x_i) + U^{j+1}(x_i) - U_i^{j+1} \right| \\ &\leq \max_{0\leq i\leq N, 0\leq j\leq M} \left| u(x_i, t_{j+1}) - U^{j+1}(x_i) \right| + \max_{0\leq i\leq N, 0\leq j\leq M} \left| U^{j+1}(x_i) - U_i^{j+1} \right| \end{aligned} \tag{4.17}$$

Using the error bounds of Lemma 4.3.3 and Theorem 4.4.1 for the result in (4.17), we get

$$\begin{aligned} \max_{0\leq i\leq N, 0\leq j\leq M} \left| u(x_i, t_{j+1}) - U^{j+1}(x) \right| + \max_{0\leq i\leq N, 0\leq j\leq M} \left| U^{j+1}(x) - U_i^{j+1} \right| &\leq C(\Delta t)^2 + Ch \\ &\leq C\left((\Delta t)^2 + h\right). \end{aligned}$$

Hence,

$$\begin{aligned} &\max_{0\leq i\leq N, 0\leq j\leq M} \left| u(x_i, t_{j+1}) - U_i^{j+1} \right| \\ &\leq C((\Delta t)^2 + h). \end{aligned}$$

■

4.5 Numerical results and discussion

To demonstrate the effectiveness of the proposed scheme in (4.9), we have implemented the following example. In this example, we have computed the maximum absolute error and the rate of convergence using the double mesh principle given in Doolan et al. (1980).

$$Err_{\varepsilon,\mu}^{N,M} = \max_{0\le i,j\le N,M} \left| U^{N,M}(x_i,\, t_j) - U^{2N,2M}(x_{2i},\, t_{2j}) \right| \quad \text{(maximum absolute errors)}$$

$$Roc_{\varepsilon,\mu}^{N,M} = \log_2 \left(\frac{Err_{\varepsilon,\mu}^{N,M}}{Err_{\varepsilon,\mu}^{2N,2M}} \right) \quad \text{(rate of convergence)}$$

Example 4.1. *Consider the following time-delay problem Kumar et al. (2020):*

$$\begin{cases} \varepsilon u_{xx}(x,t) + \mu(1+x)u_x(x,t) - u(x,t) - u_t(x,t) = \\ -u(x,t-\tau) + 16x^2(1-x)^2, (x,t) \in (0,1)\times(0,2] \\ u(x,t) = 0, \quad (x,t) \in [0,1]\times[-\gamma,0] \\ u(0,t) = 0, u(1,t) = 0, \quad t \in [0,2] \end{cases}$$

In Table 4.1 and Table 4.2, we computed the maximum absolute errors and the corresponding rates of convergence for the developed numerical scheme for Example 4.1. Thus, the results are presented using $\mu = 10^{-3}$ and different values of ε as shown in Table 4.1, and using $\varepsilon = 10^{-3}$ and different values of μ as shown in Table 4.2 with the discretization parameters N and M varying with the same ratio (N and M both multiplied by 2). Here, we see that the rate of convergence of the developed fitted operator finite difference scheme is very close to one(confirm the spatial order). Again, the result in Table 4.3 is computed using $\mu = 10^{-3}$ and different values of ε with the discretization parameters N and M varying with the ratios of 4 and 2 respectively and the rate of convergence is still first order. Table 4.4 shows the comparison of our scheme with the reference cited in Kumar et al. (2020). The comparison confirms that the maximum absolute errors, $Err_{\varepsilon,\mu}^{N,M}$ obtained by our scheme is less than the error obtained by the scheme in Kumar et al. (2020).

For the given Example 4.1 the plotted figures in 4.1 exhibit the boundary layer behavior in the solution of the given problem. Again, the log-log plot in Figure 4.2 supports our theoretical error estimates.

Table 4.1: Maximum absolute errors, $Err_{\varepsilon,\mu}^{N,M}$ and rates of convergence, $Roc^{N,M}$ using scheme (4.9) for Example 4.1 with $\mu = 10^{-3}$ and different values of ε

	N = 32	64	128	256	512
$\varepsilon \downarrow$	M = 8	16	32	64	128
10^{0}	$1.8562e-03$	$9.5156e-04$	$4.8194e-04$	$2.4254e-04$	$1.2167e-04$
	0.9640	0.9814	0.9906	0.9952	-
10^{-2}	$1.9408e-03$	$9.7348e-04$	$4.8751e-04$	$2.4395e-04$	$1.2202e-04$
	0.9954	0.9977	0.9988	0.9995	-
10^{-4}	$1.9417e-03$	$9.7371e-04$	$4.8757e-04$	$2.4396e-04$	$1.2203e-04$
	0.9958	0.9979	0.9990	0.9994	-
10^{-6}	$1.9417e-03$	$9.7371e-04$	$4.8757e-04$	$2.4396e-04$	$1.2203e-04$
	0.9958	0.9979	0.9990	0.9994	-
10^{-8}	$1.9417e-03$	$9.7371e-04$	$4.8757e-04$	$2.4396e-04$	$1.2203e-04$
	0.9958	0.9979	0.9990	0.9994	-
10^{-10}	$1.9417e-03$	$9.7371e-04$	$4.8757e-04$	$2.4396e-04$	$1.2203e-04$
	0.9958	0.9979	0.9990	0.9994	-
10^{-12}	$1.9417e-03$	$9.7371e-04$	$4.8757e-04$	$2.4396e-04$	$1.2203e-04$
	0.9958	0.9979	0.9990	0.9994	-
10^{-14}	$1.9417e-03$	$9.7371e-04$	$4.8757e-04$	$2.4396e-04$	$1.2203e-04$
	0.9958	0.9979	0.9990	0.9994	-
10^{-16}	$1.9417e-03$	$9.7371e-04$	$4.8757e-04$	$2.4396e-04$	$1.2203e-04$
	0.9958	0.9979	0.9990	0.9994	-
$\vdots$	$\vdots$	$\vdots$	$\vdots$	$\vdots$	$\vdots$
10^{-20}	$1.9417e-03$	$9.7371e-04$	$4.8757e-04$	$2.4396e-04$	$1.2203e-04$
	0.9958	0.9979	0.9990	0.9994	-
$Err_{\varepsilon,\mu}^{N,M}$	$1.9417e-03$	$9.7371e-04$	$4.8757e-04$	$2.4396e-04$	$1.2203e-04$
$Roc_{\varepsilon,\mu}^{N,M}$	0.9958	0.9979	0.9990	0.9994	-

Table 4.2: Maximum absolute errors, $Err_{\varepsilon,\mu}^{N,M}$ and rates of convergence, $Roc^{N,M}$ using scheme (4.9) for Example 4.1 with $\varepsilon = 10^{-3}$ and different values of μ

	N = 32	64	128	256	512
$\mu \downarrow$	M = 8	16	32	64	128
10^{0}	$1.9389e-03$	$9.7334e-04$	$4.8752e-04$	$2.4395e-04$	$1.2203e-04$
	0.9942	0.9975	0.9989	0.9993	-
10^{-2}	$1.9417e-03$	$9.7369e-04$	$4.8756e-04$	$2.4396e-04$	$1.2203e-04$
	0.9958	0.9979	0.9989	0.9994	-
10^{-4}	$1.9416e-03$	$9.7369e-04$	$4.8756e-04$	$2.4396e-04$	$1.2203e-04$
	0.9957	0.9979	0.9989	0.9994	-
10^{-6}	$1.9416e-03$	$9.7369e-04$	$4.8756e-04$	$2.4396e-04$	$1.2203e-04$
	0.9957	0.9979	0.9989	0.9994	-
10^{-8}	$1.9416e-03$	$9.7369e-04$	$4.8756e-04$	$2.4396e-04$	$1.2203e-04$
	0.9957	0.9979	0.9989	0.9994	-
10^{-10}	$1.9416e-03$	$9.7369e-04$	$4.8756e-04$	$2.4396e-04$	$1.2203e-04$
	0.9957	0.9979	0.9989	0.9994	-
10^{-12}	$1.9416e-03$	$9.7369e-04$	$4.8756e-04$	$2.4396e-04$	$1.2203e-04$
	0.9957	0.9979	0.9989	0.9994	-
10^{-14}	$1.9416e-03$	$9.7369e-04$	$4.8756e-04$	$2.4396e-04$	$1.2203e-04$
	0.9957	0.9979	0.9989	0.9994	-
10^{-16}	$1.9416e-03$	$9.7369e-04$	$4.8756e-04$	$2.4396e-04$	$1.2203e-04$
	0.9957	0.9979	0.9989	0.9994	-
$\vdots$	$\vdots$	$\vdots$	$\vdots$	$\vdots$	$\vdots$
10^{-20}	$1.9416e-03$	$9.7369e-04$	$4.8756e-04$	$2.4396e-04$	$1.2203e-04$
	0.9957	0.9979	0.9989	0.9994	-
$Err_{\varepsilon,\mu}^{N,M}$	$1.9416e-03$	$9.7369e-04$	$4.8756e-04$	$2.4396e-04$	$1.2203e-04$
$Roc_{\varepsilon,\mu}^{N,M}$	0.9957	0.9979	0.9989	0.9994	-

Table 4.3: Maximum absolute errors, $Err_{\varepsilon,\mu}^{N,M}$ and rates of convergence, $Roc^{N,M}$ using scheme (4.9) for Example 4.1 with $\mu = 10^{-3}$ and different values of ε.

	N = 8	32	128	512
$\varepsilon \downarrow$	M = 8	16	32	64
10^{0}	$6.5420e-03$	$3.5406e-03$	$1.8560e-03$	$9.5155e-04$
	0.8857	0.9318	0.9638	–
10^{-2}	$7.6192e-03$	$3.8573e-03$	$1.9408e-03$	$9.7348e-04$
	0.9820	0.9909	0.9954	–
10^{-4}	$7.6325e-03$	$3.8609e-03$	$1.9417e-03$	$9.7371e-04$
	0.9832	0.9916	0.9958	–
10^{-6}	$7.6325e-03$	$3.8609e-03$	$1.9417e-03$	$9.7371e-04$
	0.9832	0.9916	0.9958	–
10^{-8}	$7.6325e-03$	$3.8609e-03$	$1.9417e-03$	$9.7371e-04$
	0.9832	0.9916	0.9958	–
10^{-10}	$7.6325e-03$	$3.8609e-03$	$1.9417e-03$	$9.7371e-04$
	0.9832	0.9916	0.9958	–
10^{-12}	$7.6325e-03$	$3.8609e-03$	$1.9417e-03$	$9.7371e-04$
	0.9832	0.9916	0.9958	–
10^{-14}	$7.6325e-03$	$3.8609e-03$	$1.9417e-03$	$9.7371e-04$
	0.9832	0.9916	0.9958	–
10^{-16}	$7.6325e-03$	$3.8609e-03$	$1.9417e-03$	$9.7371e-04$
	0.9832	0.9916	0.9958	–
$\vdots$	$\vdots$	$\vdots$	$\vdots$	$\vdots$
10^{-20}	$7.6325e-03$	$3.8609e-03$	$1.9417e-03$	$9.7371e-04$
	0.9832	0.9916	0.9958	–
$Err_{\varepsilon,\mu}^{N,M}$	$7.6325e-03$	$3.8609e-03$	$1.9417e-03$	$9.7371e-04$
$Roc_{\varepsilon,\mu}^{N,M}$	0.9832	0.9916	0.9958	–

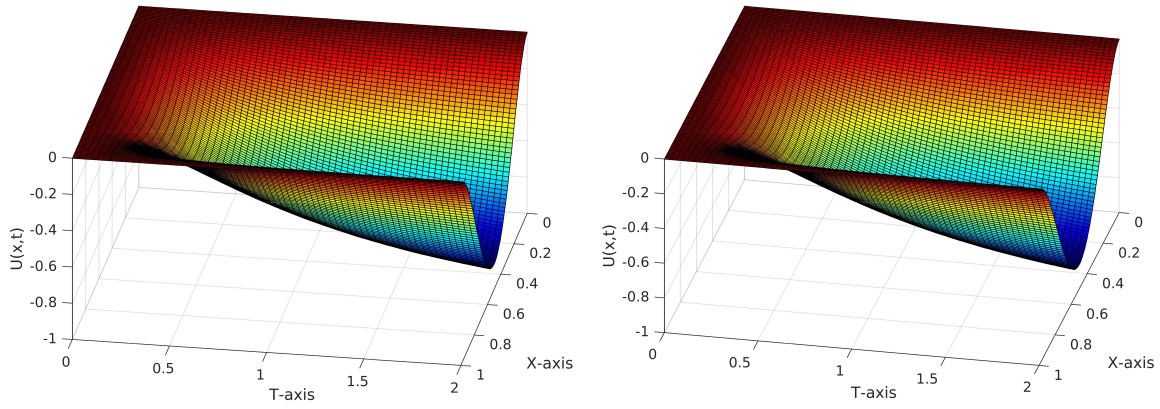

(a) (b)

Figure 4.1: Numerical solution of Example 4.1 for (a) $\mu = 10^{-10}$, $\varepsilon = 10^{-3}$ taking $N = 128$ and $M = 64$, (b) $\mu = 10^{-3}$, $\varepsilon = 10^{-10}$ taking $N = 128$ and $M = 64$

Table 4.4: Comparison of $Err_{\varepsilon,\mu}^{N,M}$ of our scheme in (4.9) with an existing schemes in Kumar et al. (2020) using Example (4.1)

$\mu = 10^{-3}$ $\varepsilon \downarrow$ **Proposed method**	$N = 128$ $M = 32$	$N = 256$ $M = 64$	$N = 512$ $M = 128$
10^{-4}	$4.8757e-04$	$2.4396e-04$	$1.2203e-04$
10^{-6}	$4.8757e-04$	$2.4396e-04$	$1.2203e-04$
10^{-8}	$4.8757e-04$	$2.4396e-04$	$1.2203e-04$
10^{-10}	$4.8757e-04$	$2.4396e-04$	$1.2203e-04$
Scheme in Kumar et al. (2020)			
10^{-4}	$2.4749e-3$	$1.2214e-3$	$6.0706e-4$
10^{-6}	$24437e-3$	$1.2073e-3$	$6,0036e-4$
10^{-8}	$24442e-3$	$1.2071e-3$	$6.0016e-4$
10^{-10}	$2.4442e-3$	$1.2071e-3$	$6.0016e-4$

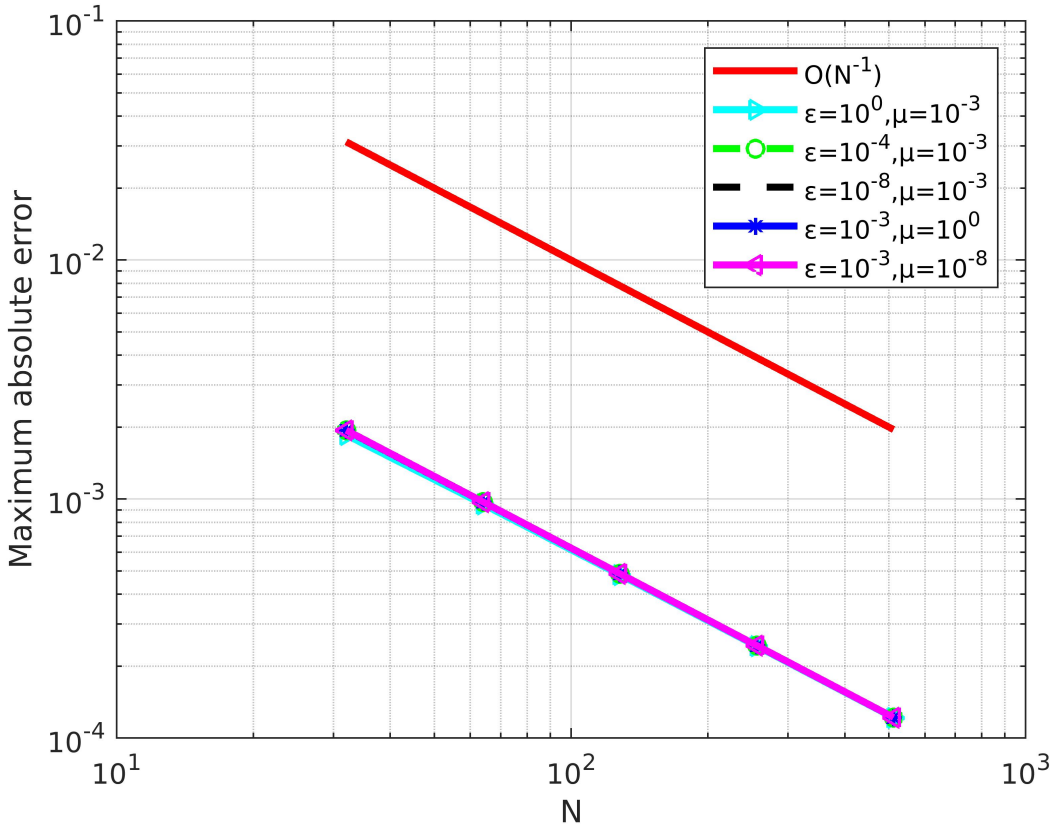

Figure 4.2: Log-Log plot of N vs maximum absolute errors for Example 4.1

4.6 Summary

In this chapter, a fitted operator finite difference method (FOFDM) is developed for solving singularly perturbed time delay partial differential equation with two parameters. In the development of the numerical scheme, the discretization was done by using the implicit Crank-Nicolson finite difference method for the time variable on a uniform mesh, and a fitted operator finite difference (FOFDM) for the space variable on a uniform mesh. The proposed numerical method converges uniformly, regardless of the perturbation parameters ε and μ. Theoretically, the scheme is shown to be first-order in space and second-order in time. To confirm the theoretical convergence results and to demonstrate the applicability of the proposed method, an example has been provided, and results are presented in tables and graphs using Matlab software. The numerical example confirms the theoretical analysis.

CHAPTER 5

ALMOST SECOND ORDER NUMERICAL METHOD FOR TWO-PARAMETER SINGULARLY PERTURBED TIME-DELAY PARABOLIC PROBLEMS

This chapter focuses on singularly perturbed time-delay parabolic convection-reaction-diffusion problems with two small parameters for both smooth and non-smooth data. The study aims to investigate the behavior of the layers in the solution, considering both smooth and non-smooth data. To achieve this, a numerical method is developed based on the Crank-Nicolson scheme for discretizing the time variable on a uniform mesh. Additionally, a hybrid finite difference scheme is employed for the space variable, incorporating central, upwind, and mid-point differencing techniques on a Shishkin-type piecewise uniform mesh. The convergence analysis demonstrates the proposed method exhibits uniform convergence of second order in both space and time. This implies that the numerical solution approaches the true solution with an accuracy proportional to the square of the mesh size. To validate the theoretical findings, numerical experiments are conducted on various test examples. These experiments confirm the theoretical results and show the accuracy and reliability of the approach in capturing the behavior of the boundary layers and providing accurate approximations for the considered problems.

5.1 The governing problem

Define the time-delay parabolic two-parameter SPP on the domain $\bar{D} = D \cup \partial D$, where $D = (0,1) \times (0,T]$ and $\partial D = L_l \cup L_d \cup L_r$ with $L_d = [0,1] \times [-\gamma, 0]$ (delay interval), $L_l = \{0\} \times (0,T]$ (left side boundary) and $L_r = \{1\} \times (0,T]$ (right side boundary) as

$$Lu(x,t) - u_t(x,t) = -c(x,t)u(x,t-\gamma) + f(x,t),\ (x,t) \in D, \tag{5.1}$$

subject to initial boundary data

$$\begin{aligned} u(x,t) &= \Phi_d(x,t),\ \ (x,t) \in L_d, \\ u(0,t) &= \Phi_l(t),\ \ u(1,t) = \Phi_r(t),\ \ t \in [0,T], \end{aligned} \tag{5.2}$$

In the above equations, $Lu(x,t) = \varepsilon u_{xx}(x,t) + \mu a(x,t)u_x(x,t) - b(x,t)u(x,t)$, where $0 < \varepsilon \leq 1$ and $0 \leq \mu \leq 1$ are perturbation parameters, and γ is a delay parameter. The coefficients

$b(x,t)$, $c(x,t)$ for $(x,t) \in \bar{D}$, $a(x,t)$ and $f(x,t)$ (on a given discontinuous interval) and $\Phi_l(t)$, $\Phi_r(t)$, and $\Phi_b(x,t)$ are assumed to be sufficiently regular such that $a(x,t) \geq \alpha > 0$, $b(x,t) \geq \beta > 0$, $c(x,t) \geq \Upsilon > 0$, for all $(x,t) \in \bar{D}$. These conditions ensure that the coefficients are positive and have sufficient regularity properties within the domain D and its boundary. At the corner points of the domain $\bar{D}$, additional compatibility conditions may be required to ensure the well-posedness of the problem. These compatibility conditions arise from the need to match the solutions from different sides of the corner, $(0,0)$ and $(1,0)$. Boundary layers may arise near the boundary region due to the small perturbation parameters ε and μ. Additionally, because of the presence of a jump (discontinuity) in the convection coefficient term $a(x,t)$ and the source term $f(x,t)$ at a point (ξ,ζ) with bounds $|[a](\xi,\zeta)| \leq C$ and $|[f](\xi,\zeta)| \leq C$, the problem (5.1)-(5.2) exhibit an interior layer near the point of discontinuity of the solution $u(x,t)$. The presence of the interior and boundary layers may require special numerical methods or techniques to accurately capture the behavior of the solution in these layer regions. Under these assumptions, the problem (5.1)-(5.2) possesses a unique solution.

5.2 Qualitative properties of the continuous problem

In Chapter 4, Section 4.2, the existence and uniqueness of analytical solutions, as well as the boundedness of their derivatives, are exhaustively discussed. This analysis is supported by Lemma 4.2.1, Lemma 4.2.2, and Lemma 4.2.3. These results provide detailed insights into the properties of the solutions and their derivatives in the context of the problem being investigated.

Remark 5.2.1. *If the convection term $a(x,t)$ and the source term $f(x,t)$ are given by discontinuous intervals, the analytical properties are considered in the defined intervals in convenient way.*

5.3 Derivation of the numerical scheme

In this section, we focus on the derivation of the proposed numerical scheme for solving the governing problem. To discretize the time domain $[0,T]$, we divide it into a uniform mesh. For the sake of simplicity, we choose a parameter γ such that $T = k\gamma$ for some positive integer $k > 1$. We define the collections of mesh points as follows:
D^M: Collection of all mesh points in $[0,T]$, where M is the number of mesh points in the time direction. It is given by $D^M = \{t_j = j\triangle t, j = 0,1,2,\ldots,M, t_M = T, \triangle t = \frac{T}{M}\}$.
D_γ^m: Collection of all mesh points in $[-\gamma,0]$, where m is the number of mesh points in the negative time direction. It is given by $D_\gamma^m = \{t_j = j\triangle t, j = 0,1,2,\ldots,m, t_m = \gamma, \triangle t = \frac{\gamma}{m}\}$.

For the mesh of the space variable, we introduce two transition parameters τ_1 and τ_2 as follows:

$$\tau_1 = \begin{cases} \min\left\{\frac{1}{4}, \frac{4\sqrt{\varepsilon}}{\sqrt{\eta\alpha}}\ln N\right\}, & \text{for } \mu^2 \leq \frac{\eta\varepsilon}{\alpha}, \\ \min\left\{\frac{1}{4}, \frac{4\varepsilon}{\eta\alpha}\ln N\right\}, & \text{for } \mu^2 \geq \frac{\eta\varepsilon}{\alpha}, \end{cases} \quad \tau_2 = \begin{cases} \min\left\{\frac{1}{4}, \frac{4\sqrt{\varepsilon}}{\sqrt{\eta\alpha}}\ln N\right\}, & \text{for } \mu^2 \leq \frac{\eta\varepsilon}{\alpha}, \\ \min\left\{\frac{1}{4}, \frac{4\mu}{\eta}\ln N\right\}, & \text{for } \mu^2 \geq \frac{\eta\varepsilon}{\alpha}, \end{cases}$$

where N is a positive integer and $0 < \tau_1 < \tau_2 < 1$. The interval $[0,1]$ is divided into three subintervals: $[0,\tau_1]$, $[\tau_1, 1-\tau_2]$, and $[1-\tau_2, 1]$. The mesh spacing in each subinterval is defined as follows:

i. In the interval $[0,\tau_1]$, we divide it into $\frac{N}{4}$ subintervals, and the mesh spacing is $h_L = x_i - x_{i-1} = \frac{4\tau_1}{N}$.

ii. In the interval $[\tau_1, 1-\tau_2]$, we divide it into $\frac{N}{2}$ subintervals, and the mesh spacing is $h_M = x_i - x_{i-1} = \frac{2(1-\tau_1-\tau_2)}{N}$.

iii. In the interval $[1-\tau_2, 1]$, we divide it into $\frac{N}{4}$ subintervals, and the mesh spacing is $h_R = x_i - x_{i-1} = \frac{4\tau_2}{N}$.

Using each mesh spacing, the mesh points in the space variable are denoted by $\bar{\Lambda}^N = \{x_i\}_{i=1}^N$, where $i = 0, 1, \ldots, N$. The expression for x_i is given by:

$$x_i = \begin{cases} ih_L, & \text{for } 0 \leq i \leq \frac{N}{4}, \\ \tau_1 + (i - \frac{N}{4})h_M, & \text{for } \frac{N}{4} < i \leq \frac{3N}{4}, \\ (1-\tau_2) + (i - \frac{3N}{4})h_R, & \text{for } \frac{3N}{4} < i \leq N. \end{cases}$$

In addition to the mesh points in the space variable, we define two quantities related to the mesh spacing. Let $h_i = x_i - x_{i-1}$ for $i = 1, \ldots, N$, which represents the mesh spacing between consecutive points x_{i-1} and x_i. Furthermore, we introduce $\hbar_i$, defined as the average of h_i and h_{i+1}, given by $\hbar_i = \frac{h_i + h_{i+1}}{2}$ for $i = 1, \ldots, N-1$.

To discretize the boundary data and boundary conditions domains, the domain is divided into three sets: $L_d^{N,M}$, $L_l^{N,M}$, and $L_r^{N,M}$, which represent the boundary data points, left boundary points, and right boundary points, respectively, as follows:

i. $L_d^{N,M} = \bar{D}^N \times \bar{D}^m$: This set consists of all mesh points in the spatial and delay interval, and $\bar{D}^m$ denotes the uniform time mesh in $[-\gamma, 0]$ with M mesh points.

ii. $L_l^{N,M} = \bar{D}^N \cap L_l$: This set consists of the mesh points in the spatial direction that lie on the left boundary of the domain. It represents the part of the discretized domain where the left boundary conditions are applied.

iii. $L_r^{N,M} = \bar{D}^N \cap L_r$: This set consists of the mesh points in the spatial direction that lie on the right boundary of the domain. It represents the part of the discretized domain where the right boundary conditions are applied.

To divide the discretized domain into sub-domains, we introduce k sub-domains denoted by $\bar{D}_r^{M,N}$, representing the mesh points within each interval of the time domain. The domain is divided into sub-domains as follows:

$$\bar{D}^{N,M} = \bar{D}^N \times \bar{D}_1^M \cup \bar{D}^N \times \bar{D}_2^M \cup \ldots \cup \bar{D}^N \times \bar{D}_k^M = \bigcup_{r=1}^{k} \bar{D}_r^{M,N}$$

Here, $\bar{D}_r^M$ represents the mesh points in the time direction corresponding to the interval $[(r-1)\gamma, r\gamma]$. It consists of $M+1$ uniform mesh points within each interval and is used for the method of steps.

After generating the rectangular grid, a finite difference method is developed, which employs a hybrid scheme consisting of the Crank-Nicolson discretization for the time variable and a combination of the central difference, upwind, and mid-point schemes for the spatial direction. To derive the Crank-Nicolson scheme in the temporal direction, Taylor's series expansion is applied to $U_t(x_i, t_j)$ at the point $(x_i, t_{j+1/2})$ as follows.

$$U_i^{j+1} = U_i^{j+1/2} + \frac{\Delta t}{2}\frac{\partial U_i^{j+1/2}}{\partial t} + \left(\frac{\Delta t}{2}\right)^2 \frac{1}{2!}\frac{\partial^2 U_i^{j+1/2}}{\partial t^2} + \left(\frac{\Delta t}{2}\right)^3 \frac{1}{3!}\frac{\partial^3 U_i^{j+1/2}}{\partial t^3} + \ldots \quad (5.3)$$

$$U_i^{j} = U_i^{j+1/2} - \frac{\Delta t}{2}\frac{\partial U_i^{j+1/2}}{\partial t} + \left(\frac{\Delta t}{2}\right)^2 \frac{1}{2!}\frac{\partial^2 U_i^{j+1/2}}{\partial t^2} - \left(\frac{\Delta t}{2}\right)^3 \frac{1}{3!}\frac{\partial^3 U_i^{j+1/2}}{\partial t^3} + \ldots \quad (5.4)$$

By subtracting Equation 5.3 from Equation 5.4, the term $U_i^{j+1/2}$ is eliminated, and the resulting expression is

$$\frac{\partial U_i^{j+1/2}}{\partial t} = \frac{U_i^{j+1} - U_i^{j}}{\Delta t} + T_i^{j+1/2}$$

In this equation, $T_i^{j+1/2}$ represents the local truncation error of the scheme, which is given by:

$$T^{j+1/2}(x) = \frac{(\Delta t)^3}{24}\frac{\partial^3 U^{j+1/2}(x)}{\partial t^3} + H.O.Ts \text{ (higher-order terms)} \quad (5.5)$$

The truncation error has an order of three, indicating that the error introduced by the scheme is proportional to $(\Delta t)^3$. Now, utilizing the previously mentioned discretizations in the tem-

poral direction, we can express the hybrid scheme as follows:

$$\begin{aligned}
\left[L_{\text{cen}}^{N,M}U_i^j\right] &= \frac{1}{2}\left[\varepsilon\delta_x^2U_i^{j+1}+\mu a_i^{j+1}D_x^0U_i^{j+1}-b_i^{j+1}U_i^{j+1}+\varepsilon\delta_x^2U_i^j+\mu a_i^jD_x^0U_i^j-b_i^jU_i^j\right]-D_tU_i^{j+1/2}\\
\left[L_{\text{up}}^{N,M}U_i^j\right] &= \frac{1}{2}\left[\varepsilon\delta_x^2U_i^{j+1}+\mu a_i^{j+1}D_x^+U_i^{j+1}-b_i^{j+1}U_i^{j+1}+\varepsilon\delta_x^2U_i^j+\mu a_i^jD_x^+U_i^j-b_i^jU_i^j\right]-D_tU_i^{j+1/2}\\
\left[L_{mp}^{N,M}U_i^j\right] &= \frac{1}{2}\left[\varepsilon\delta_x^2U_i^{j+1}+\mu\bar{a}_i^{j+1}D_x^+U_i^{j+1}-\bar{b}_i^{j+1}U_i^{j+1}+\varepsilon\delta_x^2U_i^j+\mu\bar{a}_i^jD_x^+U_i^j-\bar{b}_i^jU_i^j\right]-\overline{D_tU_i^{j+1/2}}
\end{aligned} \tag{5.6}$$

where the following definitions apply:

$$D_x^+U_i^j=\frac{U_{i+1}^j-U_i^j}{h_{i+1}},\quad D_x^0U_i^j=\frac{U_{i+1}^j-U_{i-1}^j}{2\hbar_i},\quad D_tU_i^{j+1/2}=\frac{U_i^{j+1}-U_i^j}{\Delta t}$$
$$\delta_x^2U_i^j=\frac{1}{\hbar_i}\left(\frac{U_{i+1}^j-U_i^j}{h_{i+1}}-\frac{U_i^j-U_{i-1}^j}{h_i}\right),\quad \overline{U_i^j}=\frac{U_i^j+U_{i+1}^j}{2}$$

Further, let's define $\hat{b}=b+\dfrac{1}{\Delta t}$. Then, the discretized form of problem (5.6) takes the following form:

$$\begin{aligned}
L^{N,M}=\overset{+}{\sigma}_iU_{i+1}^j+\overset{c}{\sigma}iU_i^j+\overset{-}{\sigma}iU_{i-1}^j+\overset{++}{\sigma}iU_{i+1}^{j+1}+\overset{cc}{\sigma}iU_i^{j+1}+\overset{--}{\sigma}iU_{i-1}^{j+1}=\\
F_i^j\left(x_i,t_j\right)\in D^{N,M},\\
U_i^j=u\left(x_i,t_j\right),\left(x_i,t_j\right)\in\partial D^{N,M}
\end{aligned} \tag{5.7}$$

Where

$$\left[L^{N,M}U\right]i^j=\begin{cases}
\left[L\text{cen}^{\,N,M}U_i^j\right], & \text{if } 1\le i<N/4,\\
\left[L\text{cen}^{\,N,M}U_i^j\right], & \text{if } N/4<i<3N/4 \text{ and } \mu hM|a|<2\varepsilon,\\
\left[L_{\text{mp}}^{N,M}U_i^j\right], & \text{if } N/4<i<3N/4,\mu hM|a|\ge 2\varepsilon \text{ and } hM|\hat{b}|<2\mu\alpha,\\
\left[L\text{up}^{\,N,M}U_i^j\right], & \text{if } N/4<i<3N/4,\mu hM|a|\ge 2\varepsilon \text{ and } hM|\hat{b}|\ge 2\mu\alpha,\\
\left[L\text{cen}^{\,N,M}U_i^j\right], & \text{if } 3N/4<i<N \text{ and } \mu hR|a|<2\varepsilon,\\
\left[L_{\text{mp}}^{N,M}U_i^j\right], & \text{if } 3N/4<i<N \text{ and } \mu hR|a|\ge 2\varepsilon
\end{cases} \tag{5.8}$$

For the left transition point $x_i=\tau_1=0.25$, the left layer region will be $[0,\ 0.25]$. The hybrid scheme at $x_i=\tau_1$ is given by:

$$\left[L^{N,M}U_i^j\right] = \begin{cases} \left[L\text{cen}^{\,N,M}U_i^j\right], & \text{if } \tau_1 = 0.25, \\ \left[L_{\text{mp}}^{N,M}U_i^j\right], & \text{if } \tau_1 < 0.25 \text{ and } hM|\hat{b}| < 2\mu\alpha, \\ \left[L\text{up}^{N,M}U_i^j\right], & \text{otherwise} \end{cases} \tag{5.9}$$

Similarly, for the right transition point $x_i = \tau_2$ such that $1-\tau_2 = 0.75$, the right layer region will be $[1-\tau_2, 1] = [0.75, 1]$. At $x_i = 1-\tau_2 = 0.75$, we have the following hybrid scheme:

$$\left[L^{N,M}U_i^j\right] = \begin{cases} \left[L_{\text{cen}}^{N,M}U_i^j\right], & \text{if } 1-\tau_2 = 0.75, \text{ and } \mu h_R\|a\| < 2\varepsilon, \\ \left[L_{\text{mp}}^{N,M}U_i^j\right], & \text{if } 1-\tau_2 = 0.75, \text{ and } \mu h_R\|a\| \geq 2\varepsilon, \\ \left[L_{\text{mp}}^{N,M}U_i^j\right], & \text{if } 1-\tau_2 > 0.75, \text{ and } h_R\|\hat{b}\| < 2\mu\alpha, \\ \left[L_{\text{up}}^{N,M}U_i^j\right], & \text{otherwise,} \end{cases} \tag{5.10}$$

and

$$F_i^j = \begin{cases} \dfrac{\Delta t}{2}\left[-c_i^{j+1}U_i^{j-m+1} + f_i^{j+1} + -c_i^jU_i^{j-m} + f_i^j\right], & \text{if } L^{N,M} = L_{\text{cen}}^{N,M} \text{ or } L_{up}^{N,M}, \\ \dfrac{\Delta t}{2}\left[\overline{-c_i^{j+1}U_i^{j-m+1}} + \overline{f_i^{j+1}} + \overline{-c_i^jU_i^{j-m}} + \overline{f_i^j}\right], & \text{if } L^{N,M} = L_{\text{mp}}^{N,M}. \end{cases} \tag{5.11}$$

with

$$-c_i^jU_i^{j-m} = \begin{cases} \underbrace{-c_i^j\Phi_i^{j-m}}_{j\in[0,\,m]} \textbf{ or } \underbrace{-c_i^jU_i^{j-m}}_{j\in[m+1,\,M]} \\ \overline{\underbrace{-c_i^j\Phi_i^{j-m}}_{j\in[0,\,m]}} \textbf{ or } \overline{\underbrace{-c_i^jU_i^{j-m}}_{j\in[m+1,\,M]}} \end{cases}$$

and the elements in the system of the matrix $L^{N,M}_{\varepsilon,\mu}$ of (5.7) are as follows

$$\overset{+}{\sigma}_i = \frac{\triangle t\varepsilon}{2h_{i+1}\hbar_i} + \frac{\triangle t\mu a_i^j}{4\hbar_i}, \quad \overset{c}{\sigma}_i = \frac{-\triangle t\varepsilon}{2h_{i+1}\hbar_i} - \frac{\triangle t\varepsilon}{2h_i\hbar_i} - \frac{\triangle t}{2}b_i^j + 1, \quad \overset{-}{\sigma}_i = \frac{\triangle t\varepsilon}{2h_{i+1}\hbar_i} - \frac{\triangle t\mu a_i^j}{4\hbar_i},$$
$$\text{if } L^{N,M} \equiv L^{N,M}_{cd},$$
$$\overset{+}{\sigma}_i = \frac{\triangle t\varepsilon}{2h_{i+1}\hbar_i} + \frac{\triangle t\mu a_i^j}{2h_{i+1}}, \quad \overset{c}{\sigma}_i = \frac{-\triangle t\varepsilon}{2h_{i+1}\hbar_i} - \frac{\triangle t\varepsilon}{2h_i\hbar_i} - \frac{\triangle t\mu a_i^j}{2h_{i+1}} - 0.5\triangle t b_i^j + 1, \quad \overset{-}{\sigma}_i = \frac{-\triangle t\varepsilon}{h_i\hbar_i},$$
$$\text{if } L^{N,M} \equiv L^{N,M}_{up},$$
$$\overset{+}{\sigma}_i = \frac{\triangle t\varepsilon}{h_{i+1}\hbar_i} + \frac{\triangle t\mu a_{i+1/2}^j}{h_{i+1}} - 0.5\triangle t b_{i+1/2}^j + 1, \quad \overset{c}{\sigma}_i = \frac{-\triangle t\varepsilon}{h_{i+1}\hbar_i} - \frac{\triangle t\varepsilon}{h_i\hbar_i} - \frac{\triangle t\mu a_{i+1/2}^j}{h_{i+1}} - 0.5\triangle t b_{i+1/2}^j + 1,$$
$$\overset{-}{\sigma}_i = \frac{\triangle t\varepsilon}{h_i\hbar_i}, \quad \text{if } L^{N,M} \equiv L^{N,M}_{mp},$$
$$\overset{++}{\sigma}_i = \frac{-\triangle t\varepsilon}{2h_{i+1}\hbar_i} + \frac{-\triangle t\mu a_i^{j+1}}{4\hbar_i}, \overset{cc}{\sigma}_i = \frac{\triangle t\varepsilon}{2h_{i+1}\hbar_i} + \frac{\triangle t\varepsilon}{2h_i\hbar_i} + \frac{\triangle t}{2}b_i^{j+1} + 1, \overset{--}{\sigma}_i = \frac{-\triangle t\varepsilon}{2h_{i+1}\hbar_i} + \frac{\triangle t\mu a_i^{j+1}}{24\hbar_i},$$
$$\text{if } L^{N,M} \equiv L^{N,M}_{cd},$$
$$\overset{++}{\sigma}_i = \frac{-\triangle t\varepsilon}{2h_{i+1}\hbar_i} - \frac{\triangle t\mu a_i^{j+1}}{2h_{i+1}}, \overset{cc}{\sigma}_i = \frac{\triangle t\varepsilon}{2h_{i+1}\hbar_i} + \frac{\triangle t\varepsilon}{2h_i\hbar_i} + \frac{\triangle t\mu a_i^{j+1}}{2h_{i+1}} + \frac{\triangle t}{2}b_i^{j+1} + 1, \overset{--}{\sigma}_i = \frac{\triangle t\varepsilon}{h_i\hbar_i},$$
$$\text{if } L^{N,M} \equiv L^{N,M}_{up},$$
$$\overset{++}{\sigma}_i = \frac{-\triangle t\varepsilon}{h_{i+1}\hbar_i} - \frac{\triangle t\mu a_{i+1/2}^{j+1}}{h_{i+1}} + \triangle t b_{i+1/2}^{j+1} + 1, \overset{cc}{\sigma}_i = \frac{\triangle t\varepsilon}{h_{i+1}\hbar_i} + \frac{\triangle t\varepsilon}{h_i\hbar_i} + \frac{\triangle t\mu a_{i+1/2}^{j+1}}{h_{i+1}} + 0.5\triangle t b_{i+1/2}^j + 1,$$
$$\overset{--}{\sigma}_i = \frac{-\triangle t\varepsilon}{h_i\hbar_i} \quad \text{if } L^{N,M} \equiv L^{N,M}_{mp},$$

5.4 Boundedness of discrete solution and error analysis

Lemma 5.4.1 (**Discrete minimum principle**). *The discretized form in (5.7) satisfies the discrete minimum principle, that is if for any mesh function φ with $\varphi_i^j\Big|_{\partial D^{N,M}} \geq 0$ and $\left[L^{N,M}\varphi\right]_i^j\Big|_{D^{N,M}} \leq 0$, then $\varphi_i^j\Big|_{\bar{D}^{N,M}} \geq 0$.*

Proof. In the proof of the discrete minimum principle Lemma, we consider the matrix formed by the proposed difference scheme (5.7). By examining the entries of the tridiagonal system matrix of the scheme (5.7), we can verify that it is a negative **M**-matrix. A negative **M**-matrix is a matrix where the off-diagonal entries are non-positive, and the row sums are non-negative with at least one row having a strictly positive sum. This property ensures that the matrix is invertible and that its inverse is non-negative. Since the difference operator $L^{N,M}$ is represented by a negative **M**-matrix, it satisfies the discrete minimum principle. This implies that if the mesh function φ satisfies the conditions $\varphi_i^j\Big|_{\partial D^{N,M}} \geq 0$ and $\left[L^{N,M}\varphi_i^j\right]\Big|_{D^{N,M}} < 0$, then the solution φ will be non-negative throughout the entire domain $\bar{D}^{N,M}$. ■

This discrete minimum principle is an important property that ensures that the numerical solution obtained using the discretization scheme (5.7) does not produce negative values

when the exact solution is non-negative and the source term is non-positive. It guarantees the preservation of positivity in the numerical solution.

5.4.1 Error analysis

The given decomposition of the discrete solution U is expressed as:

$$U = V + W_L + W_R, \tag{5.12}$$

where

$$\begin{cases} \left[L^{N,M}V\right]_i^j = -c_i^j V_i^{j-m} + f_i^j, & \left(x_i,t_j\right) \in D^{N,M} \\ V_i^j\Big|_{\partial D^{N,M}} = v\left(x_i,t_j\right), \end{cases} \tag{5.13}$$

$$\begin{cases} \left[L^{N,M}W_L\right]_i^j = -c_i^j \left(W_L\right)_i^{j-m}, & \left(x_i,t_j\right) \in D^{N,M} \\ \left(W_L\right)_i^j\Big|_{\partial D^{N,M}} = w_L\left(x_i,t_j\right), \end{cases} \tag{5.14}$$

$$\begin{cases} \left[L^{N,M}W_R\right]_i^j = -c_i^j \left(W_L\right)_i^{j-m}, & \left(x_i,t_j\right) \in D^{N,M} \\ \left(W_R\right)_i^j\Big|_{\partial D^{N,M}} = w_R\left(x_i,t_j\right) \end{cases} \tag{5.15}$$

where V, W_L, and W_R represent different components of the solution. Let's examine each component in more detail:

V satisfies the same equation as the original problem defined by equation (5.13). In this equation, $\left[L^{N,M}V\right]_i^j$ represents the discrete operator applied to V at grid point (i,j), and it is equal to $-c_i^j V_i^{j-m} + f_i^j$. Here, c_i^j and f_i^j are coefficients or source terms associated with the original equation. The equation is valid for grid points (x_i,t_j) within the domain $D^{N,M}$, and the boundary condition $V_i^j\Big|_{\partial D^{N,M}} = v\left(x_i,t_j\right)$ is imposed on the boundary of the domain.

W_L satisfies a similar equation as V, but with different boundary conditions. Equation (5.14) defines the equation for W_L, where $\left[L^{N,M}W_L\right]_i^j$ represents the discrete operator applied to W_L at grid point (i,j), and it is equal to $-c_i^j \left(W_L\right)_i^{j-m}$. The boundary condition for W_L is given by $\left(W_L\right)_i^j\Big|_{\partial D^{N,M}} = w_L\left(x_i,t_j\right)$.

Similarly, W_R satisfies an equation similar to V and W_L, but with a different set of boundary conditions. Equation (5.15) defines the equation for W_R, where $\left[L^{N,M}W_R\right]_i^j$ represents the discrete operator applied to W_R at grid point (i,j), and it is equal to $-c_i^j \left(W_L\right)_i^{j-m}$. The boundary condition for W_R is given by $\left(W_R\right)_i^j\Big|_{\partial D^{N,M}} = w_R\left(x_i,t_j\right)$.

By decomposing the discrete solution U into the components V, W_L, and W_R as shown in equations (5.13), (5.14), and (5.15), respectively, we can study and analyze the behavior

and properties of each component individually, which can help in understanding the overall solution.

The given excerpt introduces an error decomposition for the numerical solution U and the analytical solution u of the problem. The error decomposition is expressed as follows:

$$[U-u]_i^j = [V-v]_i^j + [W_L - w_L]_i^j + [W_R - w_R]_i^j \text{ for all } \left(x_i, t_j\right) \in \bar{\Omega}^{N,M}$$

In this expression, the error $[U-u]_i^j$ at a specific grid point (x_i, t_j) is decomposed into three components:

1. $[V-v]_i^j$ represents the error introduced by the finite difference scheme in space and time. This component captures the discrepancy between the numerical solution V and the analytical solution v in the interior of the domain.

2. $[W_L - w_L]_i^j$ represents the error associated with the left boundary of the domain. This component captures the discrepancy between the numerical solution at the left boundary, denoted as W_L, and the corresponding value of the analytical solution at the left boundary, denoted as w_L.

3. $[W_R - w_R]_i^j$ represents the error associated with the right boundary of the domain. This component captures the discrepancy between the numerical solution at the right boundary, denoted as W_R, and the corresponding value of the analytical solution at the right boundary, denoted as w_R.

Lemma 5.4.2. *For functions $s = v, w_L, w_R$ defined on $\bar{\Omega}$ and $S = V, W_L, W_R$ defined on $\bar{D}^{N,M}$, a. the local truncation error is defined as:*

$$\left[L^{N,M}(S-s)\right]_i^j = -c_i^j [S-s]_i^{j-m} + \left[\left(L_{\varepsilon,\mu} - \frac{\partial}{\partial t}\right) s - L^{N,M} s\right]_i^j$$

where $[S-s]_i^{j-m}$ represents the difference between the values of S and s at the mesh point $(x_i, t_j - m)$, and c_i^j is a coefficient. On an arbitrary mesh size h_i:

$$\begin{aligned}
&\left|\left[L_{cen}^{N,M}(S-s)\right]_i^j\right| \leq \left|[S-s]_i^{j-m}\right| + C\left[\varepsilon \hbar_i \|s_{xxx}\| + \mu \hbar_i \|s_{xx}\| + M^{-2}\|s_{tt}\|\right] \\
&\left|\left[L_{up}^{N,M}(S-s)\right]_i^j\right| \leq \left|[S-s]_i^{j-m}\right| + C\left[\varepsilon \hbar_i \|s_{xxx}\| + \mu h_{i+1} \|s_{xx}\| + M^{-2}\|s_{tt}\|\right] \\
&|\left[L_{mp}^{N,M}(S-s)\right]_i^j| \leq |[S-s]_i^{j-m}| + C\left[\varepsilon \hbar_i \|s_{xxx}\| + \mu h_{i+1}^2 \left(\|s_{xxx}\| + \|s_{xx}\|\right) + M^{-2}\|s_{tt}\|\right]
\end{aligned}$$

On a uniform mesh size h:

$$
\begin{aligned}
&| L_{cen}^{N,M}(S-s)\Big]_i^j | \leq |[S-s]_i^{j-m} | + C\left[\varepsilon h^2 \|s_{xxxx}\| + \mu h^2 \|s_{xxx}\| + M^{-2}\|s_{tt}\|\right], \\
&\left|\left[L_{up}^{N,M}(S-s)\right]_i^j\right| \leq \left|[S-s]_i^{j-m}\right| + C\left[\varepsilon h^2 \|s_{xxxx}\| + \mu h \|s_{xx}\| + M^{-2}\|s_{tt}\|\right], \\
&\left|\left[L_{mp}^{N,M}(S-s)\right]_i^j\right| \leq \left|[S-s]_i^{j-m}\right| + C\left[\varepsilon h \|s_{xxx}\| + \mu h^2 \left(\|s_{xxx}\| + \|s_{xx}\|\right) + M^{-2}\|s_{tt}\|\right].
\end{aligned}
$$

In these bounds, ε, μ, M, and C are constants, and $\hbar_i$ represents the step size in the spatial direction. The bounds for the local truncation error differ on an arbitrary mesh compared to a uniform mesh in terms of the terms involving spatial derivatives. Here's a breakdown of the key differences:
On an arbitrary mesh: - The bounds involve terms $\hbar_i$ and h_{i+1}, which represent the step sizes in the spatial direction at different mesh points. These step sizes can vary at different locations in the mesh. - The terms $\varepsilon\hbar_i\|s_{xxx}\|$, $\mu\hbar_i\|s_{xx}\|$, and $\mu h_{i+1}^2(\|s_{xxx}\| + \|s_{xx}\|)$ appear in the bounds, indicating the impact of spatial derivatives on the local truncation error estimation. - The terms $\|s_{tt}\|$ and M^{-2} are also present, representing the impact of second-order time derivatives and the inverse of the square of the mesh size in the temporal direction on the local truncation error.
On a uniform mesh: - The bounds involve a single step size h that is uniform throughout the mesh. - The terms $\varepsilon h^2\|s_{xxxx}\|$, $\mu h^2\|s_{xxx}\|$, and $\mu h(\|s_{xx}\|)$ appear in the bounds, indicating the influence of spatial derivatives on the local truncation error estimation. - The terms $\|s_{tt}\|$ and M^{-2} are also present, representing the impact of second-order time derivatives and the inverse of the square of the mesh size in the temporal direction on the local truncation error.
b. The error bound for the smooth component is

$$
\left|[V-v]_i^j\right| \leq C\left(M^{-2}+N^{-2}\right).
$$

c. The error bounds on the singular components(the layer components) satisfy

$$
\begin{aligned}
&\left|(W_L)_i^j\right| \leq CN^{-2}, \quad i = N/4,\ldots,N, j\Delta t \leq \gamma, \\
&\left|(W_R)_i^j\right| \leq CN^{-2}, \quad i = 0,\ldots,3N/4, j\Delta t \leq \gamma.
\end{aligned}
$$

Proof. The detailed proof is in Sumit et al. (2020). ■

By using the idea in *b* and *c* of lemma 5.4.2, we have obtained the following main result.

Theorem 5.4.1 (Main result). *Let U_i^{j+1} and $u(x_i,t_{j+1})$ be the numerical solution and the continuous solution of the problem in (4.1) - (4.2). Then,*

$$\sup_{\varepsilon,\mu}\left[\max_{0\le i\le N,0\le j\le M}\left|u(x_i,t_{j+1})-U_i^{j+1}\right|_{\bar{D}}^{N,M}\right]\le\begin{cases} C\left(M^{-2}+N^{-2}(\ln N)^2\right), & \text{when } \alpha\mu^2\le\eta\varepsilon \\ C\left(M^{-2}+N^{-2}(\ln N)^2\right), & \text{when } \alpha\mu^2\ge\eta\varepsilon \end{cases}$$

5.5 Numerical results and discussion

To confirm the efficiency of the proposed method, we consider test problems with smooth and non-smooth data. We present the numerical results on a uniform mesh as well as on a non-uniform mesh of Shishkin type. The maximum absolute errors and the numerical rate of convergence are computed using the double mesh principle Doolan et al. (1980) due to the unavailability of the analytical solution. Results are compared with some methods.
The maximum absolute error is given by

$$Err_{\varepsilon,\mu}^{N,M}=\max_{0\le i,j\le N,M}\left|U^{N,M}(x_i,\,t_j)-U^{2N,2M}(x_{2i},\,t_{2j})\right|$$

and the rate of convergence by the formula

$$Roc_{\varepsilon,\mu}^{N,M}=\log_2\left(\frac{Err_{\varepsilon,\mu}^{N,M}}{Err_{\varepsilon,\mu}^{2N,2M}}\right)$$

To investigate the applicability of the developed scheme in (5.7), the following two test examples with smooth data are considered:

Example 5.1.

$$\begin{cases} \varepsilon u_{xx}(x,t)+\mu(1+x)u_x(x,t)-u(x,t)-u_t(x,t)= \\ -u(x,t-\gamma)+16x^2(1-x)^2,(x,t)\in(0,1)\times(0,2] \\ u(x,t)=0,\quad (x,t)\in[0,1]\times[-\tau,0] \\ u(0,t)=0,u(1,t)=0,\quad t\in[0,2] \end{cases}$$

Example 5.2.

$$\begin{cases} \varepsilon u_{xx}(x,t)+\mu\left(1+x(1-x)+t^2\right)u_x(x,t)-(1+5xt)u(x,t) \\ -u_t(x,t)=-u(x,t-\gamma)+x(1-x)\left(e^t-1\right),\quad (x,t)\in(0,1)\times(0,2] \\ u(x,t)=0,\quad (x,t)\in[0,1]\times[-\tau,0] \\ u(0,t)=0,u(1,t)=0,\quad t\in(0,2] \end{cases}$$

We consider the following two-parameter singularly perturbed time delay parabolic problem for our third and fourth examples. This problem involves a non-smooth convection coefficient term $a(x,t)$ and a source term $f(x,t)$ in (5.1)-(5.2), as described in Chandru et al.

(2018).

Example 5.3.

$$a(x,t)=\begin{cases}-(1+e^{-xt}),0\le x\le 0.5,\\ 2+x+t,0.5<x\le 1,\end{cases}\qquad f(x,t)=\begin{cases}\left(e^{t^2}-1\right)(1+xt),0\le x\le 0.5\\ -(2+x)t^2,0.5<x\le 1\end{cases}$$
$$b(x,t)=2+xt,\ c(x,t)=1,\ \text{and}\quad u(0,t)=u(1,t)=u(x,0)=0$$

Example 5.4.

$$a(x,t)=\begin{cases}1+x(1-x)+t,0\le x\le 0.5,\\ -(1+3xt),0.5<x\le 1,\end{cases}\qquad f(x,t)=\begin{cases}(1+x)\left(e^t-1\right),0\le x\le 0.5,\\ (-2+x)t,0.5<x\le 1,\end{cases}$$
$$b(x,t)=1+x+t,\ c(x,t)=1,\ \text{and}\quad u(0,t)=u(1,t)=u(x,0)=0.$$

We utilized scheme (5.7) to obtain the numerical solutions for the given test examples, as the analytical solutions are not available in closed form. The results are presented in Table 5.1-Table 5.9, corresponding to Example 5.1- Example 5.4.

For Example 5.1, the numerical implementation results are shown in Table 5.1 and Table 5.2. The experimental results for Example 5.2 are displayed in Table 5.3 and Table 5.4. Both examples demonstrate that our scheme (5.7) achieves uniform convergence with a second order in both variables, regardless of the perturbation parameters.

Tables 5.6 and 5.7 present the numerical solution of the test problem in Example 5.3, while Tables 5.8 and 5.9 present the obtained numerical results of Example 5.4. In both examples, the convection and source terms contain non-smooth data. As a result, the solutions to these problems exhibit interior layers and boundary layers, as illustrated in Figures 5.3 and 5.4. Once again, our scheme (5.7) demonstrates uniform convergence with a second order in both variables, as supported by the numerical results of Examples 5.3 and 5.4.

To compare our proposed scheme with the existing scheme in Sumit et al. (2020), we refer to Table 5.5. The comparison reveals that our scheme exhibits a lower maximum point-wise error compared to the scheme in Sumit et al. (2020). This indicates that our scheme is more accurate.

In all of our test examples, the errors remain independent of the perturbation parameters. This confirms that the present method is parameter-uniform. The uniform convergence is further supported by the log-log plots in Figures 5.3 and 5.4.

Examples 5.1 and 5.2 feature smooth data in the convection coefficient and source term, resulting in boundary layers near the boundary regions. On the other hand, Examples 5.3 and 5.4 involve non-smooth data with discontinuities in the convection coefficient and source

term. Due to this non-smoothness, the solutions exhibit both interior layers and boundary layers, as depicted graphically in Figures 5.3 and 5.4. The theoretical behavior of the numerical solutions is supported by Figures 5.1-5.4.

Table 5.1: Maximum absolute errors, $Err_{\varepsilon,\mu}^{N,M}$ and rates of convergence, $Roc_{\varepsilon,\mu}^{N,M}$ using scheme (5.7) for Example 5.1 with $\mu = 10^{-3}$ and different values of ε.

	N $\rightarrow$	32	64	128	256	512
$\varepsilon \downarrow$	M $\rightarrow$	8	16	32	64	128
10^{0}	$Err_{\varepsilon,\mu}^{N,M} \rightarrow$	7.1784e-04	1.8213e-04	4.5704e-05	1.1437e-05	2.8598e-06
	$Roc_{\varepsilon,\mu}^{N,M} \rightarrow$	1.9787	1.9946	1.9986	1.9997	-
10^{-2}	$Err_{\varepsilon,\mu}^{N,M} \rightarrow$	5.6025e-03	1.4060e-03	3.5184e-04	8.7980e-05	2.1996e-05
	$Roc_{\varepsilon,\mu}^{N,M} \rightarrow$	1.9945	1.9986	1.9997	1.9999	-
10^{-4}	$Err_{\varepsilon,\mu}^{N,M} \rightarrow$	5.8291e-03	1.4625e-03	3.6596e-04	9.1510e-05	2.2879e-05
	$Roc_{\varepsilon,\mu}^{N,M} \rightarrow$	1.9948	1.9987	1.9997	1.9999	-
10^{-6}	$Err_{\varepsilon,\mu}^{N,M} \rightarrow$	5.8314e-03	1.4631e-03	3.6611e-04	9.1547e-05	2.2888e-05
	$Roc_{\varepsilon,\mu}^{N,M} \rightarrow$	1.9948	1.9987	1.9997	1.9999	-
10^{-8}	$Err_{\varepsilon,\mu}^{N,M} \rightarrow$	5.8314e-03	1.4631e-03	3.6611e-04	9.1547e-05	2.2888e-05
	$Roc_{\varepsilon,\mu}^{N,M} \rightarrow$	1.9948	1.9987	1.9997	1.9999	-
10^{-10}	$Err_{\varepsilon,\mu}^{N,M} \rightarrow$	5.8314e-03	1.4631e-03	3.6611e-04	9.1547e-05	2.2888e-05
	$Roc_{\varepsilon,\mu}^{N,M} \rightarrow$	1.9948	1.9987	1.9997	1.9999	-
10^{-12}	$Err_{\varepsilon,\mu}^{N,M} \rightarrow$	5.8314e-03	1.4631e-03	3.6611e-04	9.1547e-05	2.2888e-05
	$Roc_{\varepsilon,\mu}^{N,M} \rightarrow$	1.9948	1.9987	1.9997	1.9999	-
10^{-14}	$Err_{\varepsilon,\mu}^{N,M} \rightarrow$	5.8314e-03	1.4631e-03	3.6611e-04	9.1547e-05	2.2888e-05
	$Roc_{\varepsilon,\mu}^{N,M} \rightarrow$	1.9948	1.9987	1.9997	1.9999	-
$\vdots$	$\vdots$	$\vdots$	$\vdots$	$\vdots$	$\vdots$	$\vdots$
10^{-40}	$Err_{\varepsilon,\mu}^{N,M} \rightarrow$	5.8314e-03	1.4631e-03	3.6611e-04	9.1547e-05	2.2888e-05
	$Roc_{\varepsilon,\mu}^{N,M} \rightarrow$	1.9948	1.9987	1.9997	1.9999	-
$Err_{\varepsilon,\mu}^{N,M}$	$\rightarrow$	5.8314e-03	1.4631e-03	3.6611e-04	9.1547e-05	2.2888e-05
$Roc_{\varepsilon,\mu}^{N,M}$	$\rightarrow$	1.9948	1.9987	1.9997	1.9999	-

Table 5.2: Maximum absolute errors, $Err_{\varepsilon,\mu}^{N,M}$ and rates of convergence, $Roc_{\varepsilon,\mu}^{N,M}$ using scheme (5.7) for Example 5.1 with $\varepsilon = 10^{-3}$ and different values of μ.

	N $\rightarrow$	32	64	128	256	512
$\mu \downarrow$	M $\rightarrow$	8	16	32	64	128
10^{0}	$Err_{\varepsilon,\mu}^{N,M} \rightarrow$	6.4634e-03	1.5384e-03	3.7470e-04	9.2432e-05	2.2952e-05
	$Roc_{\varepsilon,\mu}^{N,M} \rightarrow$	2.0709	2.0376	2.0193	2.0098	-
10^{-2}	$Err_{\varepsilon,\mu}^{N,M} \rightarrow$	5.8135e-03	1.4580e-03	3.6474e-04	9.1193e-05	2.2798e-05
	$Roc_{\varepsilon,\mu}^{N,M} \rightarrow$	1.9954	1.9991	1.9999	2.0000	-
10^{-4}	$Err_{\varepsilon,\mu}^{N,M} \rightarrow$	5.8075e-03	1.4572e-03	3.6464e-04	9.1181e-05	2.2796e-05
	$Roc_{\varepsilon,\mu}^{N,M} \rightarrow$	1.9947	1.9987	1.9997	2.0000	-
10^{-6}	$Err_{\varepsilon,\mu}^{N,M} \rightarrow$	5.8074e-03	1.4572e-03	3.6464e-04	9.1180e-05	2.2796e-05
	$Roc_{\varepsilon,\mu}^{N,M} \rightarrow$	1.9947	1.9987	1.9997	1.9999	-
10^{-8}	$Err_{\varepsilon,\mu}^{N,M} \rightarrow$	5.8074e-03	1.4572e-03	3.6464e-04	9.1180e-05	2.2796e-05
	$Roc_{\varepsilon,\mu}^{N,M} \rightarrow$	1.9947	1.9987	1.9997	1.9999	-
10^{-10}	$Err_{\varepsilon,\mu}^{N,M} \rightarrow$	5.8074e-03	1.4572e-03	3.6464e-04	9.1180e-05	2.2796e-05
	$Roc_{\varepsilon,\mu}^{N,M} \rightarrow$	1.9947	1.9987	1.9997	1.9999	-
10^{-12}	$Err_{\varepsilon,\mu}^{N,M} \rightarrow$	5.8074e-03	1.4572e-03	3.6464e-04	9.1180e-05	2.2796e-05
	$Roc_{\varepsilon,\mu}^{N,M} \rightarrow$	1.9947	1.9987	1.9997	1.9999	-
10^{-14}	$Err_{\varepsilon,\mu}^{N,M} \rightarrow$	5.8074e-03	1.4572e-03	3.6464e-04	9.1180e-05	2.2796e-05
	$Roc_{\varepsilon,\mu}^{N,M} \rightarrow$	1.9947	1.9987	1.9997	1.9999	-
10^{-16}	$Err_{\varepsilon,\mu}^{N,M} \rightarrow$	5.8074e-03	1.4572e-03	3.6464e-04	9.1180e-05	2.2796e-05
	$Roc_{\varepsilon,\mu}^{N,M} \rightarrow$	1.9947	1.9987	1.9997	1.9999	-
$\vdots$	$\vdots$	$\vdots$	$\vdots$	$\vdots$	$\vdots$	$\vdots$
10^{-40}	$Err_{\varepsilon,\mu}^{N,M} \rightarrow$	5.8074e-03	1.4572e-03	3.6464e-04	9.1180e-05	2.2796e-05
	$Roc_{\varepsilon,\mu}^{N,M} \rightarrow$	1.9947	1.9987	1.9997	1.9999	-
$Err_{\varepsilon,\mu}^{N,M}$	$\rightarrow$	5.8074e-03	1.4572e-03	3.6464e-04	9.1180e-05	2.2796e-05
$Roc_{\varepsilon,\mu}^{N,M}$	$\rightarrow$	1.9947	1.9987	1.9997	1.9999	-

Table 5.3: Maximum absolute errors, $Err_{\varepsilon,\mu}^{N,M}$ and rates of convergence, $Roc_{\varepsilon,\mu}^{N,M}$ using scheme (5.7) for Example 5.2 with $\mu = 10^{-3}$ and different values of ε.

	N $\rightarrow$	32	64	128	256
$\varepsilon \downarrow$	M $\rightarrow$	8	16	32	64
10^{0}	$Err_{\varepsilon,\mu}^{N,M} \rightarrow$	8.9042e-04	2.2425e-04	5.6169e-05	1.4049e-05
	$Roc_{\varepsilon,\mu}^{N,M} \rightarrow$	1.9894	1.9973	1.9993	-
10^{-2}	$Err_{\varepsilon,\mu}^{N,M} \rightarrow$	3.1319e-03	7.8541e-04	1.9655e-04	4.9150e-05
	$Roc_{\varepsilon,\mu}^{N,M} \rightarrow$	1.9955	1.9985	1.9996	-
10^{-4}	$Err_{\varepsilon,\mu}^{N,M} \rightarrow$	3.2007e-03	8.0247e-04	2.0080e-04	5.0214e-05
	$Roc_{\varepsilon,\mu}^{N,M} \rightarrow$	1.9959	1.9987	1.9996	-
10^{-6}	$Err_{\varepsilon,\mu}^{N,M} \rightarrow$	3.2014e-03	8.0264e-04	2.0085e-04	5.0225e-05
	$Roc_{\varepsilon,\mu}^{N,M} \rightarrow$	1.9959	1.9986	1.9996	-
10^{-8}	$Err_{\varepsilon,\mu}^{N,M} \rightarrow$	3.2014e-03	8.0264e-04	2.0085e-04	5.0225e-05
	$Roc_{\varepsilon,\mu}^{N,M} \rightarrow$	1.9959	1.9986	1.9996	-
10^{-10}	$Err_{\varepsilon,\mu}^{N,M} \rightarrow$	3.2014e-03	8.0264e-04	2.0085e-04	5.0225e-05
	$Roc_{\varepsilon,\mu}^{N,M} \rightarrow$	1.9959	1.9986	1.9996	-
10^{-12}	$Err_{\varepsilon,\mu}^{N,M} \rightarrow$	3.2014e-03	8.0264e-04	2.0085e-04	5.0225e-05
	$Roc_{\varepsilon,\mu}^{N,M} \rightarrow$	1.9959	1.9986	1.9996	-
10^{-14}	$Err_{\varepsilon,\mu}^{N,M} \rightarrow$	3.2014e-03	8.0264e-04	2.0085e-04	5.0225e-05
	$Roc_{\varepsilon,\mu}^{N,M} \rightarrow$	1.9959	1.9986	1.9996	-
10^{-16}	$Err_{\varepsilon,\mu}^{N,M} \rightarrow$	3.2014e-03	8.0264e-04	2.0085e-04	5.0225e-05
	$Roc_{\varepsilon,\mu}^{N,M} \rightarrow$	1.9959	1.9986	1.9996	-
10^{-18}	$Err_{\varepsilon,\mu}^{N,M} \rightarrow$	3.2014e-03	8.0264e-04	2.0085e-04	5.0225e-05
	$Roc_{\varepsilon,\mu}^{N,M} \rightarrow$	1.9959	1.9986	1.9996	-
$\vdots$	$\vdots$	$\vdots$	$\vdots$	$\vdots$	$\vdots$
10^{-40}	$Err_{\varepsilon,\mu}^{N,M} \rightarrow$	3.2014e-03	8.0264e-04	2.0085e-04	5.0225e-05
	$Roc_{\varepsilon,\mu}^{N,M} \rightarrow$	1.9959	1.9986	1.9996	-
$Err_{\varepsilon,\mu}^{N,M}$	$\rightarrow$	3.2014e-03	8.0264e-04	2.0085e-04	5.0225e-05
$Roc_{\varepsilon,\mu}^{N,M}$	$\rightarrow$	1.9959	1.9986	1.9996	-

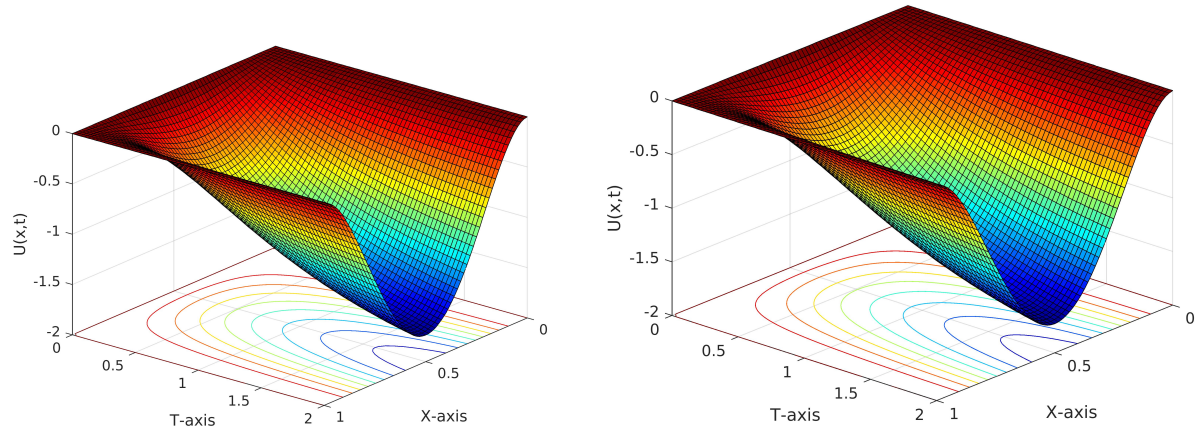

(a) (b)

Figure 5.1: Surface plot for Example 5.1 using scheme in (5.7) with $N = M = 64$ and (a) $\varepsilon = 10^{-8}, \mu = 10^{-4}$, (b) $\varepsilon = 10^{-4}, \mu = 10^{-8}$

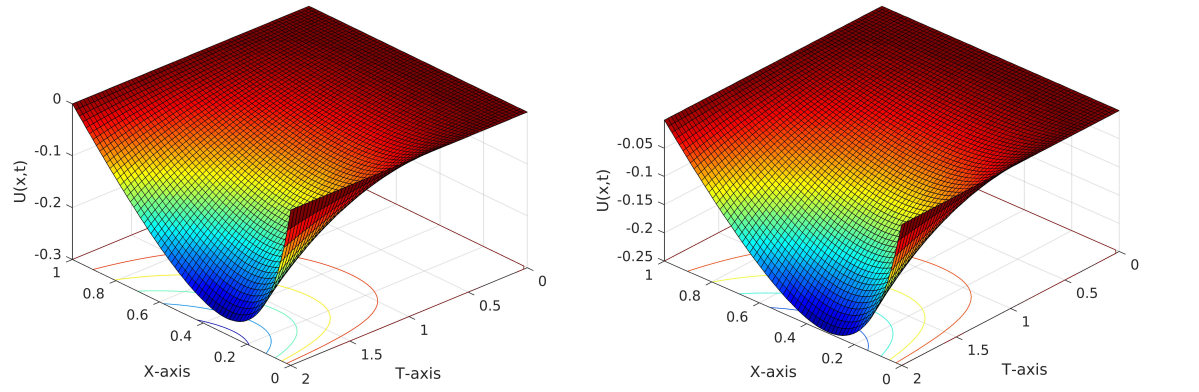

Figure 5.2: Surface plot for Example 5.2 using scheme in (5.7) with $N = M = 64$ and (a) $\varepsilon = 10^{-8}, \mu = 10^{-4}$, (b) $\varepsilon = 10^{-4}, \mu = 10^{-8}$

Table 5.4: Maximum v errors, $Err_{\varepsilon,\mu}^{N,M}$ and rates of convergence, $Roc_{\varepsilon,\mu}^{N,M}$ using scheme (5.7) for Example 5.2 with $\varepsilon = 10^{-3}$ and different values of μ.

	N →	32	64	128	256
$\mu \downarrow$	M →	8	16	32	64
10^{0}	$Err_{\varepsilon,\mu}^{N,M} \rightarrow$	3.5162e-03	8.4508e-04	2.0685e-04	5.0155e-05
	$Roc_{\varepsilon,\mu}^{N,M} \rightarrow$	2.0569	2.0305	2.0441	-
10^{-2}	$Err_{\varepsilon,\mu}^{N,M} \rightarrow$	3.1970e-03	8.0128e-04	2.0046e-04	5.0122e-05
	$Roc_{\varepsilon,\mu}^{N,M} \rightarrow$	1.9963	1.9990	1.9998	-
10^{-4}	$Err_{\varepsilon,\mu}^{N,M} \rightarrow$	3.1940e-03	8.0086e-04	2.0041e-04	5.0115e-05
	$Roc_{\varepsilon,\mu}^{N,M} \rightarrow$	1.9957	1.9986	1.9996	-
10^{-6}	$Err_{\varepsilon,\mu}^{N,M} \rightarrow$	3.1940e-03	8.0085e-04	2.0040e-04	5.0115e-05
	$Roc_{\varepsilon,\mu}^{N,M} \rightarrow$	1.9958	1.9986	1.9996	-
10^{-8}	$Err_{\varepsilon,\mu}^{N,M} \rightarrow$	3.1940e-03	8.0085e-04	2.0040e-04	5.0115e-05
	$Roc_{\varepsilon,\mu}^{N,M} \rightarrow$	1.9958	1.9986	1.9996	-
10^{-10}	$Err_{\varepsilon,\mu}^{N,M} \rightarrow$	3.1940e-03	8.0085e-04	2.0040e-04	5.0115e-05
	$Roc_{\varepsilon,\mu}^{N,M} \rightarrow$	1.9958	1.9986	1.9996	-
10^{-12}	$Err_{\varepsilon,\mu}^{N,M} \rightarrow$	3.1940e-03	8.0085e-04	2.0040e-04	5.0115e-05
	$Roc_{\varepsilon,\mu}^{N,M} \rightarrow$	1.9958	1.9986	1.9996	-
10^{-14}	$Err_{\varepsilon,\mu}^{N,M} \rightarrow$	3.1940e-03	8.0085e-04	2.0040e-04	5.0115e-05
	$Roc_{\varepsilon,\mu}^{N,M} \rightarrow$	1.9958	1.9986	1.9996	-
⋮	⋮	⋮	⋮	⋮	⋮
10^{-40}	$Err_{\varepsilon,\mu}^{N,M} \rightarrow$	3.1940e-03	8.0085e-04	2.0040e-04	5.0115e-05
	$Roc_{\varepsilon,\mu}^{N,M} \rightarrow$	1.9958	1.9986	1.9996	-
$Err_{\varepsilon,\mu}^{N,M}$	→	3.1940e-03	8.0085e-04	2.0040e-04	5.0115e-05
$Roc_{\varepsilon,\mu}^{N,M}$	→	1.9958	1.9986	1.9996	-

Table 5.5: Comparison of the proposed scheme in (5.7) with an existing schemes in Kumar et al. (2020) using Example 5.1

$\mu = 10^{-3}$ $\varepsilon \downarrow$ **Proposed method**	$N = 32$ $M = 8$	$N = 64$ $M = 16$	$N = 128$ $M = 32$	$N = 256$ $M = 64$	$N = 512$ $M = 128$
10^{-4}	5.8291e-03	1.4625e-03	3.6596e-04	9.1510e-05	2.2879e-05
10^{-6}	5.8314e-03	1.4631e-03	3.6611e-04	9.1547e-05	2.2888e-05
10^{-8}	5.8314e-03	1.4631e-03	3.6611e-04	9.1547e-05	2.2888e-05
10^{-10}	5.8314e-03	1.4631e-03	3.6611e-04	9.1547e-05	2.2888e-05
scheme in Sumit et al. (2020)					
10^{-4}	$4.3705e-2$	$1.6704e-2$	$7.3802e-3$	$3.7406e-3$	$1.8967e-3$
10^{-6}	$4.3471e-2$	$1.6596e-2$	$7.3290e-3$	$3.7218e-3$	$1.8873e-3$
10^{-8}	$4.3429e-2$	$1.6573e-2$	$7.3303e-3$	$3.7211e-3$	$1.8870e-3$
10^{-10}	$4.4343e-2$	$1.6572e-2$	$7.3303e-3$	$3.7211e-3$	$1.8870e-3$

Table 5.6: Maximum absolute errors, $Err_{\varepsilon,\mu}^{N,M}$ and rates of convergence, $Roc_{\varepsilon,\mu}^{N,M}$ using scheme (5.7) for Example 5.3 with $\mu = 10^{-3}$ and different values of ε.

	N $\rightarrow$	32	64	128	256
$\varepsilon \downarrow$	M $\rightarrow$	8	16	32	64
10^{0}	$Err_{\varepsilon,\mu}^{N,M} \rightarrow$	5.5107e-03	1.4134e-03	3.5905e-04	9.0543e-05
	$Roc_{\varepsilon,\mu}^{N,M} \rightarrow$	1.9631	1.9769	1.9875	-
10^{-2}	$Err_{\varepsilon,\mu}^{N,M} \rightarrow$	5.7686e-03	1.4501e-03	3.6416e-04	9.1280e-05
	$Roc_{\varepsilon,\mu}^{N,M} \rightarrow$	1.9921	1.9935	1.9962	-
10^{-4}	$Err_{\varepsilon,\mu}^{N,M} \rightarrow$	5.8369e-03	1.4589e-03	3.6526e-04	9.1417e-05
	$Roc_{\varepsilon,\mu}^{N,M} \rightarrow$	2.0003	1.9979	1.9984	-
10^{-6}	$Err_{\varepsilon,\mu}^{N,M} \rightarrow$	5.8375e-03	1.4591e-03	3.6529e-04	9.1426e-05
	$Roc_{\varepsilon,\mu}^{N,M} \rightarrow$	2.0003	1.9980	1.9984	-
10^{-8}	$Err_{\varepsilon,\mu}^{N,M} \rightarrow$	5.8375e-03	1.4591e-03	3.6529e-04	9.1426e-05
	$Roc_{\varepsilon,\mu}^{N,M} \rightarrow$	2.0003	1.9980	1.9984	-
10^{-10}	$Err_{\varepsilon,\mu}^{N,M} \rightarrow$	5.8375e-03	1.4591e-03	3.6529e-04	9.1426e-05
	$Roc_{\varepsilon,\mu}^{N,M} \rightarrow$	2.0003	1.9980	1.9984	-
10^{-12}	$Err_{\varepsilon,\mu}^{N,M} \rightarrow$	5.8375e-03	1.4591e-03	3.6529e-04	9.1426e-05
	$Roc_{\varepsilon,\mu}^{N,M} \rightarrow$	2.0003	1.9980	1.9984	-
10^{-14}	$Err_{\varepsilon,\mu}^{N,M} \rightarrow$	5.8375e-03	1.4591e-03	3.6529e-04	9.1426e-05
	$Roc_{\varepsilon,\mu}^{N,M} \rightarrow$	2.0003	1.9980	1.9984	-
10^{-16}	$Err_{\varepsilon,\mu}^{N,M} \rightarrow$	5.8375e-03	1.4591e-03	3.6529e-04	9.1426e-05
	$Roc_{\varepsilon,\mu}^{N,M} \rightarrow$	2.0003	1.9980	1.9984	-
$\vdots$	$\vdots$	$\vdots$	$\vdots$	$\vdots$	$\vdots$
10^{-20}	$Err_{\varepsilon,\mu}^{N,M} \rightarrow$	5.8375e-03	1.4591e-03	3.6529e-04	9.1426e-05
	$Roc_{\varepsilon,\mu}^{N,M} \rightarrow$	2.0003	1.9980	1.9984	-
$Err_{\varepsilon,\mu}^{N,M}$	$\rightarrow$	5.8375e-03	1.4591e-03	3.6529e-04	9.1426e-05
$Roc_{\varepsilon,\mu}^{N,M}$	$\rightarrow$	2.0003	1.9980	1.9984	-

Table 5.7: Maximum absolute errors, $Err_{\varepsilon,\mu}^{N,M}$ and rates of convergence, $Roc_{\varepsilon,\mu}^{N,M}$ using scheme (5.7) for Example 5.3 with $\varepsilon = 10^{-3}$ and different values of μ.

	N $\rightarrow$	32	64	128	256
$\mu \downarrow$	M $\rightarrow$	8	16	32	64
10^{0}	$Err_{\varepsilon,\mu}^{N,M} \rightarrow$	6.1608e-03	1.5011e-03	3.7069e-04	9.2110e-05
	$Roc_{\varepsilon,\mu}^{N,M} \rightarrow$	2.0371	2.0177	2.0088	-
10^{-2}	$Err_{\varepsilon,\mu}^{N,M} \rightarrow$	5.8314e-03	1.4576e-03	3.6493e-04	9.1323e-05
	$Roc_{\varepsilon,\mu}^{N,M} \rightarrow$	2.0002	1.9979	1.9986	-
10^{-4}	$Err_{\varepsilon,\mu}^{N,M} \rightarrow$	5.8314e-03	1.4576e-03	3.6493e-04	9.1324e-05
	$Roc_{\varepsilon,\mu}^{N,M} \rightarrow$	2.0002	1.9979	1.9986	-
10^{-6}	$Err_{\varepsilon,\mu}^{N,M} \rightarrow$	5.8314e-03	1.4576e-03	3.6493e-04	9.1324e-05
	$Roc_{\varepsilon,\mu}^{N,M} \rightarrow$	2.0002	1.9979	1.9986	-
10^{-8}	$Err_{\varepsilon,\mu}^{N,M} \rightarrow$	5.8314e-03	1.4576e-03	3.6493e-04	9.1324e-05
	$Roc_{\varepsilon,\mu}^{N,M} \rightarrow$	2.0002	1.9979	1.9986	-
10^{-10}	$Err_{\varepsilon,\mu}^{N,M} \rightarrow$	5.8314e-03	1.4576e-03	3.6493e-04	9.1324e-05
	$Roc_{\varepsilon,\mu}^{N,M} \rightarrow$	2.0002	1.9979	1.9986	-
10^{-12}	$Err_{\varepsilon,\mu}^{N,M} \rightarrow$	5.8314e-03	1.4576e-03	3.6493e-04	9.1324e-05
	$Roc_{\varepsilon,\mu}^{N,M} \rightarrow$	2.0002	1.9979	1.9986	-
10^{-14}	$Err_{\varepsilon,\mu}^{N,M} \rightarrow$	5.8314e-03	1.4576e-03	3.6493e-04	9.1324e-05
	$Roc_{\varepsilon,\mu}^{N,M} \rightarrow$	2.0002	1.9979	1.9986	-
10^{-16}	$Err_{\varepsilon,\mu}^{N,M} \rightarrow$	5.8314e-03	1.4576e-03	3.6493e-04	9.1324e-05
	$Roc_{\varepsilon,\mu}^{N,M} \rightarrow$	2.0002	1.9979	1.9986	-
$\vdots$	$\vdots$	$\vdots$	$\vdots$	$\vdots$	$\vdots$
10^{-20}	$Err_{\varepsilon,\mu}^{N,M} \rightarrow$	5.8314e-03	1.4576e-03	3.6493e-04	9.1324e-05
	$Roc_{\varepsilon,\mu}^{N,M} \rightarrow$	2.0002	1.9979	1.9986	-
$Err_{\varepsilon,\mu}^{N,M}$	$\rightarrow$	5.8314e-03	1.4576e-03	3.6493e-04	9.1324e-05
$Roc_{\varepsilon,\mu}^{N,M}$	$\rightarrow$	2.0002	1.9979	1.9986	-

Table 5.8: Maximum absolute errors, $Err_{\varepsilon,\mu}^{N,M}$ and rates of convergence, $Roc_{\varepsilon,\mu}^{N,M}$ using scheme (5.7) for Example 5.4 with $\mu = 10^{-3}$ and different values of ε.

	N $\rightarrow$	32	64	128	256
$\varepsilon \downarrow$	M $\rightarrow$	8	16	32	64
10^{0}	$Err_{\varepsilon,\mu}^{N,M} \rightarrow$	3.8029e-03	1.1072e-03	3.0071e-04	7.8684e-05
	$Roc_{\varepsilon,\mu}^{N,M} \rightarrow$	1.7802	1.8805	1.9342	-
10^{-2}	$Err_{\varepsilon,\mu}^{N,M} \rightarrow$	4.8349e-03	1.2524e-03	3.2301e-04	8.2004e-05
	$Roc_{\varepsilon,\mu}^{N,M} \rightarrow$	1.9488	1.9550	1.9778	-
10^{-4}	$Err_{\varepsilon,\mu}^{N,M} \rightarrow$	5.0002e-03	1.2915e-03	3.2799e-04	8.2634e-05
	$Roc_{\varepsilon,\mu}^{N,M} \rightarrow$	1.9529	1.9773	1.9888	-
10^{-6}	$Err_{\varepsilon,\mu}^{N,M} \rightarrow$	5.0019e-03	1.2919e-03	3.2809e-04	8.2660e-05
	$Roc_{\varepsilon,\mu}^{N,M} \rightarrow$	1.9530	1.9773	1.9888	-
10^{-8}	$Err_{\varepsilon,\mu}^{N,M} \rightarrow$	5.0019e-03	1.2919e-03	3.2809e-04	8.2660e-05
	$Roc_{\varepsilon,\mu}^{N,M} \rightarrow$	1.9530	1.9773	1.9888	-
10^{-10}	$Err_{\varepsilon,\mu}^{N,M} \rightarrow$	5.0019e-03	1.2919e-03	3.2809e-04	8.2660e-05
	$Roc_{\varepsilon,\mu}^{N,M} \rightarrow$	1.9530	1.9773	1.9888	-
10^{-12}	$Err_{\varepsilon,\mu}^{N,M} \rightarrow$	5.0019e-03	1.2919e-03	3.2809e-04	8.2660e-05
	$Roc_{\varepsilon,\mu}^{N,M} \rightarrow$	1.9530	1.9773	1.9888	-
10^{-14}	$Err_{\varepsilon,\mu}^{N,M} \rightarrow$	5.0019e-03	1.2919e-03	3.2809e-04	8.2660e-05
	$Roc_{\varepsilon,\mu}^{N,M} \rightarrow$	1.9530	1.9773	1.9888	-
10^{-16}	$Err_{\varepsilon,\mu}^{N,M} \rightarrow$	5.0019e-03	1.2919e-03	3.2809e-04	8.2660e-05
	$Roc_{\varepsilon,\mu}^{N,M} \rightarrow$	1.9530	1.9773	1.9888	-
$\vdots$	$\vdots$	$\vdots$	$\vdots$	$\vdots$	$\vdots$
10^{-20}	$Err_{\varepsilon,\mu}^{N,M} \rightarrow$	5.0019e-03	1.2919e-03	3.2809e-04	8.2660e-05
	$Roc_{\varepsilon,\mu}^{N,M} \rightarrow$	1.9530	1.9773	1.9888	-
$Err_{\varepsilon,\mu}^{N,M}$	$\rightarrow$	5.0019e-03	1.2919e-03	3.2809e-04	8.2660e-05
$Roc_{\varepsilon,\mu}^{N,M}$	$\rightarrow$	1.9530	1.9773	1.9888	-

Table 5.9: Maximum absolute errors, $Err_{\varepsilon,\mu}^{N,M}$ and rates of convergence, $Roc_{\varepsilon,\mu}^{N,M}$ using scheme (5.7) for Example 5.4 with $\varepsilon = 10^{-3}$ and different values of μ.

	N $\rightarrow$	32	64	128	256
$\mu \downarrow$	M $\rightarrow$	8	16	32	64
10^{0}	$Err_{\varepsilon,\mu}^{N,M} \rightarrow$	5.0529e-03	1.3020e-03	3.2960e-04	8.2863e-05
	$Roc_{\varepsilon,\mu}^{N,M} \rightarrow$	1.9564	1.9819	1.9919	-
10^{-2}	$Err_{\varepsilon,\mu}^{N,M} \rightarrow$	4.9835e-03	1.2875e-03	3.2703e-04	8.2399e-05
	$Roc_{\varepsilon,\mu}^{N,M} \rightarrow$	1.9526	1.9771	1.9887	-
10^{-4}	$Err_{\varepsilon,\mu}^{N,M} \rightarrow$	4.9856e-03	1.2878e-03	3.2707e-04	8.2403e-05
	$Roc_{\varepsilon,\mu}^{N,M} \rightarrow$	1.9529	1.9772	1.9888	-
10^{-6}	$Err_{\varepsilon,\mu}^{N,M} \rightarrow$	4.9856e-03	1.2878e-03	3.2707e-04	8.2403e-05
	$Roc_{\varepsilon,\mu}^{N,M} \rightarrow$	1.9529	1.9772	1.9888	-
10^{-8}	$Err_{\varepsilon,\mu}^{N,M} \rightarrow$	4.9856e-03	1.2878e-03	3.2707e-04	8.2403e-05
	$Roc_{\varepsilon,\mu}^{N,M} \rightarrow$	1.9529	1.9772	1.9888	-
10^{-10}	$Err_{\varepsilon,\mu}^{N,M} \rightarrow$	4.9856e-03	1.2878e-03	3.2707e-04	8.2403e-05
	$Roc_{\varepsilon,\mu}^{N,M} \rightarrow$	1.9529	1.9772	1.9888	-
10^{-12}	$Err_{\varepsilon,\mu}^{N,M} \rightarrow$	4.9856e-03	1.2878e-03	3.2707e-04	8.2403e-05
	$Roc_{\varepsilon,\mu}^{N,M} \rightarrow$	1.9529	1.9772	1.9888	-
10^{-14}	$Err_{\varepsilon,\mu}^{N,M} \rightarrow$	4.9856e-03	1.2878e-03	3.2707e-04	8.2403e-05
	$Roc_{\varepsilon,\mu}^{N,M} \rightarrow$	1.9529	1.9772	1.9888	-
10^{-16}	$Err_{\varepsilon,\mu}^{N,M} \rightarrow$	4.9856e-03	1.2878e-03	3.2707e-04	8.2403e-05
	$Roc_{\varepsilon,\mu}^{N,M} \rightarrow$	1.9529	1.9772	1.9888	-
$\vdots$	$\vdots$	$\vdots$	$\vdots$	$\vdots$	$\vdots$
10^{-20}	$Err_{\varepsilon,\mu}^{N,M} \rightarrow$	4.9856e-03	1.2878e-03	3.2707e-04	8.2403e-05
	$Roc_{\varepsilon,\mu}^{N,M} \rightarrow$	1.9529	1.9772	1.9888	-
$Err_{\varepsilon,\mu}^{N,M}$	$\rightarrow$	4.9856e-03	1.2878e-03	3.2707e-04	8.2403e-05
$Roc_{\varepsilon,\mu}^{N,M}$	$\rightarrow$	1.9529	1.9772	1.9888	-

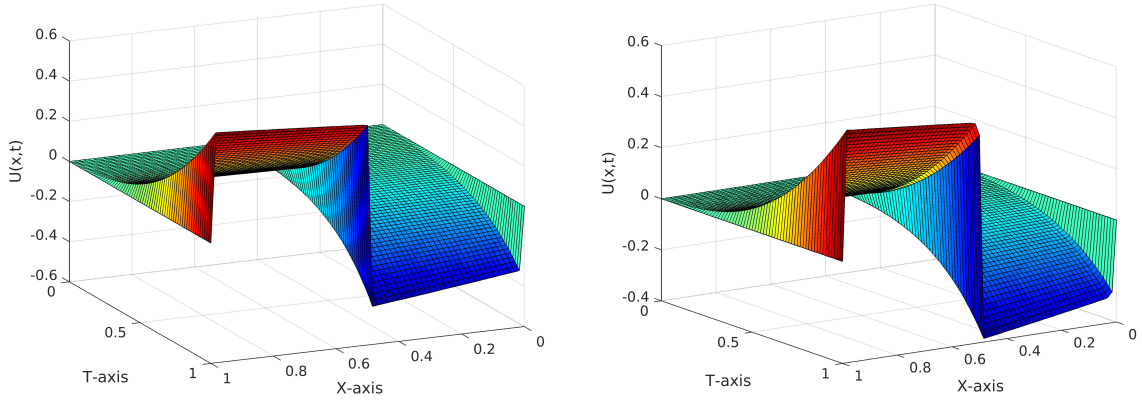

(a) (b)

Figure 5.3: Surface plot for Example 5.3 using scheme in (5.7) with $N = M = 64$ and (a) $\varepsilon = 10^{-8}, \mu = 10^{-4}$, (b) $\varepsilon = 10^{-4}, \mu = 10^{-8}$

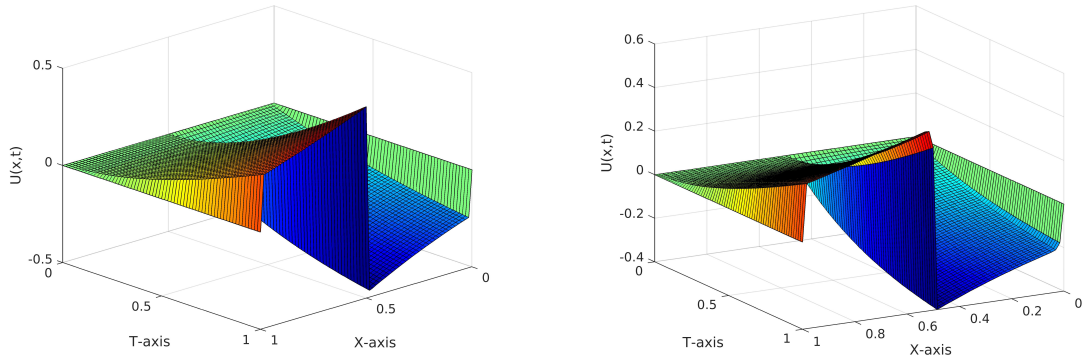

(a) (b)

Figure 5.4: Surface plot for Example 5.4 using scheme in (5.7) with $N = M = 64$ and (a) $\varepsilon = 10^{-8}, \mu = 10^{-4}$, (b) $\varepsilon = 10^{-4}, \mu = 10^{-8}$

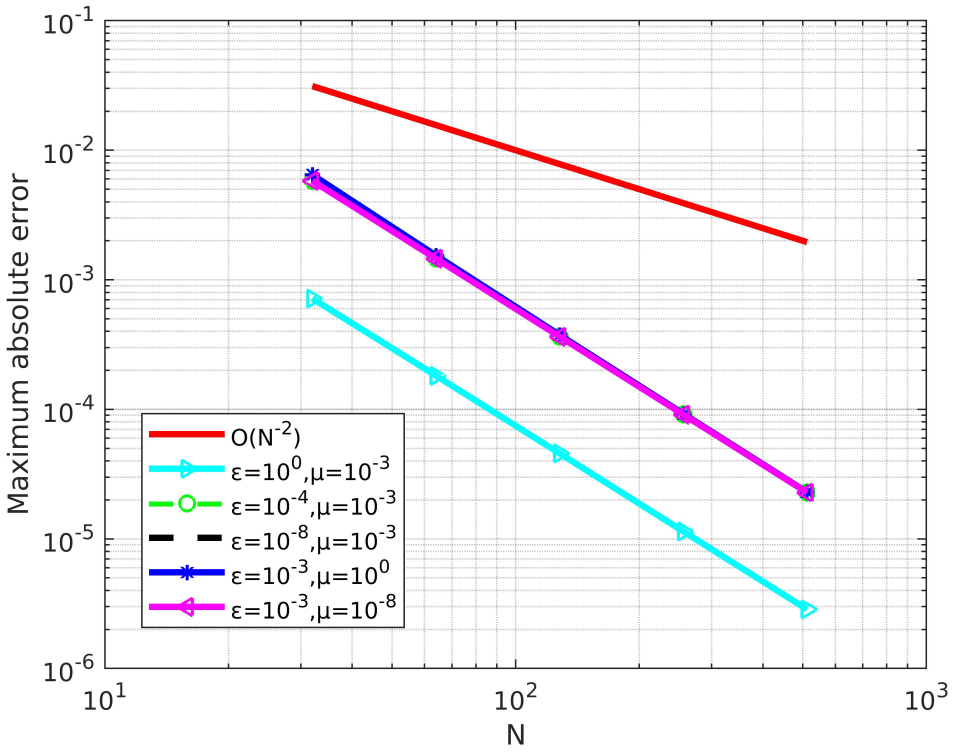

Figure 5.5: Log-Log plot of N vs maximum absolute error for Example 5.1.

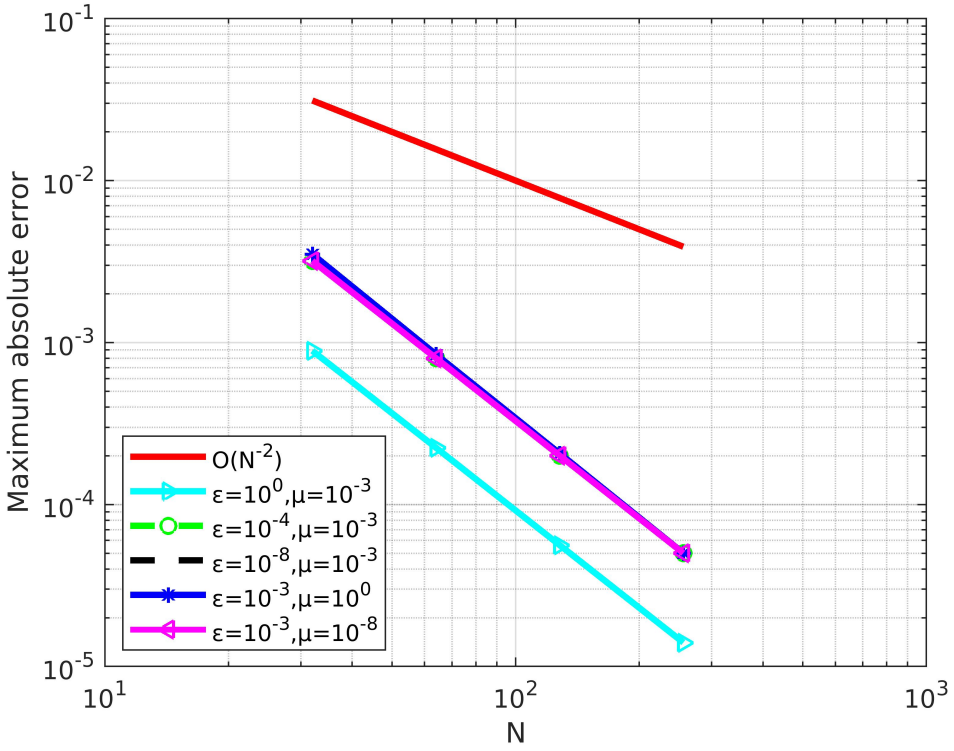

Figure 5.6: Log-Log plot of N vs maximum absolute error for Example 5.2.

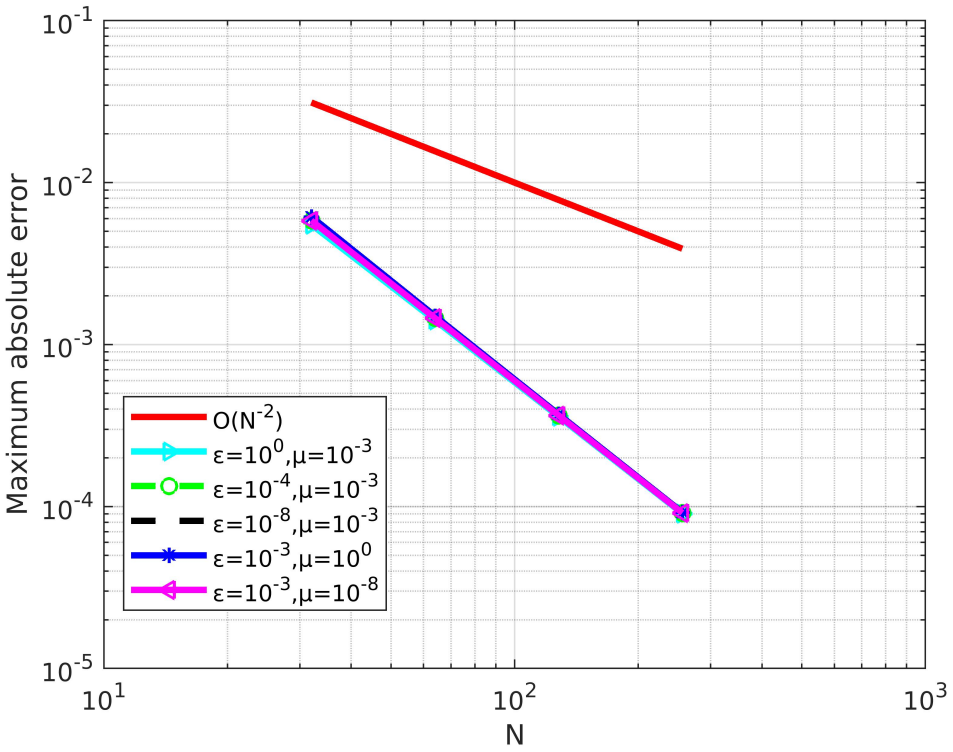

Figure 5.7: Log-Log plot of N vs maximum absolute error, for Example, 5.3.

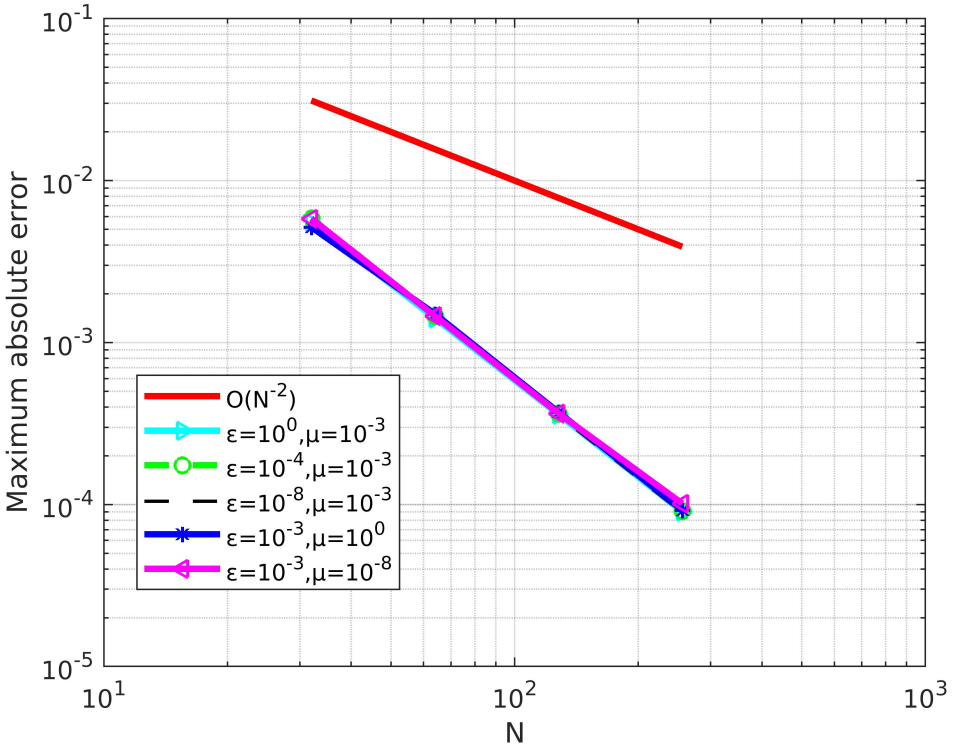

Figure 5.8: Log-Log plot of N vs maximum absolute error, for Example, 5.4.

5.6 Summary

This chapter introduced a hybrid-fitted finite difference scheme to solve two-parameter singularly perturbed time delay parabolic differential equations for both smooth and non-smooth data. The problem was discretized using the difference operator comprising the Crank-Nicolson method for time and a blend of the central, upwind, and midpoint difference operators for space. The convergence analysis proved that the method is uniformly convergent with second-order time variables and almost second-order space variables. The method was further implemented using test examples (with smooth and non-smooth data). In both cases, the theoretical results were confirmed. Tabulated results show practically a second-order uniform convergence. Furthermore, a performance comparison with an existing method in the literature indicates that the proposed method is more accurate.

CHAPTER 6

A FITTED PARAMETER CONVERGENT FINITE DIFFERENCE SCHEME FOR TWO-PARAMETER SINGULARLY PERTURBED PARABOLIC DIFFERENTIAL EQUATIONS

This chapter focuses on the formulation of a numerical scheme that is uniform in its parameters for a class of time-dependent parabolic SPPs with two perturbation parameters without delay. In these problems, the existence of the two parameters results in the formation of boundary layer(s) in the solution regions. Solving these model problems using classical methods does not yield satisfactory results due to the layer behavior. Therefore, nonstandard finite difference schemes have been developed as a means to obtain numerical solutions for these problems. To develop the scheme, the Crank-Nicolson discretization on a uniform time mesh and a fitted operator method with a uniform spatial mesh are employed. The stability and convergence analysis of the proposed scheme is also discussed, and it exhibits uniform convergence of second order in the temporal direction and first order in the spatial direction. However, temporal mesh refinements are used to enhance the order to two in both directions. Model examples are provided to validate the practicality of the proposed numerical scheme.

6.1 The governing problem

Consider the problem with Dirichlet boundary conditions on the domain $D = (0,1) \times (0,T]$ with boundary $\partial D = \bar{D} \backslash D$ as

$$L_{\varepsilon,\mu} u(x,t) = \varepsilon u_{xx}(x,t) + \mu a(x,t) u_x(x,t) - b(x,t) u_t(x,t) - c(x,t) u(x,t) = f(x,t), \quad (x,t) \in D, \tag{6.1}$$

$$u(x,0) = u_0(x), \quad x \in [0,1], \tag{6.2}$$

$$u(0,t) = \Phi_0(t), \quad u(1,t) = \Phi_1(t), \quad t \in [0,T]. \tag{6.3}$$

Here, ε and μ are small positive parameters with $0 < \varepsilon \leq 1$ and $0 \leq \mu \leq 1$. From (6.1)-(6.3), the coefficients $a(x,t)$, $b(x,t)$, $c(x,t)$, and $f(x,t)$ for $(x,t) \in \bar{D}$, are assumed to be smooth. Additionally, it is assumed $a(x,t) \geq \alpha > 0$, $b(x,t) \geq \beta > 0$, $c(x,t) \geq \gamma > 0$. Again, at the corners $(0,0)$ and $(1,0)$, we make the assumption of adequate regularity and compatibility conditions based on the idea as stated in Ladyzhenskaya et al. (1968). If all of the stated as-

sumptions are satisfied, then the problem described in (6.1)-(6.3) possesses a unique solution on $\bar{D}$.

6.2 Some qualitative properties of the continuous problem

This section presents a discussion on certain analytical properties of the governing problem (6.1)-(6.3) in a one-dimensional spatial domain, denoted as $\bar{\Omega}$.

Lemma 6.2.1. *Let* $\Psi(x,t) \in C^{2,1}(\bar{D})$. *If* $\Psi|_{\partial D} \geq 0$ *and* $\left(L_{\varepsilon,\mu} - \frac{\partial}{\partial t}\right)\Psi|_D \leq 0$, *then* $\Psi|_{\bar{D}} \geq 0$.

Proof. We prove this lemma by contradiction. Assume there exists an arbitrary point (x^*,t^*) in the plane $D = (0,1)\times(0,T)$ such that $\Psi(x^*,t^*) = \min\{\Psi(x,t)\}_{(x,t)\in\bar{D}}$, and suppose $\Psi(x^*,t^*) < 0$. By the definition of (x^*,t^*), it is clear that $(x^*,t^*) \notin \{0,1\}\times\{0,T\}$. Applying the first and second derivative tests for multivariable functions in calculus, we have $\Psi_{xx}(x^*,t^*) \geq 0$, $\nabla_x\Psi(x^*,t^*) = 0$, and $\nabla_t\Psi(x^*,t^*) = 0$. Consequently, we can observe that

$$\left(L_{\varepsilon,\mu} - \frac{\partial}{\partial t}\right)\Psi|_D \geq 0$$

which leads to a contradiction. Hence, our initial assumption, $\Psi(x^*,t^*) < 0$, is incorrect. Therefore, $\Psi(x^*,t^*)|_{\bar{D}} \geq 0$. Since (x^*,t^*) was arbitrarily chosen, it follows that $\Psi(x,t) \geq 0$ for all $(x,t) \in \bar{D}$. ■

Lemma 6.2.2. *Gupta et al. (2019). Let* $u(x,t)$ *be the solution of (6.1)-(6.3), then for* $0 < \varepsilon \leq 1$ *and* $0 \leq \mu \leq 1$, *we have*

$$\|u\|_{\bar{\Omega}} \leq \frac{\xi\|f\|_{\bar{D}}}{\beta} + \|u\|_{\partial D}.$$

Proof. We can prove this Lemma using the concept of barrier functions. Therefore, let us introduce two comparison (barrier) functions as follows:

$$\varphi^{\pm}(x,t) = \frac{\xi\|f\|_{\bar{D}}}{\beta} + \|u\|_{\partial D} \pm u(x,t) \forall (x,t) \in \bar{D}$$

when $x = 0$, $\varphi^{\pm}(0,t) = \frac{\xi\|f\|_{\bar{D}}}{\beta} + \|u\|_{\partial D} \pm u(0,t) = \frac{\xi\|f\|_{\bar{D}}}{\beta} + \|u\|_{\partial D} \pm \Phi_0(t) \geq 0$ and
when $x = 1$, $\varphi^{\pm}(1,t) = \frac{\xi\|f\|_{\bar{D}}}{\beta} + \|u\|_{\partial D} \pm u(1,t) = \frac{\xi\|f\|_{\bar{D}}}{\beta} + \|u\|_{\partial} \pm \Phi_1(t) \geq 0$.
Then, we have $\varphi^{\pm}(x,t) \geq 0\, \forall (x,t) \in \partial D$. Again, since $b(x,t) \geq \beta > 0$ and $\|f\|_{\bar{D}} \geq f(x,t) \forall (x,t) \in \bar{D}$, we have $-b(x,t)\beta^{-1}\|f\|_{\bar{D}} \pm f(x,t) \leq 0$. This inequality implies

$$L_{\varepsilon,\mu}\varphi^{\pm}(x,t) \leq 0, \quad \forall (x,t) \in D.$$

Applying the minimum principle in Lemma 4.2.1, we get $\varphi^{\pm}(x,t) \geq 0, \forall (x,t) \in \bar{D}$, which gives the desired estimate. ■

Lemma 6.2.3 (**The bounds of the continuous problem and its derivatives**). *In the continuous problem described in 6.1)-(6.3), consider the solution u, which can be decomposed as* $u = v + w_L + w_R$. *Here, v represents the regular component,* w_L *represents the left singular components, and* w_R *represents the right singular components. These components are accompanied by a sufficiently large constant C, which remains independent of the perturbation parameters Kumar et al. (2020). Then,*

a. $\|u\| \leq C$.

b. For all non- negative integers i and j $(0 \leq i+2j \leq 4)$*, the derivatives of the solution u of problem (6.1)- (6.3) satisfy*

$$\left\| \frac{\partial^{i+j} u}{\partial x^i \partial t^j} \right\| \leq \begin{cases} C \dfrac{1}{(\sqrt{\varepsilon})^i}, & \text{when } \alpha\mu^2 \leq \eta\varepsilon \\ C \left(\dfrac{\mu}{\varepsilon}\right)^i \left(\dfrac{\mu^2}{\varepsilon}\right)^j, & \text{when } \alpha\mu^2 \geq \eta\varepsilon \end{cases}$$

c. $|w_L(x,t)| \leq Ce^{-\theta_L x}, \quad |w_R(x,t)| \leq Ce^{-\theta_R(1-x)}$

where

$$\theta_L = \begin{cases} \frac{\sqrt{\eta\alpha}}{\sqrt{\varepsilon}}, & \alpha\mu^2 \leq \eta\varepsilon, \\ \frac{\alpha\mu}{\varepsilon}, & \alpha\mu^2 \geq \eta\varepsilon, \end{cases} \qquad \theta_R = \begin{cases} \frac{\sqrt{\eta a}}{2\sqrt{\varepsilon}}, & \alpha\mu^2 \leq \eta\varepsilon, \\ \frac{\eta}{2\mu}, & \alpha\mu^2 \geq \eta\varepsilon. \end{cases}$$

6.3 Derivation of the numerical scheme

6.3.1 Temporal discretization

To develop the numerical scheme, we first divide the time domain $[0,\ T]$ into a uniform mesh using the given time step size $\triangle t$. The mesh points in the temporal domain are denoted by $\Omega^M = \{t_j = j\triangle t,\ \ j = 0,\ 1,\ 2,\ ...,\ M,\ t_M = T\}$, where M represents the number of mesh points in the time interval.

Next, we apply the implicit Crank-Nicolson discretization in the temporal direction to formulate the semi-discrete scheme for the problem described in (6.1)-(6.2). The derivation of the Crank-Nicolson scheme for $U_t(x,t_j)$ at the $(x, j+1/2)$ time step involves utilizing Taylor's

series expansion for U^{j+1} and U^{j}.

$$U^{j+1}(x) = U^{j+1/2}(x) + \frac{\Delta t}{2}\frac{\partial U^{j+1/2}(x)}{\partial t} + \left(\frac{\Delta t}{2}\right)^2 \frac{1}{2!}\frac{\partial^2 U^{j+1/2}(x)}{\partial t^2} + \left(\frac{\Delta t}{2}\right)^3 \frac{1}{3!}\frac{\partial^3 U^{j+1/2}(x)}{\partial t^3} + \ldots \tag{6.4}$$

$$U^{j}(x) = U^{j+1/2}(x) - \frac{\Delta t}{2}\frac{\partial U^{j+1/2}(x)}{\partial t} + \left(\frac{\Delta t}{2}\right)^2 \frac{1}{2!}\frac{\partial^2 U^{j+1/2}(x)}{\partial t^2} - \left(\frac{\Delta t}{2}\right)^3 \frac{1}{3!}\frac{\partial^3 U^{j+1/2}(x)}{\partial t^3} + \ldots \tag{6.5}$$

Subtracting Eq. (6.5) from Eq. (6.4), and eliminating the term $U^{j+1/2}(x)$, we get

$$\frac{U^{j+1}(x) - U^{j}(x)}{\Delta t} = \frac{\partial U^{j+1/2}(x)}{\partial t} + O(\Delta t)^3. \tag{6.6}$$

The local truncation error value $(T^{j+1/2}(x))$ obtained from the Taylor's series expansion is

$$T^{j+1/2}(x) = \frac{(\Delta t)^3}{24}\frac{\partial^3 U^{j+1/2}(x)}{\partial t^3} + (\text{higher order terms})$$

and its order three, ($O((\Delta t)^3)$). After substituting Eq. (6.6) into (6.1)) and rearranging, we obtained the semi-discretized scheme as

$$\left[L^{N,M}U(x)\right]^{j} \equiv b(x,t_{j+1/2})\left(\frac{u\left(x,t_{j+1}\right) - u\left(x,t_{j}\right)}{\Delta t}\right) = \varepsilon u_{xx}\left(x,t_{j+1/2}\right) + \mu a(x,t_{j+1/2})u_x\left(x,t_{j+1/2}\right) - c\left(x,t_{j+1/2}\right)u\left(x,t_{j+1/2}\right) - f\left(x,t_{j+1/2}\right) + O\left((\Delta t)^3\right)\}, \tag{6.7}$$

where

$$u\left(x,t_{j+1/2}\right) = \frac{u\left(x,t_{j+1}\right) + u\left(x,t_{j}\right)}{2} + O\left((\Delta t)^3\right), \text{ and}$$

$$f\left(x,t_{j+1/2}\right) = \frac{f\left(x,t_{j+1}\right) + f\left(x,t_{j}\right)}{2} + O\left((\Delta t)^3\right)$$

Lemma 6.3.1. ***(The minimum principle for the semi-discrete scheme)****. Assume that* $\left[L^M U(x)\right]^{j+1}$ *is the discrete operator given in (6.7) and* $\Psi^{j+1}(x)$ *is any mesh function satisfying* $\Psi^{j+1}(x) \geq 0$ *on* $\partial\Omega$ *and* $\left[L^M\Psi(x)^{j+1}\right] \leq 0$ *on* Ω *for* $0 \leq j \leq M$, *then* $\Psi^{j+1}(x) \geq 0$ *on* $\bar{\Omega}$

Proof. This Lemma can be proven using a proof by contradiction. Therefore, let $r^\star \in \Omega$ be any arbitrary point, such that $\Psi^{j+1}(r^\star) = \min_{x\in\Omega}\Psi^{j+1}(x)$. Again, suppose $\Psi^{j+1}(x) < 0$. It is clear that the set $((r^\star, t_{j+1}) \notin \{(0,t_{j+1}),(1,t_{j+1})\}$. Applying the concept of the calculus of several-variable functions, we obtain $(\Psi_{xx})^{j+1}(r^\star) \geq 0$, $(\varphi_x)^{j+1}(s^\star) = 0$. This gives $L^M\Psi(r^\star)^{j+1} > 0$ which contradict to the fact that $L^M\Psi(x)^{j+1} \leq 0$. Therefore, $\Psi^{j+1}(x) \geq 0$ on $\bar{\Omega}$ which is our claim. ■

Lemma 6.3.2. ***(The local error estimate).*** *Suppose that* $\|\frac{\partial^k u(x,t)}{\partial t^k}\| \leq C, (x,t) \in \overline{\Omega},\ k = 0,1,2$. *The local error estimate in temporal direction* $E_{j+1} = U^{j+1}(x) - u(x,t_{j+1})$ *is given by*

$$\left\|E_{j+1}\right\| \leq C(\Delta t)^3.$$

for sufficiently large constant C.

Proof. The time derivative is approximated by the fourth-order Taylor's series expansion of the Crank-Nicholson finite difference discretization in the temporal direction, given by:

$$\frac{U^{j+1}(x) - U^j(x)}{\Delta t} = U_t^{j+1/2}(x) + O((\Delta t)^3). \tag{6.8}$$

Upon substituting Eq. (6.8) into (6.1)-(6.2), we obtain the following equation

$$L_{\varepsilon,\mu} u(x,t_{j+1}) = u_t(x,t_{j+1}) + O((\Delta t)^3)$$

Furthermore, considering E_{k+1} as the semi-discrete minimum operator, we have

$$L^M_{\varepsilon,\mu} E(x,t_{j+1}) = O((\Delta t)^3)$$

Then, by using Lemma 6.3.1, the bound of the local error is estimated as $\left\|E_{j+1}\right\| \leq C(\Delta t)^3$ ■

Lemma 6.3.3 (**The global error estimation**). *The global error,* $G_j = U^j(x) - u(x,t_j$ *of the time discretization satisfies*

$$\left\|G_{j+1}\right\| \leq C(\Delta t)^2.$$

where C *is a constant independent of* ε, μ *and* Δt.

Proof. By using the estimation of local errors, the global error at $j+1$ nodal points is given as

$$\left\|G_{j+1}\right\| = \left\|\sum_{\xi=1}^{j} E_\xi\right\|, j(\Delta t) \leq T$$

$$\begin{aligned}
&= \left\|E_1 + E_2 + E_3 + E_4 + \ldots + E_j\right\| \\
&\leq \|E_1\| + \|E_2\| + \|E_3\| + \|E_4\| + \ldots + \left\|E_j\right\| \\
&\leq C_1(j)(\Delta t)^3 \\
&\leq C_1 \frac{T}{\Delta t}(\Delta t)^3 = C_1 T(\Delta t)^2, \ \text{ because } \ j \leq \frac{T}{\Delta t} \\
&\leq C(\Delta t)^2, \quad \text{where, } \ C = C_1 T
\end{aligned}$$

■

This lemma shows that the convergence of the semi-discrete scheme is order two in time.

6.3.2 Spatial discretization for full-discrete scheme

The given domain $\bar{\Omega}^N = [0,1]$ is subdivided into N sub-intervals such that

$$x_0 = 0, x_1 = x_0 + i = h, x_2 = x_1 + h, \cdots x_N = N(h) = 1$$

Now, the full discretized problem is

$$\begin{aligned}\left[L^{N,M}U\right]_i^j \equiv b(x_i,t_{j+1/2})\left(\frac{u\left(x_i,t_{j+1}\right)-u\left(x_i,t_j\right)}{\Delta t}\right) = \varepsilon u_{x_i x}\left(x_i,t_{j+1/2}\right)+ \\ \mu a(x_i,t_{j+1/2})u_x\left(x_i,t_{j+1/2}\right) \\ -c\left(x_i,t_{j+1/2}\right)u\left(x_i,t_{j+1/2}\right)-f\left(x_i,t_{j+1/2}\right)+O\left((\Delta t)^2\right)\}\end{aligned} \tag{6.9}$$

Using fitted finite difference methods the fully discrete scheme in (6.9) can be expressed as

$$\begin{aligned}\left[L^{N,M}U\right]_i^j \equiv \frac{1}{2}\left[\varepsilon\delta_x^2 U_i^{j+1}+\mu {a_i}^{j+1}D_x^+ U_i^{j+1}-{c_i}^{j+1}U_i^{j+1}+\varepsilon\delta_x^2 U_i^j+\mu {a_i}^j D_x^+ U_i^j-{c_i}^j U_i^j\right]- \\ {b_i}^{j+1/2}D_t U_i^{j+1/2} = F_i^j \quad i=0,1,2,\cdots,N-1, \quad j=0,1,2,\cdots,M-1\end{aligned} \tag{6.10}$$

where

$$D_x^+ U_i^j = \frac{U_{i+1}^j - U_i^j}{h_x}, \quad D_t U_i^{j+1/2} = \frac{U_i^{j+1}-U_i^j}{\Delta t} \qquad \delta_x^2 U_i^j = \left(\frac{U_{i+1}^j - 2U_i^j + u_{i-1}^j}{\phi_i^2}\right)$$

$$D_x^+ U_i^{j+1} = \frac{U_{i+1}^{j+1}-U_i^{j+1}}{h_x},$$

and

$$\delta_x^2 U_i^{j+1} = \left(\frac{U_{i+1}^{j+1} - 2U_i^{j+1} + u_{i-1}^{j+1}}{\phi_i^2}\right) \quad F_i^j = \frac{f\left(x_i,t_{j+1}\right)+f\left(x_i,t_j\right)}{2}$$

Again, from Munyakazi (2015), the denominator function ϕ_i^2 is given by

$$\phi_i^2(h,\varepsilon,\mu) \equiv \phi_i^2 = \frac{h\varepsilon}{\mu a\left(x_i\right)}\left(\exp\left(\frac{\mu a\left(x_i\right)h}{\varepsilon}\right)-1\right) \tag{6.11}$$

Using the finite difference schemes and the value of ϕ_i^2 above, Eq. (6.10) can be written in compact form as

$$\left[L^{N,M}U\right]_i^j \equiv \delta^+ U_{i+1}^{j+1} + \delta^c U_i^{j+1} + \delta^- U_{i-1}^{j+1} + \delta_1^+ U_{i+1}^j + \delta_1^c U_i^j + \delta_1^- U_{i-1}^j = F_i^j \qquad (6.12)$$

where, the coefficients $\delta^+, \delta_1^+, \delta^c, \delta_1^c, \delta^m$ and δ_1^m are

$$\delta^+ = \left(\frac{\varepsilon}{2\phi(i)^2} + \frac{\mu a_i^{j+1}}{2h}\right),\ \delta_1^+ = \left(\frac{\varepsilon}{2\phi(i)^2} + \frac{\mu a_i^{j}}{2h}\right),\ \delta^- = \delta_1^- = \frac{\varepsilon}{2\phi(i)^2}$$
$$\delta^c = \left(\frac{-\varepsilon}{\phi(i)^2} - \frac{\mu a_i^{j+1}}{2h} - \frac{c_i^{j+1}}{2} - \frac{b_i^{j+1}}{\Delta t}\right) \delta_1^c = \left(\frac{-\varepsilon}{\phi(i)^2} - \frac{\mu a_i^{j}}{2h} - \frac{c_i^{j}}{2} - \frac{b_i^{j}}{\Delta t}\right),$$

6.4 The convergence analysis of the numerical scheme

This section analyzed uniformly stability and uniformly convergence of the developed scheme.

Lemma 6.4.1. *(**Discrete minimum principle**) Assume that $\left[L^{N,M}U\right]_i^{j+1}$ is the discrete operator given in (4.11) and ϕ_i^{j+1} is any mesh function satisfying $\phi_i^{j+1} \geq 0$ on $\partial\Omega^{N,M}$ and $\left[L^{N,M}\phi\right]_i^{j+1} \leq 0$ on $\Omega^{N,M}$ for $0 \leq i \leq N$, $0 \leq j \leq M$, then $\phi_i^{j+1} \geq 0$ on $\bar{\Omega}^{N,M}$*

Proof. Let s and l be indices such that $\phi_s^{l+1} = \min_{(i,j)} \phi_i^{j+1}$, for $\phi_i^{j+1} \in \bar{\Omega}^{N,M}$. Again, assume that $\phi_s^{l+1} < 0$. It is clear to see that $(s,l) \notin \{1,N\} \times \{1,M\}$, because $\phi_s^{l+1} \geq 0$. It follows that $\phi_{s+1}^{l+1} - \phi_s^{l+1} > 0$ and $\phi_s^{l+1} - \phi_{s-1}^{l+1} < 0$.

$$L^{N,M}\phi_s^{l+1} = \varepsilon\left(\frac{\phi_{s+1}^{l+1} - 2\phi_s^{l+1} + \phi_{s-1}^{l+1}}{\phi_s^2}\right) + \mu a_s^{l+1}\left(\frac{\phi_{s+1}^{l} + \phi_s^{l+1}}{h_s}\right) - c_s^{l+1}\phi_s^{l+1}$$
$$L^{N,M}\phi_s^{l+1} = \varepsilon\left(\frac{\phi_{s+1}^{l+1} - \phi_s^{l+1} + \phi_{s-1}^{l+1} - \phi_{s+1}^{l+1}}{\frac{h\varepsilon}{\mu a(x_s)}\left(\exp\left(\frac{\mu a(x_s)h}{\varepsilon}\right) - 1\right)}\right) + \mu a_s^{l+1}\left(\frac{\phi_{s+1}^{l+1} + \phi_s^{l+1}}{h_s}\right) - c_s^{l+1}\phi_s^{l+1} > 0$$

which is a contradiction to the fact that $L^{N,M}\phi_s^{l+1} \leq 0$. Therefore $\phi_s^{l+1} \geq 0$. The indices s and l being arbitrary, we obtain $\phi_i^{j+1} \geq 0$ in $\bar{\Omega}^{N,M}$. ■

Lemma 6.4.2. *(**Uniform stability estimate**) At any time level t_j, if H_i^{j+1} is any mesh function such that $H_0^{j+1} = H_N^{j+1} = 0$, then*

$$\left|H_i^{j+1}\right| \leq \frac{1}{\Upsilon} \max_{1 \leq i \leq N-1} \left|L^{N,M}H_i^{j+1}\right|, \text{ for } 0 < j < M.$$

Theorem 6.4.1 (Error estimate in the spatial discretization). *Let $U(x_i, t_{j+1})$ and U_i^{j+1} are the exact solution and approximate solution of (6.1)-(6.2) respectively. If N and C are mesh*

numbers and sufficiently large constants, then the following error bound holds.

$$\left|L_{\varepsilon,\mu}^{N,M}\left(U(x_i,t_{j+1})-U_i^{j+1}\right)\right| \leq CN^{-1}. \tag{6.13}$$

Proof. To proof Lemma 6.4.2 and Theorem 6.4.1, follow the steps in (4.4.1). ■

Combining Lemma 4.3.3 and Theorem 4.4.1, we can state the following theorem as the main result of this paper.

Theorem 6.4.2. ***(The main result)*** *Let $u(x,t)$ be the exact solution of (6.1)- (6.2) and U_i^{j+1} is its numerical approximation obtained using (6.10). Then there exists a constant C independent of ε,μ, h and Δt such that*

$$\sup_{\varepsilon,\mu}\left[\max_{0\leq i\leq N,0\leq j\leq M}\left|U_i^{j+1}-u(x_i,t_{j+1})\right|\right] \leq C(h+(\Delta t)^2). \tag{6.14}$$

Proof. This Lemma can be proved by combining Lemma 6.3.3 and Theorem 6.4.1, and it confirms the developed method is uniformly convergent of second order in time and first order in space directions. ■

6.5 Numerical implementations and discussions

To demonstrate the applicability of the proposed scheme in (6.10), two examples are provided. The maximum absolute errors and numerical rate of convergence are calculated on the considered using the double mesh principle given in Doolan et al. (1980) as follows.

$$Err_{\varepsilon,\mu}^{N,M} = \max_{0\leq i,j\leq N,M}\left|U^{N,M}(x_i,\,t_j)-U^{2N,2M}(x_{2i},\,t_{2j})\right| \quad \text{(maximum absolute errors)}$$

$$Roc_{\varepsilon,\mu}^{N,M} = \log_2\left(\frac{Err_{\varepsilon,\mu}^{N,M}}{Err_{\varepsilon,\mu}^{2N,2M}}\right) \quad \text{(rate of convergence)}$$

Example 6.1. *Munyakazi (2015) We consider the following time-dependent problem*

$$\begin{aligned}
&\varepsilon\frac{\partial^2 u}{\partial x^2}+\mu(1+x)\frac{\partial u}{\partial x}-\frac{\partial u}{\partial t}-u=16x^2(1-x)^2, \quad (x,t)\in\Omega=(0,1)\times(0,1]\\
&u(x,0)=0, \quad x\in\bar{\Omega}_x=[0,1]\\
&u(0,t)=0, \quad u(1,t)=0, \quad t\in\bar{\Omega}_t=[0,1]
\end{aligned}$$

Example 6.2. *Das and Mehrmann (2016) For our second example, we consider the following time-dependent Initial Value Boundary Problem (IVBP) of*

$$u_t - \varepsilon u_{xx} + \mu(1+\exp(x))u_x + \left(1+x^4\,|x|\right)u = 10\exp\left(t^2\right)\left(x^2-x^4\right), (x,t) \in (0,1)\times(0,1]$$
$$u(x,0) = x^3(1-x)^3, \quad x \in (0,1)$$
$$u(0,t) = u(1,t) = 0, \quad t \in (0,1]$$

The exact solution of the two given problems is not known. So, we have used the developed scheme in (6.10) to solve such problems and to investigate the applicability of our scheme. Tables 6.1 and 6.2 show the result of Example 6.1 by using the scheme in (6.10). From these tables, results ensure that our scheme is first order which confirms the spatial order. But, by using temporal mesh refinement, we have improved this order to two as shown in Tables 6.3 and 6.4. Tables 6.6 and 6.7 show the numerical implementation of Example 6.2 using the developed scheme in (6.10), and the results from these tables show that the linear convergence of the scheme. Using a similar technique that we did in Tables 6.3 and 6.4, we modified the linear convergence of the scheme to quadratic convergence (see Table 6.8). A comparison of our scheme to existing schemes was done in Tables 6.5 and 6.9, and our scheme shows better accuracy than the existing schemes. Figure 6.1 and Figure 6.2 describe the graphical result of Example 6.1, while Figure 6.2 is for Example 6.2. The plotted figures exhibit that the boundary layer behavior in the solution of the given problem. Also, the log-log plots in Figure 6.3 are plotted for the considered examples, and these plots support our theoretical error estimates.

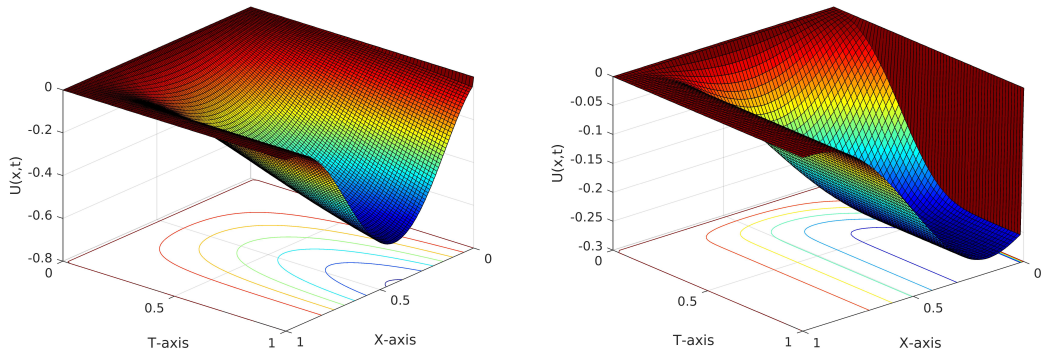

(a) (b)

Figure 6.1: Numerical results of Example 6.1 using scheme (6.10) (a) for $N = M = 64$, $\varepsilon = 2^{-20}$, $\mu = 2^{-3}$ and (b) for $N = M = 64, \varepsilon = 2^{-20}, \mu = 1$

Table 6.1: Maximum absolute errors, $Err_{\varepsilon,\mu}^{N,M}$ and rates of convergence, $Roc_{\varepsilon,\mu}^{N,M}$ using scheme (6.10) for Example 6.1 with $\mu = 2^{-3}$ and different values of ε.

	N $\rightarrow$	16	32	64	128	256
$\varepsilon \downarrow$	M $\rightarrow$	8	16	32	64	128
10^{0}	$Err_{\varepsilon,\mu}^{N,M}$	3.8894e-04	5.4676e-05	1.3382e-05	3.1627e-06	7.0143e-07
	$Roc_{\varepsilon,\mu}^{N,M}$	2.8306	2.0306	2.0811	2.1728	-
2^{-2}	$Err_{\varepsilon,\mu}^{N,M} \rightarrow$	2.9658e-03	1.4713e-03	7.4156e-04	3.6828e-04	1.8377e-04
	$Roc_{\varepsilon,\mu}^{N,M} \rightarrow$	1.0113	0.9885	1.0098	1.0029	-
2^{-4}	$Err_{\varepsilon,\mu}^{N,M} \rightarrow$	3.4955e-03	1.7391e-03	8.7940e-04	4.3455e-04	2.1807e-04
	$Roc_{\varepsilon,\mu}^{N,M} \rightarrow$	1.0072	0.9837	1.0170	0.9947	-
2^{-6}	$Err_{\varepsilon,\mu}^{N,M} \rightarrow$	3.6659e-03	1.8261e-03	9.2406e-04	4.5617e-04	2.2918e-04
	$Roc_{\varepsilon,\mu}^{N,M} \rightarrow$	1.0054	0.9827	1.0184	0.9931	-
2^{-8}	$Err_{\varepsilon,\mu}^{N,M} \rightarrow$	3.7438e-03	1.8710e-03	9.4711e-04	4.6727e-04	2.3476e-04
	$Roc_{\varepsilon,\mu}^{N,M} \rightarrow$	1.0007	0.9822	1.0193	0.9931	-
2^{-10}	$Err_{\varepsilon,\mu}^{N,M} \rightarrow$	3.7424e-03	1.8914e-03	9.7841e-04	4.8873e-04	2.4644e-04
	$Roc_{\varepsilon,\mu}^{N,M} \rightarrow$	0.9845	0.9509	1.0014	0.9878	-
2^{-12}	$Err_{\varepsilon,\mu}^{N,M} \rightarrow$	3.7399e-03	1.8728e-03	9.5354e-04	4.9208e-04	2.7039e-04
	$Roc_{\varepsilon,\mu}^{N,M} \rightarrow$	0.9978	0.9738	0.9544	0.8639	-
2^{-14}	$Err_{\varepsilon,\mu}^{N,M} \rightarrow$	3.7399e-03	1.8728e-03	9.5069e-04	4.6984e-04	2.3925e-04
	$Roc_{\varepsilon,\mu}^{N,M} \rightarrow$	0.9978	0.9781	1.0168	0.9912	-
2^{-16}	$Err_{\varepsilon,\mu}^{N,M} \rightarrow$	3.7399e-03	1.8728e-03	9.5069e-04	4.6983e-04	2.3635e-04
	$Roc_{\varepsilon,\mu}^{N,M} \rightarrow$	0.9978	0.9781	1.0168	0.9912	-
$\vdots$	$\vdots$	$\vdots$	$\vdots$	$\vdots$	$\vdots$	$\vdots$
2^{-40}	$Err_{\varepsilon,\mu}^{N,M}$	3.7399e-03	1.8728e-03	9.5069e-04	4.6983e-04	2.3635e-04
	$Roc_{\varepsilon,\mu}^{N,M}$	0.9978	0.9781	1.0168	0.9912	-
$Err_{\varepsilon,\mu}^{N,M}$	$\rightarrow$	3.7399e-03	1.8728e-03	9.5069e-04	4.6983e-04	2.3635e-04
$Roc_{\varepsilon,\mu}^{N,M}$	$\rightarrow$	0.9978	0.9781	1.0168	0.9912	-

Table 6.2: Maximum absolute errors, $Err_{\varepsilon,\mu}^{N,M}$ and rates of convergence, $Roc_{\varepsilon,\mu}^{N,M}$ using scheme (6.10) for Example 6.1 with $\varepsilon = 10^{-3}$ and different values of μ.

	N $\rightarrow$	16	32	64	128	256
$\mu \downarrow$	M $\rightarrow$	8	16	32	64	128
2^{0}	$Err_{\varepsilon,\mu}^{N,M}$	3.8894e-04	5.4676e-05	1.3382e-05	3.1627e-06	7.0143e-07
	$Roc_{\varepsilon,\mu}^{N,M}$	2.8306	2.0306	2.0811	2.1728	-
2^{-2}	$Err_{\varepsilon,\mu}^{N,M} \rightarrow$	3.3064e-03	1.6808e-03	8.2753e-04	4.1419e-04	2.0490e-04
	$Roc_{\varepsilon,\mu}^{N,M} \rightarrow$	0.9761	1.0223	0.9985	1.0154	-
2^{-4}	$Err_{\varepsilon,\mu}^{N,M} \rightarrow$	3.2956e-03	1.6376e-03	8.1657e-04	4.1055e-04	2.0407e-04
	$Roc_{\varepsilon,\mu}^{N,M} \rightarrow$	1.0090	1.0039	0.9920	1.0085	-
2^{-6}	$Err_{\varepsilon,\mu}^{N,M} \rightarrow$	3.2919e-03	1.6359e-03	8.1575e-04	4.0737e-04	2.0356e-04
	$Roc_{\varepsilon,\mu}^{N,M} \rightarrow$	1.0088	1.0039	1.0018	1.0009	-
2^{-8}	$Err_{\varepsilon,\mu}^{N,M} \rightarrow$	3.2909e-03	1.6354e-03	8.1552e-04	4.0725e-04	2.0350e-04
	$Roc_{\varepsilon,\mu}^{N,M} \rightarrow$	1.0088	1.0039	1.0018	1.0009	-
2^{-10}	$Err_{\varepsilon,\mu}^{N,M} \rightarrow$	3.2906e-03	1.6353e-03	8.1547e-04	4.0722e-04	2.0349e-04
	$Roc_{\varepsilon,\mu}^{N,M} \rightarrow$	1.0088	1.0039	1.0018	1.0009	-
2^{-12}	$Err_{\varepsilon,\mu}^{N,M} \rightarrow$	3.2906e-03	1.6353e-03	8.1547e-04	4.0722e-04	2.0349e-04
	$Roc_{\varepsilon,\mu}^{N,M} \rightarrow$	1.0088	1.0039	1.0018	1.0009	-
2^{-14}	$Err_{\varepsilon,\mu}^{N,M} \rightarrow$	3.2906e-03	1.6353e-03	8.1547e-04	4.0722e-04	2.0349e-04
	$Roc_{\varepsilon,\mu}^{N,M} \rightarrow$	1.0088	1.0039	1.0018	1.0009	-
$\vdots$	$\vdots$	$\vdots$	$\vdots$	$\vdots$	$\vdots$	$\vdots$
2^{-30}	$Err_{\varepsilon,\mu}^{N,M}$	3.7399e-03	1.8728e-03	9.5069e-04	4.6983e-04	2.3635e-04
	$Roc_{\varepsilon,\mu}^{N,M}$	1.0088	1.0039	1.0018	1.0009	-
$Err_{\varepsilon,\mu}^{N,M}$	$\rightarrow$	3.7399e-03	1.8728e-03	9.5069e-04	4.6983e-04	2.3635e-04
$Roc_{\varepsilon,\mu}^{N,M}$	$\rightarrow$	1.0088	1.0039	1.0018	1.0009	-

Table 6.3: Maximum absolute errors, $Err_{\varepsilon,\mu}^{N,M}$ and rates of convergence, $Roc_{\varepsilon,\mu}^{N,M}$ using scheme (6.10) for Example 6.1 with $\mu = 10^{-3}$ and different values of ε.

	N $\rightarrow$	16	32	64	128
$\varepsilon \downarrow$	M $\rightarrow$	8	32	128	512
10^{0}	$Err_{\varepsilon,\mu}^{N,M} \rightarrow$	3.7154e-04	5.1172e-05	1.2743e-05	3.1831e-06
	$Roc_{\varepsilon,\mu}^{N,M} \rightarrow$	2.8601	2.0056	2.0012	-
10^{-2}	$Err_{\varepsilon,\mu}^{N,M} \rightarrow$	3.1715e-02	7.4881e-03	1.8460e-03	4.5989e-04
	$Roc_{\varepsilon,\mu}^{N,M} \rightarrow$	2.0825	2.0202	2.0050	-
10^{-4}	$Err_{\varepsilon,\mu}^{N,M} \rightarrow$	3.6848e-02	8.7688e-03	2.1682e-03	5.4171e-04
	$Roc_{\varepsilon,\mu}^{N,M} \rightarrow$	2.0711	2.0159	2.0009	-
10^{-6}	$Err_{\varepsilon,\mu}^{N,M} \rightarrow$	3.6921e-02	8.8083e-03	2.1882e-03	5.5165e-04
	$Roc_{\varepsilon,\mu}^{N,M} \rightarrow$	2.0675	2.0091	1.9879	-
10^{-8}	$Err_{\varepsilon,\mu}^{N,M} \rightarrow$	3.6921e-02	8.8083e-03	2.1882e-03	5.5165e-04
	$Roc_{\varepsilon,\mu}^{N,M} \rightarrow$	2.0675	2.0091	1.9879	-
10^{-10}	$Err_{\varepsilon,\mu}^{N,M} \rightarrow$	3.6921e-02	8.8083e-03	2.1882e-03	5.5165e-04
	$Roc_{\varepsilon,\mu}^{N,M} \rightarrow$	2.0675	2.0091	1.9879	-
10^{-12}	$Err_{\varepsilon,\mu}^{N,M} \rightarrow$	3.6921e-02	8.8083e-03	2.1882e-03	5.5165e-04
	$Roc_{\varepsilon,\mu}^{N,M} \rightarrow$	2.0675	2.0091	1.9879	-
10^{-14}	$Err_{\varepsilon,\mu}^{N,M} \rightarrow$	3.6921e-02	8.8083e-03	2.1882e-03	5.5165e-04
	$Roc_{\varepsilon,\mu}^{N,M} \rightarrow$	2.0675	2.0091	1.9879	-
10^{-16}	$Err_{\varepsilon,\mu}^{N,M} \rightarrow$	3.6921e-02	8.8083e-03	2.1882e-03	5.5165e-04
	$Roc_{\varepsilon,\mu}^{N,M} \rightarrow$	2.0675	2.0091	1.9879	-
10^{-18}	$Err_{\varepsilon,\mu}^{N,M} \rightarrow$	3.6921e-02	8.8083e-03	2.1882e-03	5.5165e-04
	$Roc_{\varepsilon,\mu}^{N,M} \rightarrow$	2.0675	2.0091	1.9879	-
$\vdots$	$\vdots$	$\vdots$	$\vdots$	$\vdots$	$\vdots$
10^{-20}	$Err_{\varepsilon,\mu}^{N,M} \rightarrow$	3.6921e-02	8.8083e-03	2.1882e-03	5.5165e-04
	$Roc_{\varepsilon,\mu}^{N,M} \rightarrow$	2.0675	2.0091	1.9879	-
$Err_{\varepsilon,\mu}^{N,M}$	$\rightarrow$	3.6921e-02	8.8083e-03	2.1882e-03	5.5165e-04
$Roc_{\varepsilon,\mu}^{N,M}$	$\rightarrow$	2.0675	2.0091	1.9879	-

Table 6.4: Maximum absolute errors, $Err_{\varepsilon,\mu}^{N,M}$ and rates of convergence, $Roc_{\varepsilon,\mu}^{N,M}$ using scheme (6.10) for Example 6.1 with $\mu = 10^{-3}$ and different values of μ.

	N $\rightarrow$	16	32	64	128
$\varepsilon \downarrow$	M $\rightarrow$	8	32	128	512
10^{-2}	$Err_{\varepsilon,\mu}^{N,M} \rightarrow$	3.6681e-02	8.7863e-03	2.3760e-03	5.6170e-04
	$Roc_{\varepsilon,\mu}^{N,M} \rightarrow$	2.0617	1.8867	2.0807	-
10^{-4}	$Err_{\varepsilon,\mu}^{N,M} \rightarrow$	3.6290e-02	8.6223e-03	2.1288e-03	5.3056e-04
	$Roc_{\varepsilon,\mu}^{N,M} \rightarrow$	2.0734	2.0180	2.0045	-
10^{-6}	$Err_{\varepsilon,\mu}^{N,M} \rightarrow$	3.6288e-02	8.6218e-03	2.1287e-03	5.3053e-04
	$Roc_{\varepsilon,\mu}^{N,M} \rightarrow$	2.0734	2.0180	2.0045	-
10^{-8}	$Err_{\varepsilon,\mu}^{N,M} \rightarrow$	3.6288e-02	8.6218e-03	2.1287e-03	5.3053e-04
	$Roc_{\varepsilon,\mu}^{N,M} \rightarrow$	2.0734	2.0180	2.0045	-
10^{-10}	$Err_{\varepsilon,\mu}^{N,M} \rightarrow$	3.6288e-02	8.6218e-03	2.1287e-03	5.3053e-04
	$Roc_{\varepsilon,\mu}^{N,M} \rightarrow$	2.0734	2.0180	2.0045	-
$\vdots$	$\vdots$	$\vdots$	$\vdots$	$\vdots$	$\vdots$
10^{-20}	$Err_{\varepsilon,\mu}^{N,M} \rightarrow$	3.6288e-02	8.6218e-03	2.1287e-03	5.3053e-04
	$Roc_{\varepsilon,\mu}^{N,M} \rightarrow$	2.0734	2.0180	2.0045	-
$Err_{\varepsilon,\mu}^{N,M}$	$\rightarrow$	3.6288e-02	8.6218e-03	2.1287e-03	5.3053e-04
$Roc_{\varepsilon,\mu}^{N,M}$	$\rightarrow$	2.0734	2.0180	2.0045	-

Table 6.5: Comparison of $Err_{\varepsilon,\mu}^{N,M}$ of our scheme in (6.10) with an existing schemes in Munyakazi (2015) using Example 6.1

$\mu = 10^{-2}$, $(N = M) \rightarrow$	16	32	64	128	256
$\varepsilon \downarrow$ **Proposed method**					
2^{-2}	3.5408e-03	1.4406e-03	7.2367e-04	3.6274e-04	1.8160e-04
2^{-6}	7.6891e-03	3.5741e-03	1.6758e-03	8.3861e-04	4.1005e-04
2^{-8}	8.8804e-03	4.8270e-03	2.3954e-03	1.1960e-03	5.9488e-04
scheme in Munyakazi (2015)					
2^{-2}	7.10e-3	3.11e-3	1.44e-3	6.89e-4	3.37e-4
2^{-6}	1.95e-2	7.29e-3	2.91e-3	1.27e-3	5.89e-4
2^{-8}	3.21e-2	1.31e-2	4.91e-3	1.92e-3	8.19e-4

Table 6.6: Maximum absolute errors, $Err_{\varepsilon,\mu}^{N,M}$ and rates of convergence, $Roc_{\varepsilon,\mu}^{N,M}$ using scheme (6.10) for Example 6.2 with $\mu = 10^{-2}$ and different values of ε.

	N $\rightarrow$	32	64	128	256	512
$\varepsilon \downarrow$	M $\rightarrow$	8	16	32	64	128
10^{-2}	$Err_{\varepsilon,\mu}^{N,M} \rightarrow$	4.8396e-03	2.4330e-03	1.2184e-03	6.0984e-04	3.0505e-04
	$Roc_{\varepsilon,\mu}^{N,M} \rightarrow$	0.9922	0.9977	0.9985	0.9994	-
10^{-4}	$Err_{\varepsilon,\mu}^{N,M} \rightarrow$	4.8440e-03	2.4340e-03	1.2186e-03	6.0991e-04	3.0506e-04
	$Roc_{\varepsilon,\mu}^{N,M} \rightarrow$	0.9929	0.9981	0.9986	0.9995	-
10^{-6}	$Err_{\varepsilon,\mu}^{N,M} \rightarrow$	4.8440e-03	2.4340e-03	1.2186e-03	6.0990e-04	3.0506e-04
	$Roc_{\varepsilon,\mu}^{N,M} \rightarrow$	0.9929	0.9981	0.9986	0.9995	-
10^{-8}	$Err_{\varepsilon,\mu}^{N,M} \rightarrow$	4.8440e-03	2.4340e-03	1.2186e-03	6.0990e-04	3.0506e-04
	$Roc_{\varepsilon,\mu}^{N,M} \rightarrow$	0.9929	0.9981	0.9986	0.9995	-
10^{-10}	$Err_{\varepsilon,\mu}^{N,M} \rightarrow$	4.8440e-03	2.4340e-03	1.2186e-03	6.0990e-04	3.0506e-04
	$Roc_{\varepsilon,\mu}^{N,M} \rightarrow$	0.9929	0.9981	0.9986	0.9995	-
$\vdots$	$\vdots$	$\vdots$	$\vdots$	$\vdots$	$\vdots$	$\vdots$
10^{-40}	$Err_{\varepsilon,\mu}^{N,M}$	4.8440e-03	2.4340e-03	1.2186e-03	6.0990e-04	3.0506e-04
	$Roc_{\varepsilon,\mu}^{N,M} \rightarrow$	0.9929	0.9981	0.9986	0.9995	-
$Err_{\varepsilon,\mu}^{N,M}$	$\rightarrow$	4.8440e-03	2.4340e-03	1.2186e-03	6.0990e-04	3.0506e-04
$Roc_{\varepsilon,\mu}^{N,M}$	$\rightarrow$	0.9929	0.9981	0.9986	0.9995	-

Table 6.7: Maximum absolute errors, $Err_{\varepsilon,\mu}^{N,M}$ and rates of convergence, $Roc_{\varepsilon,\mu}^{N,M}$ using scheme (6.10) for Example 6.2 with $\varepsilon = 10^{-2}$ and different values of μ.

	N $\rightarrow$	32	64	128	256	512
$\mu \downarrow$	M $\rightarrow$	8	16	32	64	128
10^{-2}	$Err_{\varepsilon,\mu}^{N,M} \rightarrow$	4.8396e-03	2.4330e-03	1.2184e-03	6.0984e-04	3.0505e-04
	$Roc_{\varepsilon,\mu}^{N,M} \rightarrow$	0.9922	0.9977	0.9985	0.9994	-
10^{-4}	$Err_{\varepsilon,\mu}^{N,M} \rightarrow$	4.8396e-03	2.4329e-03	1.2183e-03	6.0983e-04	3.0505e-04
	$Roc_{\varepsilon,\mu}^{N,M} \rightarrow$	0.9922	0.9978	0.9984	0.9994	-
10^{-6}	$Err_{\varepsilon,\mu}^{N,M} \rightarrow$	4.8396e-03	2.4329e-03	1.2183e-03	6.0983e-04	3.0505e-04
	$Roc_{\varepsilon,\mu}^{N,M} \rightarrow$	0.9922	0.9978	0.9984	0.9994	-
10^{-8}	$Err_{\varepsilon,\mu}^{N,M} \rightarrow$	4.8396e-03	2.4329e-03	1.2183e-03	6.0983e-04	3.0505e-04
	$Roc_{\varepsilon,\mu}^{N,M} \rightarrow$	0.9922	0.9978	0.9984	0.9994	-
10^{-10}	$Err_{\varepsilon,\mu}^{N,M} \rightarrow$	4.8396e-03	2.4329e-03	1.2183e-03	6.0983e-04	3.0505e-04
	$Roc_{\varepsilon,\mu}^{N,M} \rightarrow$	0.9922	0.9978	0.9984	0.9994	-
$\vdots$	$\vdots$	$\vdots$	$\vdots$	$\vdots$	$\vdots$	$\vdots$
10^{-40}	$Err_{\varepsilon,\mu}^{N,M}$	4.8396e-03	2.4329e-03	1.2183e-03	6.0983e-04	3.0505e-04
	$Roc_{\varepsilon,\mu}^{N,M} \rightarrow$	0.9922	0.9978	0.9984	0.9994	-
$Err_{\varepsilon,\mu}^{N,M}$	$\rightarrow$	4.8396e-03	2.4329e-03	1.2183e-03	6.0983e-04	3.0505e-04
$Roc_{\varepsilon,\mu}^{N,M}$	$\rightarrow$	0.9922	0.9978	0.9984	0.9994	-

Table 6.8: Maximum absolute errors, $Err_{\varepsilon,\mu}^{N,M}$ and rates of convergence, $Roc_{\varepsilon,\mu}^{N,M}$ using scheme (6.10) for Example 6.2 with $\mu = 10^{-3}$ and different values of ε.

	N $\rightarrow$	32	64	128	256
$\varepsilon \downarrow$	M $\rightarrow$	16	64	256	1024
10^{-4}	$Err_{\varepsilon,\mu}^{N,M} \rightarrow$	6.2804e-02	1.6164e-02	4.0679e-03	1.0188e-03
	$Roc_{\varepsilon,\mu}^{N,M} \rightarrow$	1.9581	1.9904	1.9974	-
10^{-6}	$Err_{\varepsilon,\mu}^{N,M} \rightarrow$	6.2807e-02	1.6165e-02	4.0682e-03	1.0189e-03
	$Roc_{\varepsilon,\mu}^{N,M} \rightarrow$	1.9581	1.9904	1.9974	-
10^{-8}	$Err_{\varepsilon,\mu}^{N,M} \rightarrow$	6.2807e-02	1.6165e-02	4.0682e-03	1.0189e-03
	$Roc_{\varepsilon,\mu}^{N,M} \rightarrow$	1.9581	1.9904	1.9974	-
$\vdots$	$\vdots$	$\vdots$	$\vdots$	$\vdots$	$\vdots$
10^{-20}	$Err_{\varepsilon,\mu}^{N,M} \rightarrow$	6.2807e-02	1.6165e-02	4.0682e-03	1.0189e-03
	$Roc_{\varepsilon,\mu}^{N,M} \rightarrow$	1.9581	1.9904	1.9974	-
$Err_{\varepsilon,\mu}^{N,M}$	$\rightarrow$	6.2807e-02	1.6165e-02	4.0682e-03	1.0189e-03
$Roc_{\varepsilon,\mu}^{N,M}$	$\rightarrow$	1.9581	1.9904	1.9974	-

Table 6.9: Comparison of $Err_{\varepsilon,\mu}^{N,M}$ of our scheme in (6.10) with an existing schemes in Das and Mehrmann (2016) using Example 6.2

$\mu = 10^{-4}$, $(N) \rightarrow$	64	128	256	512
$(M) \rightarrow$	16	32	64	128
$\varepsilon \downarrow$ **Proposed method**				
10^{-2}	2.4330e-03	1.2184e-03	6.0984e-04	3.0505e-04
10^{-4}	2.4340e-03	1.2186e-03	6.0991e-04	3.0506e-04
scheme in Das and Mehrmann (2016)				
10^{-2}	2.2542e-2	1.1005e-2	5.3920e-3	2.6870e-3
10^{-4}	2.4125e-2	1.1985e-2	5.9160e-3	2.9660e-3

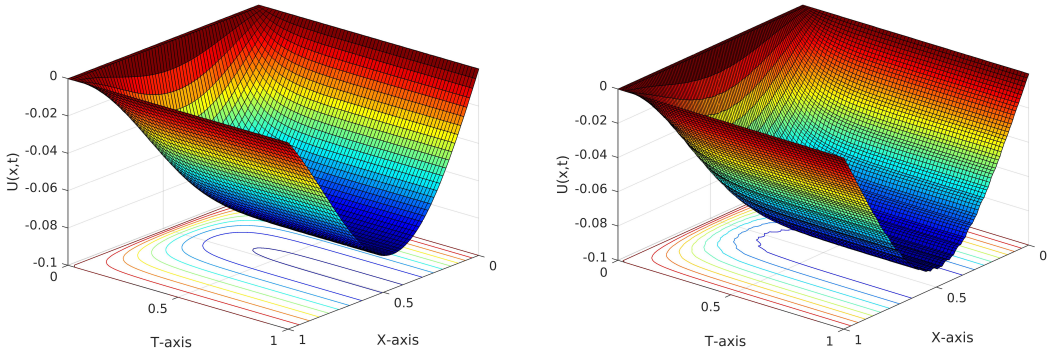

(a) (b)

Figure 6.2: Numerical results of Example 6.1 using scheme (6.10) (a) for $N = M = 64$, $\varepsilon = 1 = \mu$ and (b) for $N = 128, M = 64, \varepsilon = 1, \mu = 2^{-40}$

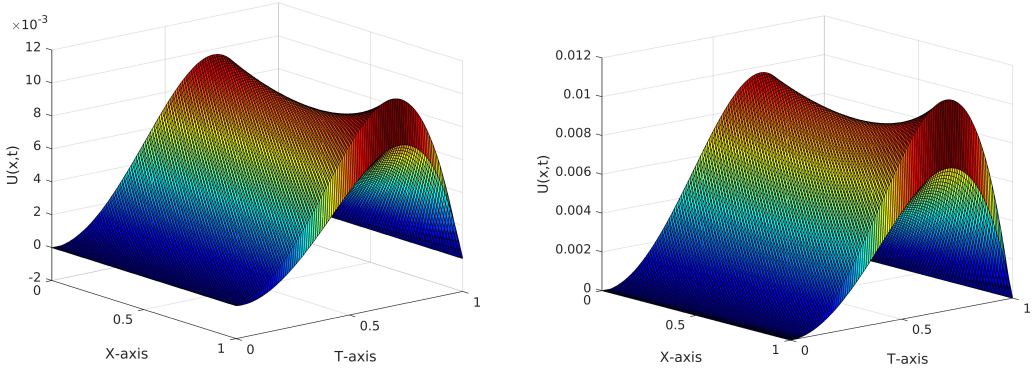

(a) (b)

Figure 6.3: Numerical results of Example 6.2 using scheme (6.10) (a) for $N = 128 = M$, $\varepsilon = \mu = 2^{-2}$ and (b) for $N = 128 = M, \varepsilon = \mu = 2^{-12}$

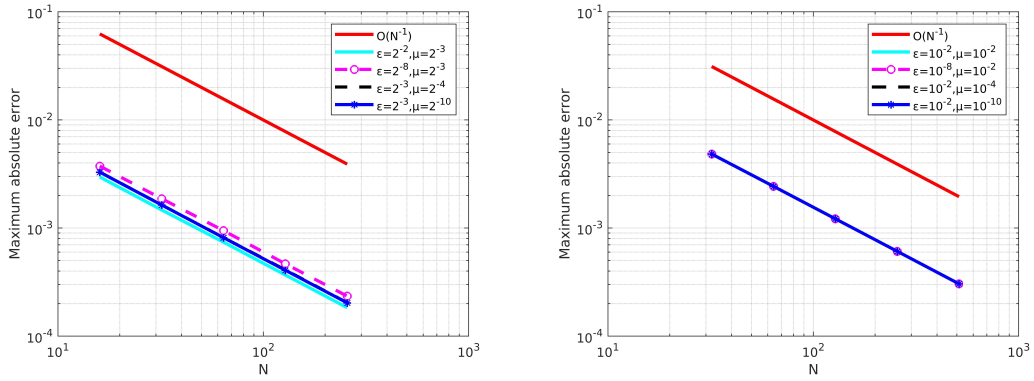

(a) (b)

Figure 6.4: Log-Log plots of (a) Example 6.1 and (b) Example 6.2

6.6 Summary

In this chapter, a fitted operator finite difference method (FOFDM) for solving singularly perturbed partial differential equations with two perturbation parameters are formulated. A uniform mesh has been considered in both space and time directions while we discretized the given domain. The discretization used the Crank-Nicolson method for time variable and nonstandard finite difference method (NSFDM) for space variable. The proposed the numerical method is uniformly convergent and independent of both the perturbation parameters, ε and μ. The scheme is shown to be first order in space and second order in time theoretically. To confirm the theoretical convergence results and to demonstrate the applicability of the proposed scheme, we have implemented two tested examples, and results have been provided and presented in tables and graphs. The numerical examples and the graphical results confirm the theoretical analyses and findings.

CHAPTER 7

A STABLE NUMERICAL TECHNIQUE FOR SOLVING NONLINEAR TWO-PARAMETER SINGULARLY PERTURBED PDES

In this chapter, a new numerical approach is developed for a nonlinear two-parameter singularly perturbed initial-boundary value problem. The implicit backward Euler's discretization for time derivative and the fitted operator technique in the the spatial domain are employed. Newton's quasilinearization technique is carried out for the nonlinear terms. Investigation of parameter-uniform error estimates shows that the developed approach is first-order accurate in both time and space. But temporal mesh refinement technique is introduced to improve the order of accuracy to two. Two examples are provided and implemented in Python to validate the applicability of the method and results are displayed in tables and graphs.

7.1 The governing problem

The nonlinear two-parameter problem in the domain $D = (0,1) \times (0,T]$ is considered as

$$\begin{cases} Lu(x,t) + u_t(x,t) = f(x,t), \ (x,t) \in D, \\ u(x,0) = g(x), \ \ x \in D_x = (0,1), \\ u(0,t) = s(t), \ \ u(1,t) = m(t), \ \ t \in D_t = [0,T], \end{cases} \tag{7.1}$$

where $Lu(x,t) \equiv -\varepsilon u_{xx}(x,t) + \mu a(x,t)u(x,t)u_x(x,t) - b(x,t)(u^2(x,t))$, $0 < \varepsilon \leq 1$ and $0 \leq \mu \leq 1$ are perturbation parameters. The coefficient functions $a(x,t), b(x,t)$ and $f(x,t)$, $(x,t) \in \bar{D}$, the initial function $g(x)$ for $x \in \bar{D}_x$, and the functions $s(t)$ and $m(t)$ for $t \in \bar{D}_t$ are assumed to be sufficiently smooth, and bounded with $a(x,t) \geq \alpha > 0$ and $b(x,t) \geq \beta > 0$. Also, we assume the compatibility conditions of the data at the corners, that means $u(0,0) = s(0)$ and $u(1,0) = m(0)$.

7.1.1 Properties of the continuous problem

Lemma 7.1.1. Assume $\Psi(x,t) \in C^{2,1}\bar{D}$. If $\Psi|_{\partial D} \geq 0$ and $\left(L_{\varepsilon,\mu} + \dfrac{\partial}{\partial t}\right)\Psi|_D \geq 0$, then $\Psi|_{\bar{D}} \geq 0$.

Proof. Let $(x^\star, t^\star)$ be an arbitrary point in the domain $D = (0,1) \times (0,T)$ such that $\Psi(x^\star, t^\star) =$

$\min\{\Psi(x,t)\}_{(x,t)\in\bar{D}}$. We will assume that $\Psi(x^\star,t^\star)<0$. Since $(x^\star,t^\star)\notin\{0,1\}\times\{0,T\}$, we can apply the first and second derivative tests for multivariable functions and use the definition of $(x^\star,t^\star)$ to obtain the following properties:

$$\Psi_{xx}(x^\star,t^\star)\geq 0,\quad \nabla_x\Psi(x^\star,t^\star)=0,\quad \nabla_t\Psi(x^\star,t^\star)=0.$$

Hence,

$$\left(L_{\varepsilon,\mu}+\frac{\partial}{\partial t}\right)\Psi|_D=-\varepsilon\Psi_{xx}(x^\star,t^\star)+\mu a(x^\star,t^\star)\Psi(x^\star,t^\star)\nabla_x\Psi(x^\star,t^\star)\quad -b(x^\star,t^\star)(\Psi(x^\star,t^\star))^2+\nabla_t\Psi(x^\star,t^\star)$$

Since $\Psi_{xx}(x^\star,t^\star)\geq 0$ and $\nabla_x\Psi(x^\star,t^\star)=0$, the terms involving these derivatives become zero. Additionally, $\nabla_t\Psi(x^\star,t^\star)=0$. Hence;

$$\left(L_{\varepsilon,\mu}+\frac{\partial}{\partial t}\right)\Psi|_D=\underbrace{-\varepsilon\Psi_{xx}(x^\star,\,t^\star)}_{\leq 0}+\underbrace{\mu a(x^\star,\,t^\star)\Psi(x^\star,\,t^\star)\nabla_x\Psi(x^\star,t^\star)}_{=0}\underbrace{-b(x^\star,t^\star)(\Psi(x^\star,\,t^\star))^2}_{\leq 0}\underbrace{+\nabla_t\Psi(x^\star,t^\star)}_{=0} \tag{7.2}$$

$$\leq 0.$$

where the inequality follows from $\varepsilon>0$ and $(\Psi(x^\star,t^\star))^2\geq 0$. However, this contradicts our assumption that $\left(L_{\varepsilon,\mu}+\frac{\partial}{\partial t}\right)\Psi|_D\geq 0$. Here, our initial assumption that $\Psi(x^\star,t^\star)<0$ is incorrect. Hence, we conclude that $\Psi(x^\star,t^\star)|_{\bar{D}}\geq 0$. As $(x^\star,t^\star)$ was chosen arbitrarily, it follows that $\Psi(x,t)\geq 0$ for all $(x,t)\in\bar{D}$. ■

Due to the prevalence of multiple solutions in most nonlinear problems, the task of obtaining a unique solution becomes challenging when studying nonlinear TPSPPs. Consequently, we introduce the following theorem, which assures that the considered problem possesses a unique solution.

Theorem 7.1.1 (**Existence and Uniqueness**). *The problem given in (7.1) possesses a unique solution.*

Proof. To prove this theorem, we need to define an energy function. We can define by introducing a suitable function that captures the energy or Lyapunov-like structure of the problem as follows.

$$E(t)=\frac{-\varepsilon}{2}\int_0^1 u_x^2(x,t)dx+\frac{\mu\alpha}{2}\int_0^1 u^2(x,t)dx-\frac{\beta}{3}\int_0^1 u^3(x,t)dx. \tag{7.3}$$

Taking the derivative of (7.3), we have:

$$E'(t) = -\varepsilon \int_0^1 u_x(x,t)u_{xt}(x,t)dx + \mu\alpha \int_0^1 u(x,t)u_t(x,t)dx - \beta \int_0^1 u^2(x,t)u_t(x,t)dx. \quad (7.4)$$

Using integration by parts and utilizing the value of $u_t(x,t)$ from (7.1), we obtain

$$-\varepsilon \int_0^1 u_x^2(x,t)dx = -\varepsilon \left(u_x(x,t)u_t(x,t) - \int_0^1 u_t(x,t)u_{xx}(x,t)dx \right) \quad (7.5)$$

$$\mu\alpha \int_0^1 u(x,t)u_t(x,t)dx = \mu\alpha \int_0^1 u(x,t)\left(\varepsilon u_{xx}(x,t) - \mu a(x,t)u(x,t)u_x(x,t) + b(x,t)(u(x,t))^2 + f(x,t)\right)dx \quad (7.6)$$

$$-\beta \int_0^1 u^2(x,t)u_t(x,t)dx = -\beta \int_0^1 u^2(x,t)\left(\varepsilon u_{xx}(x,t) - \mu a(x,t)u(x,t)u_x(x,t) + b(x,t)(u(x,t))^2 + f(x,t)\right)dx. \quad (7.7)$$

This will allow us to express (7.4) in a different form.

$$\begin{aligned} E'(t) = &-\varepsilon \left(u_x(x,t)u_t(x,t) - \int_0^1 u_t(x,t)u_{xx}(x,t)dx \right) + \\ &\mu\alpha \int_0^1 u(x,t)\left(\varepsilon u_{xx}(x,t) - \mu a(x,t)u(x,t)u_x(x,t) + b(x,t)(u(x,t))^2 + f(x,t)\right)dx \\ &-\beta \int_0^1 u^2(x,t)\left(\varepsilon u_{xx}(x,t) - \mu a(x,t)u(x,t)u_x(x,t) + b(x,t)(u(x,t))^2 + f(x,t)\right)dx. \end{aligned} \quad (7.8)$$

Equation (7.8) becomes

$$\begin{aligned} E'(t) = &-\varepsilon \int_0^1 u_t(x,t)u_{xt}(x,t)dx + \\ &\mu\alpha \int_0^1 u(x,t)\left(\varepsilon u_{xx}(x,t) - \mu a(x,t)u(x,t)u_x(x,t) + b(x,t)(u(x,t))^2 + f(x,t)\right)dx \\ &-\beta \int_0^1 u^2(x,t)\left(\varepsilon u_{xx}(x,t) - \mu a(x,t)u(x,t)u_x(x,t) + b(x,t)(u(x,t))^2 + f(x,t)\right)dx \end{aligned} \quad (7.9)$$

Using Cauchy-Schwarz and Hölder's inequalities, we can bound the integral terms in Equation (7.9).

$$\begin{aligned} &\left| \int u_x u_{xt}\, dx \right| \le \sqrt{\int (u_x)^2\, dx}\sqrt{\int (u_{xt})^2\, dx} = \|u_x\|_{L_2(\Omega)}\|u_{xt}\|_{L_2(\Omega)} \\ &\left| \int u(f + \varepsilon u_{xx} - \mu\alpha u u_x + \beta u^2)\, dx \right| \le \|u\|_{L_p(\Omega)}\|f + \varepsilon u_{xx} - \mu\alpha u u_x + \beta u^2\|_{L_q(\Omega)} \\ &\left| \int u^2(f + \varepsilon u_{xx} - \mu\alpha u u_x + \beta u^2)\, dx \right| \le \|u^2\|_{L_p(\Omega)}\|f + \varepsilon u_{xx} - \mu\alpha u u_x + \beta u^2\|_{L_q(\Omega)} \end{aligned} \quad (7.10)$$

To obtain the overall bounds for the integrals in equation (7.10), we need to combine the individual bounds for each integral.

$$E'(t) \leq -\varepsilon \left(\|u_x\|_{L_2(\Omega)} \|u_{xt}\|_{L_2(\Omega)} \right) + \mu\alpha \left(\|u\|_{L_p(\Omega)} \|f + \varepsilon u_{xx} - \mu\alpha u u_x + \beta u^2\|_{L_q(\Omega)} \right) \\ -\beta \left(\|u^2\|_{L_p(\Omega)} \|f + \varepsilon u_{xx} - \mu\alpha u u_x + \beta u^2\|_{L_q(\Omega)} \right). \tag{7.11}$$

We are considering the case where $\varepsilon + \beta \leq \mu\alpha$ to estimate the terms on the right-hand side. This leads to

$$\frac{dE}{dt} \leq 0. \tag{7.12}$$

Hence,

$$E(t) \leq E(0) \quad \text{for } 0 \leq t \leq T. \tag{7.13}$$

Again, if we consider the case $3\varepsilon + 2\beta \leq 3\mu\alpha$, we get

$$E(t) \geq E(0) \quad \text{for } 0 \leq t \leq T. \tag{7.14}$$

Now, combining (7.13) and (7.14), we have

$$E(t) = 0. \tag{7.15}$$

Now, let us assume the given problem in (7.1) has two distinct solutions, say u and v. Again, define difference function $w(x,t)$ that satisfies the given conditions of (7.1) such that $w(x,t) = u(x,t) - v(x,t)$. Then substituting $w(x,t)$ in (7.3), and using the result in (7.15), we have:

$$E(w(x,t)) = 0 \Rightarrow \frac{-\varepsilon}{2} \int_0^1 w_x^2(x,t)dx + \frac{\mu\alpha}{2} \int_0^1 w^2(x,t)dx - \frac{\beta}{3} \int_0^1 w^3(x,t)dx = 0.$$
$$w(x,t) = 0$$
$$u(x,t) - v(x,t) = 0$$
$$u(x,t) = v(x,t),$$

and this contradicts to our assumption problem in (7.1) has two distinct solutions. Therefore, the problem in (7.1) has a unique solution. ■

Lemma 7.1.2 (Continuous uniform stability estimate). *Assume $u(x,t)$ is the solution of (7.1). For any $\varepsilon > 0$ and $\mu \geq 0$, it follows that*

$$\|u\|_{\bar{D}} \leq \beta^{-1}\|f\|_{\bar{D}} + \|u\|_{\partial D}.$$

Proof. We define two comparison functions as

$$\varphi^{\pm}(x,t) = \beta^{-1}\|f\|_{\bar{D}} + \|u\|_{\partial D} \pm u(x,t) \quad \text{for all } (x,t) \in \bar{D}.$$

Now, let's investigate the behavior of $\varphi^{\pm}$ on the boundary of D:

$$\begin{aligned} \text{When } x = 0, \quad \varphi^{\pm}(0,t) &= \beta^{-1}\|f\|_{\bar{D}} + \|u\|_{\partial D} \pm u(0,t) \\ &= \beta^{-1}\|f\|_{\bar{D}} + \|u\|_{\partial D} \pm s(t), \end{aligned}$$

where $s(t)$ is the boundary function at $x = 0$. Since $s(t) \geq 0$, we have $\varphi^{\pm}(0,t) \geq 0$.
Similarly, when $x = 1$, we have $\varphi^{\pm}(1,t) \geq 0$. Therefore, we have shown that $\varphi^{\pm}(x,t) \geq 0$ for all $(x,t) \in \partial D$. Next, we consider the operator $L_{\varepsilon,\mu}$ applied to $\varphi^{\pm}$:

$$L_{\varepsilon,\mu}\varphi^{\pm}(x,t) = \varepsilon\varphi^{\pm}_{xx}(x,t) + \mu a(x,t)\varphi^{\pm}(x,t)\nabla_x\varphi^{\pm}(x,t) - b(x,t)(\varphi^{\pm}(x,t))^2.$$

Since $\varphi^{\pm}_{xx}(x,t) \leq 0$ and $\nabla_x\varphi^{\pm}(x,t) = 0$ for all $(x,t) \in D$, we can simplify the expression:

$$L_{\varepsilon,\mu}\varphi^{\pm}(x,t) = -b(x,t)(\varphi^{\pm}(x,t))^2.$$

Now, by applying the maximum principle in Lemma 7.1.1, we conclude that $\varphi^{\pm}(x,t) \geq 0$ for all $(x,t) \in \bar{D}$.
Since $\varphi^{\pm}(x,t) = \beta^{-1}\|f\|_{\bar{D}} + \|u\|_{\partial D} \pm u(x,t)$, we have

$$\varphi^{\pm}(x,t) \geq 0 \quad \Rightarrow \quad \beta^{-1}\|f\|_{\bar{D}} + \|u\|_{\partial D} \pm u(x,t) \geq 0.$$

This implies that $-u(x,t) \leq \beta^{-1}\|f\|_{\bar{D}} + \|u\|_{\partial D}$ and $u(x,t) \leq \beta^{-1}\|f\|_{\bar{D}} + \|u\|_{\partial D}$ for all $(x,t) \in \bar{D}$. Therefore, we have $\|u\|_{\bar{D}} \leq \beta^{-1}\|f\|_{\bar{D}} + \|u\|_{\partial D}$, which gives the desired estimate. ■

Therefore, this Lemma establishes the continuous uniform stability estimate for the solution $u(x,t)$ of (7.1).

Lemma 7.1.3 (Derivative bounds). *Assume $u(x,t)$ is the solution to the problem described in (6.1). For $j = 0,1,2$, there exists a constant C such that*

$$\left|\frac{\partial^j u(x,t)}{\partial t^j}\right| \leq C, \quad \forall (x,t) \in \bar{D}.$$

Here, C represents a constant value that remains unaffected by the perturbation parameters ε and μ.

Proof. From the initial condition, we have $u(x,0) = h_0(x)$ for $t = 0$. Upon differentiating with respect to t, we obtain

$$\frac{\partial u(x,0)}{\partial t} = \varepsilon \frac{\partial^2 u(x,0)}{\partial x^2} - a(x,0)u(x,0)\frac{\partial u(x,0)}{\partial x} + b(x,0)(u(x,0))^2 + f(x,0), \quad x \in [0,1]. \tag{7.16}$$

At the boundaries $x = 0$ and $x = 1$, we have:

$$\frac{\partial u(0,t)}{\partial t} = s_0'(t), \tag{7.17}$$

$$\frac{\partial u(1,t)}{\partial t} = m_1'(t), \quad t \in (0,T]. \tag{7.18}$$

Using the smoothness of $h_0(x)$, $s_0(t)$, and $m_1(t)$, we can find a constant C_1 such that:

$$\left|\frac{\partial u(x,t)}{\partial t}\right| \leq C_1 \text{ for all } (x,t) \in \partial D.$$

For any $(x,t) \in D$, the differential equation $Lu - f = \frac{\partial u(x,t)}{\partial t} = 0$ holds. Since the linear operator L is uniformly stable, we can apply Lemma 7.1.2 to conclude that

$$\left|\frac{\partial u(x,t)}{\partial t}\right| \leq C \text{ for all } (x,t) \in \bar{D}$$

This completes the proof of the Lemma. ■

7.2 Construction of the numerical scheme

7.2.1 Time discretization

To discretize the time interval $[0,T]$ into M equally sized intervals of length Δt given as $\Delta t = \dfrac{T}{M}$ such that $t_0 = 0, t_M = T$ and $t_j = j\Delta t$ for $j = 0,1,2,3,...,M$. To write the semi-discrete form for the problem in (7.1), we discretize the time variable using implicit Euler method with a uniform time step Δt.

$$\begin{cases} u(x,0) = u^0(x) = g^0(x), \\ \left(\dfrac{u^{j+1}(x) - u^j}{\Delta t}\right) - \varepsilon u_{xx}^{j+1}(x) + \mu a^{j+1}(x) u^{j+1}(x) u_x^{j+1}(x) - b^{j+1}(x)(u^{j+1}(x))^2 = f^{j+1}(x), \\ u(0,t) = u^{j+1}(0) = s^{j+1}(0), \quad u(1,t) = u^{j+1}(1) = m^{j+1}(1). \end{cases} \tag{7.19}$$

After rearranging Eq. (7.19), we obtain the following system.

$$\begin{cases} u^0(x) = g^0(x), \\ -\Delta t \varepsilon u_{xx}^{j+1}(x) + \Delta t \mu a^{j+1}(x) u^{j+1}(x) u_x^{j+1}(x) - \Delta t b^{j+1}(x)(u^{j+1}(x))^2 - \\ \Delta t f^{j+1}(x) + u^{j+1}(x) = u^j(x), \\ u(0,t_{j+1}) = s^{j+1}(0), \quad u(1,t_{j+1}) = m^{j+1}(1). \end{cases} \tag{7.20}$$

Eq. (7.20) can be reduced to

$$\begin{cases} u^0(x) = g^0(x), \\ L_{\varepsilon,\mu}^{-} u^{j+1} = \mathscr{F}^{j+1}, \\ u(0,t_{j+1}) = s^{j+1}(0), \quad u(1,t_{j+1}) = m^{j+1}(1). \end{cases} \tag{7.21}$$

where $L_{\varepsilon,\mu}^{-} u^{j+1} = -\varepsilon u_{xx}^{j+1}(x) + \mu a^{j+1}(x) u^{j+1}(x) u_x^{j+1}(x) - b^{j+1}(x)(u^{j+1}(x))^2$ and $\mathscr{F}^{j+1} = f^{j+1}(x) - \dfrac{1}{\Delta t} u^{j+1}(x) + \dfrac{1}{\Delta t} u^j(x)$. The above Eq. (7.21) is a nonlinear semi-discrete form of the given problem for $j = 0, 1, 2, 3, ..., M-1$.

7.2.2 Analysis of the semi-discrete scheme

Lemma 7.2.1 (Semi-discrete maximum principle). If $\Psi^{j+1}(0) \geq 0$, $\Psi^{j+1}(1) \geq 0$, and $\left(L_{\varepsilon,\mu}^{-}\right)\Psi^{j+1}(x) \geq 0$ for all $x \in D$, then it follows that $\Psi^{j+1}(x) \geq 0$ for all $x \in \bar{D}$.

Proof. Suppose there exists $x^* \in \bar{D}$ such that $\Psi^{j+1}(x^*) = \min_{x\in\bar{D}} \Psi^{j+1}(x) < 0$. Since $x^* \neq \{0,1\}$, we can employ the second derivative test and first derivative test on the function $\Psi^{j+1}(x)$ to establish that $\Psi_x^{j+1}(x^*) = 0$ and $\Psi_{xx}^{j+1}(x^*) > 0$. By substituting $\Psi^{j+1}(x^*)$ into Equation (7.21), we obtain:

$$L_{\varepsilon,\mu}^{-} \Psi^{j+1}(x^*) = \underbrace{-\varepsilon \Psi_{xx}^{j+1}(x)}_{<0} + \underbrace{\mu a^{j+1}(x) \Psi^{j+1}(x) \Psi_x^{j+1}(x)}_{=0} - \underbrace{b^{j+1}(x)(\Psi^{j+1}(x))^2}_{<0} \leq 0$$

This contradicts the assumption $\left(L_{\varepsilon,\mu}^{-}\right)\Psi^{j+1}(x) \geq 0$, thereby establishing that $\Psi^{j+1}(x) \geq 0$

for all $x \in \bar{D}$. ■

The semi-discrete maximum principle establishes the non-negativity of the solution at the mesh points given certain conditions on the boundary values and the operator $L^{-}_{\varepsilon,\mu}$.
The above semi-discrete maximum principle leads to the following stability estimate result

$$\left\|L^{-}_{\varepsilon,\mu}\right\| \leq C. \tag{7.22}$$

where C is a constant independent of ε, μ and Δt. For the semi-discrete scheme (7.21), the local truncation error e_{j+1} is estimated as $e_{j+1} = u\left(x,t_{j+1}\right) - \hat{u}^{j+1}(x)$, where $\hat{u}^{j+1}(x)$ is the solution of the following boundary value problem

$$\begin{cases} \hat{u}^0(x) = g^0(x)\ x \in D, \\ L^{-}_{\varepsilon,\mu}\hat{u}^{j+1} = \mathscr{F}^{j+1}, \\ \hat{u}(0,t_{j+1}) = s^{j+1}(0), \quad \hat{u}(1,t_{j+1}) = m^{j+1}(1), \quad j = 0,1,2,....,M-1. \end{cases} \tag{7.23}$$

Lemma 7.2.2 (Local error estimate). *Given that* $\left|\dfrac{\partial^k}{\partial t^k}u(x,t)\right| \leq C$ *holds for all* $(x,t) \in \bar{D}$ *and* $k = 0,1,2$, *the local error estimate* e_{j+1} *in the temporal direction can be expressed as:*

$$\left\|e_{j+1}\right\| \leq C(\Delta t)^2. \tag{7.24}$$

Proof. Due to the sufficient smoothness of the solution $u(x,t)$ for the problem (7.1), we can employ a Taylor series expansion to represent $u(x,t_j)$ at the time level t_j:

$$u(x,t_j) = u(x,t_{j+1}) - \Delta t u_t(x,t_{j+1}) + \frac{\Delta t^2}{2}u_{tt}(x,t_{j+1}) - \frac{\Delta t^3}{6}u_{ttt}(x,\xi) \tag{7.25}$$

for some $\xi \in [t_j,t_{j+1}]$. Substituting the expression for $u_t(x,t_j)$ from Equation (7.19) into Equation (7.25), we obtain:

$$\begin{aligned} u(x,t_j) =& u(x,t_{j+1}) - \Delta t\left(\varepsilon u_{xx}^{j+1} - \mu a^{j+1}u^{j+1}u_x^{j+1} + b^{j+1}(u^{j+1})^2 + f^{j+1}(x)\right) + O(\Delta t)^2 \\ =& u(x,t_{j+1}) - \Delta t\varepsilon u_{xx}^{j+1} + \Delta t\mu a^{j+1}u^{j+1}u_x^{j+1} - \Delta t b^{j+1}(u^{j+1})^2 - \Delta t f^{j+1}(x) + O(\Delta t)^2 \end{aligned} \tag{7.26}$$

Now, subtracting Equation (7.20) from Equation (7.26) yields the local truncation error e_{j+1},

which fulfills the subsequent boundary value problem:

$$\begin{cases} e^0_{j+1}(x) = g^0(x), \\ \bar{L_{\varepsilon,\mu}} e_{j+1} = O(\Delta t)^2, \\ e_{j+1}(0) = s^{j+1}(0), \;\; e_{j+1}(1) = m^{j+1}(1). \end{cases}$$

The stability estimate in Equation (7.22) of the semi-discrete scheme guarantees the intended outcome. Consequently, we obtain:

$$\left\| e_{j+1} \right\| \leq C(\Delta t)^2.$$

■

Lemma 7.2.3 (Global error estimate). The temporal direction global error estimate, $E_{j+1} = u(x,t_{j+1}) - u^{j+1}(x)$ is given by

$$\left\| E_{j+1} \right\| \leq C\left(\Delta t\right), \quad j\left(\Delta t\right) \leq T. \tag{7.27}$$

Proof. Start by expressing the global error E_{j+1} as the sum of the local truncation errors e_ι up to time step j:

$$\left\| E_{j+1} \right\| = \left\| \sum_{\iota=1}^{j} e_\iota \right\|, \quad j(\Delta t) \leq T.$$

By the triangle inequality, we can bound the norm of the sum by the sum of the norms:

$$\begin{aligned} &= \left\| e_1 + e_2 + e_3 + \cdots + e_j \right\| \\ &\leq \left\| e_1 \right\| + \left\| e_2 \right\| + \left\| e_3 \right\| + \cdots + \left\| e_j \right\| \end{aligned}$$

Since the local truncation errors e_ι are bounded by $C_\iota(\Delta t)^2$, as shown in the Local Error Estimate lemma, we can substitute these bounds into the inequality:

$$\begin{aligned} &\leq C_1(\Delta t)^2 + C_2(\Delta t)^2 + C_3(\Delta t)^2 + \cdots + C_j(\Delta t)^2 \\ &\leq C'(j)(\Delta t)^2 \end{aligned}$$

Here, $C'(j)$ represents a function of j that depends on the specific coefficients and conditions

of the problem. However, since $j(\Delta t) \leq T$, we can further simplify the expression:

$$\begin{aligned} &\leq C'\left(\frac{T}{\Delta t}\right)(\Delta t)^2 = C'T(\Delta t) \\ &\leq C(\Delta t) \end{aligned}$$

where $C = C'T$. ■

Therefore, the global error estimate $\left\|E_{j+1}\right\|$ is bounded by $C(\Delta t)$, which implies that the semi-discrete scheme is convergent of order one in time.

7.2.3 Quasilinearization

In order to construct a computational method for the boundary value problem stated in (7.1), it is necessary to linearize the semi-discrete problem (7.20) that involves nonlinearity. This can be accomplished by employing Newton's quasilinearization approach (see Bellman and Kalaba (1965)). The non-linear scheme given in (7.20) can be expressed as

$$\begin{cases} u^0(x) = g^0(x), \\ -\varepsilon u_{xx}^{j+1}(x) = -\mu a^{j+1}(x)u^{j+1}(x)u_x^{j+1}(x) + b^{j+1}(x)(u^{j+1}(x))^2 + f^{j+1}(x) - \dfrac{1}{\Delta t}u^{j+1}(x) + \dfrac{1}{\Delta t}u^j(x), \\ u(0,t_{j+1}) = s^{j+1}(0), \quad u(1,t_{j+1}) = m^{j+1}(1). \end{cases} \tag{7.28}$$

Let $F(u^{j+1}, u_x^{j+1}) = -\mu a^{j+1}(x)u^{j+1}(x)u_x^{j+1}(x) + b^{j+1}(x)(u^{j+1}(x))^2 + f^{j+1}(x) - \dfrac{1}{\Delta t}u^{j+1}(x) + \dfrac{1}{\Delta t}u^j(x)$ and rewrite (7.28) as

$$\begin{cases} u^0(x) = g^0(x), \\ -\varepsilon u_{xx}^{j+1}(x) = F(u^{j+1}, u_x^{j+1}), \\ u(0,t_{j+1}) = s^{j+1}(0), \quad u(1,t_{j+1}) = m^{j+1}(1). \end{cases} \tag{7.29}$$

Let $\left(u^{j+1,(k)}(x), u_x^{j+1,k}(x)\right)$ denote the k^{th} nominal solution of (7.29). By employing a two-variable Taylor series expansion of $F\left(u^{j+1,(k+1)}(x), u_x^{j+1,k+1}(x)\right)$ around the nominal solution $\left(u^{j+1,(k)}(x), u_x^{j+1,k}(x)\right)$ and considering only the first-order term, we obtain:

$$\begin{aligned} F\left(u^{j+1,(k+1)}, u_x^{j+1,k+1}\right) =& F\left(u^{j+1,(k)}, u_x^{j+1,k}\right) \\ &+ \left(u^{j+1,(k+1)} - u^{j+1,k}(x)\right) F_{u^{j+1}}\left(u^{j+1,(k)} - u^{j+1,k}(x)\right) \\ &+ \left(u_x^{j+1,(k+1)} - u_x^{j+1,k}(x)\right) F_{u_x^{j+1}}\left(u_x^{j+1,(k)} u_x^{j+1,k}(x)\right) \end{aligned} \tag{7.30}$$

Using the value of (7.30) in (7.29), and performing some simplifications, we obtain the following system.

$$\begin{cases} u^{0,(k+1)}(x) = g^{0,(k+1)}(x), \\ -\varepsilon u_{xx}^{j+1,(k+1)}(x) + \mu a^{j+1,(k)} u^{j+1,(k)} u_x^{j+1,(k+1)} - \left(\dfrac{-1}{\Delta t} - \mu a^{j+1,(k)} u_x^{j+1,(k)} + 2\mu b^{j+1,(k)} u^{j+1,(k)} \right) u^{j+1,(k+1)} \\ = \mu a^{j+1,(k)} u^{j+1,(k)} u_x^{j+1,(k)} - b^{j+1,(k)} \left(u^{j+1,(k)} \right)^2 + f^{j+1,(k)} + \dfrac{1}{\Delta t} u^{j,(k)}, \\ u^{j+1,(k+1)}(0) = s^{j+1,(k+1)}(0), \quad u^{j+1,(k+1)}(1) = m^{j+1,(k+1)}(1). \end{cases} \tag{7.31}$$

where $u^{j+1,(0)}$ is initial guess of the nominal solution $\left(u^{j+1,(k)}(x), u_x^{j+1,k}(x) \right)$ for $k = 0, 1, 2, \ldots$ is the iteration counter.

Using the following notations to write (7.31) in simplest form.

$$\begin{cases} U^{j+1}(x) = u^{j+1,(k+1)}(x) \\ c(x) = \mu a^{j+1,(k)} u^{j+1,(k)} \\ d(x) = -\dfrac{1}{\Delta t} - \mu a^{j+1,(k)} u_x^{j+1,(k)} + 2\mu b^{j+1,(k)} u^{j+1,(k)} \\ H(x) = \mu a^{j+1,(k)} u^{j+1,(k)} u_x^{j+1,(k)} - b^{j+1,(k)} \left(u^{j+1,(k)} \right)^2 + f^{j+1,(k)} + \dfrac{1}{\Delta t} u^{j,(k)} \end{cases} \tag{7.32}$$

Then, using the above notations (7.31) can be written as:

$$\begin{cases} U^0(x) = g^0(x), \\ -\varepsilon U_{xx}^{j+1}(x) + \mu c(x) U_x^{j+1} - d(x) U^{j+1} = H(x), \\ U^{j+1}(0) = s^{j+1}(0), \quad U^{j+1}(1) = m^{j+1}(1). \end{cases} \tag{7.33}$$

Equation (7.33) is the linearized form of the semi-discrete singularly perturbed nonlinear problem in (7.20).

To obtain a unique solution for the linearized singularly perturbed problem in (7.33), we assumed that the coefficient functions, $c(x)$, $d(x)$ and $H(x)$ are smooth with $c(x) \geq \lambda > 0$ and $d(x) \geq \rho > 0$, where λ and ρ are positive numbers.

Lemma 7.2.4. Let $U^{j+1}(x)$ be the semi-discrete solution of (7.33). For a certain order of derivative q that depends on the smoothness of data $U^{j+1}(x)$ satisfies the following bound

$$\left| \frac{d^\xi U^j(x)}{dx^\xi} \right| \leq C \left(1 + \Theta_1^\xi e^{-p\Theta_1 x} + \Theta_2^\xi e^{-p\Theta_2(1-x)} \right), \quad for \;\; 0 \leq \xi \leq q$$

where p is any real constant such that $0 < p < 1$

Proof. See Kadalbajoo and Yadaw (2012) ■

The above lemma provides insights into the asymptotic behavior of the solution u^{j+1} and its spatial derivatives in (7.2.4). This lemma plays a crucial role in analyzing the convergence of the fully-discrete solution.

7.2.4 Full-discrete scheme

In this section, the spatial domain $\bar{D} = [0,1]$ is subdivided into N equal sub-intervals, with each sub-interval consisting of a mesh element of length $1/N$ such that

$$x_0 = 0,\ \ x_1 = x_0 + i = h,\ \ x_2 = x_1 + h = 2h,\ \ \cdots\ \ x_N = Nh = 1.$$

Utilizing the discretization of the spatial domain, the semi-discrete linearized problem (7.33) can be transformed into its complete discrete formulation as presented below.

$$\begin{cases} u^0(x) = g^0(x_i),\ i = 0,1,2,3...,N-1, \\ \left[L^{N,M}U\right]_i^{j+1} \equiv -\varepsilon\delta_x^2 U_i^{j+1} + \mu c(x) D_x^+ U_i^{j+1} - d(x)U_i^{j+1} = H_i^{j+1}, \\ U_0^{j+1} = s_0^{t_{j+1}},\ U_N^{j+1} = m_N^{t_{j+1}}. \end{cases} \tag{7.34}$$

where

$$\delta_x^2 U_i^{j+1} = \left[\frac{U_{i+1}^{j+1} - 2U_i^{j+1} + U_{i-1}^{j+1}}{\phi_i^2(h,\varepsilon,\mu)}\right],\ \text{and}\ \ D_x^+ U_i^{j+1} = \left[\frac{U_i^{j+1} - U_{i-1}^{j+1}}{h}\right] \tag{7.35}$$

Employing FOFDM based on the technique of Mickens (1994), then we can express equation (7.34) in a discretized form.

$$\begin{cases} u^0(x) = g^0(x_i),\ i = 1,2,3...,N-1 \\ \left[L^{N,M}U\right]_i^{j+1} \equiv -\varepsilon\left[\dfrac{U_{i+1}^{j+1} - 2U_i^{j+1} + U_{i-1}^{j+1}}{\phi_i^2(h,\varepsilon,\mu)}\right] + \mu c(x)\left[\dfrac{U_i^{j+1} - U_{i-1}^{j+1}}{h}\right] - d(x)U_i^{j+1} = H_i^{j+1} \\ U_0^{j+1} = s_0^{t_{j+1}},\ U_N^{j+1} = m_N^{t_{j+1}},\ \ j = 1,2,3,...,M-1 \end{cases} \tag{7.36}$$

where the denominator function $\phi_i^2(h,\varepsilon,\mu)$ is written as

$$\phi_i^2(h,\varepsilon,\mu) \equiv \phi_i^2 = \frac{h\varepsilon}{\mu c(x)}\left(\exp\left(\frac{\mu c(x)h}{\varepsilon}\right) - 1\right)$$

Now, the equation (7.36) can be expressed as.

$$\begin{cases} u^0(x) = g^0(x_i), 1 \le i \le N-1 \\ E_i^{j+1}U_{i+1}^{j+1} + F_i^{j+1}U_i^{j+1} + G_i^{j+1}U_{i-1}^{j+1} = H_i^{j+1} \\ U_0^{j+1} = s_0^{t_{j+1}},\ U_N^{j+1} = m_N^{t_{j+1}} 1 \le j \le M-1 \end{cases} \tag{7.37}$$

with

$$E_i^{j+1} = \left(-\frac{\varepsilon}{\phi_i^2}\right), \quad F_i^{j+1} = \left(\frac{2\varepsilon}{\phi_i^2} - \frac{\mu c(x)}{h} - d(x)\right), \ G_i^{j+1} = \left(-\frac{\varepsilon}{\phi_i^2} - \frac{\mu c(x)}{h}\right),$$
$$H_i^{j+1} = \mu a_i^{j+1}U_i^{j+1}\left(\frac{U_{i+1}^{j+1} - U_i^{j+1}}{h}\right) - b_i^{j+1}\left(U_i^{j+1}\right)^2 + f_i^{j+1} + \frac{1}{\Delta t}U_i^j.$$

7.3 Analysis of the developed numerical scheme

Lemma 7.3.1. Let Ψ_i^{j+1} be any mesh function for $i = 0,1,2,3,...,N$. If $\Psi_0^{j+1} \ge 0$, $\Psi_N^{j+1} \ge 0$ and $\left[L_{\varepsilon,\mu}^{N,M}\Psi\right]_i^{j+1} \ge 0$ for $1 \le i \le N$, then $\Psi_i^{j+1} \ge 0$, for $i \in [0,N]$.

Proof. Assume there is $i^\star$ such that $\Psi^N(x_{i^\star}) = \min_{x\in\bar{D}}\Psi^N(x_i)$. We also assume that $\Psi_i^{j+1} < 0$ for some i. Based on the given hypothesis, we have $i^* \ne \{0,N\}$ and the following inequalities hold:
$\Psi_{i^*+1}^{j+1} - \Psi_{i^*}^{j+1} \ge 0$, and $\Psi_{i^*-1}^{j+1} - \Psi_{i^*}^{j+1} \ge 0$.
Now, let's consider the expression $\left[L_{\varepsilon,\mu}^{N,M}\Psi\right]_i^{j+1}$, which corresponds to the discrete operator applied to Ψ_i^{j+1}.

$$\begin{aligned} \left[L_{\varepsilon,\mu}^{N,M}\Psi\right]_{i^*}^{j+1} &= -\varepsilon\left[\frac{\Psi_{i^*+1}^{j+1} - 2\Psi_{i^*}^{j+1} + \Psi_{i^*-1}^{j+1}}{\Psi_{i^*}^2}\right] + c_{i^*}^{j+1}\left[\frac{\Psi_{i^*}^{j+1} - \Psi_{i^*-1}^{j+1}}{h}\right] - d_{i^*}^{j+1}\Psi_{i^*}^{j+1} \\ &= -\varepsilon\left[\frac{\Psi_{i^*+1}^{j+1} - \Psi_{i^*}^{j+1} + \Psi_{i^*-1}^{j-1} - \Psi_{i^*}^{j+1}}{\Psi_{i^*}^2}\right] + c_{i^*}^{j+1}\left[\frac{\Psi_{i^*}^{j+1} - \Psi_{i^*-1}^{j+1}}{h}\right] - d_{i^*}^{j+1}\Psi_{i^*}^{j+1} < 0 \end{aligned}$$

This contradicts the assumption that $\left[L_{\varepsilon,\mu}^{N,M}\Psi\right]_i^{j+1} \ge 0$ for $i \in [1,N-1]$. Hence, we conclude that $\Psi_i^{j+1} \ge 0$ for $i \in [0,N]$. ■

From this Lemma, the full-discrete maximum principle ensures that if the given conditions are satisfied, the mesh function Ψ_i^{j+1} remains non-negative for all grid points in the discrete domain.

Lemma 7.3.2 (Discrete uniform stability). Let $\Psi_i^{j+1}, i = 0,1,\ldots,N$ be any mesh functions such that $\Psi_0^{j+1} = \Psi_N^{j+1} = 0$, then

$$\left|\Psi_i^{j+1}\right| \leq \frac{1}{\rho} \max_{1\leq i\leq N-1} \left|L_\varepsilon^{N,M}\Psi_i^{j+1}\right|, \quad 0 \leq i \leq N,$$

where $d(x_i) \geq \rho > 0$.

Proof. Define

$$\left[\Psi^{\pm}\right]_m^{n+1} = \frac{1}{\rho} \max_{1\leq i\leq N-1} \left|L_\varepsilon^{N,M}\Psi_i^{n+1}\right| \pm \Psi_m^{n+1}.$$

Now, we can show that these comparison functions satisfy the required properties. For $i = 0$:

$$\left[\Psi^{\pm}\right]_0^{j+1} = \frac{1}{\rho} \max_{1\leq i\leq N-1} \left|L_\varepsilon^{N,M}\Psi_i^{j+1}\right| \pm \Psi_0^{j+1} = \frac{1}{\rho} \max_{1\leq i\leq N-1} \left|L_\varepsilon^{N,M}\Psi_i^{j+1}\right| \pm s_0^{j+1} \geq 0,$$

and for $i = N$:

$$\left[\Psi^{\pm}\right]_N^{j+1} = \frac{1}{\rho} \max_{1\leq i\leq N-1} \left|L_\varepsilon^{N,M}\Psi_i^{j+1}\right| \pm \Psi_N^{j+1} = \frac{1}{\rho} \max_{1\leq i\leq N-1} \left|L_\varepsilon^{N,M}\Psi_i^{j+1}\right| \pm m_N^{j+1} \geq 0.$$

For $i = 1, 2, \ldots, N-1$, we have:

$$\begin{aligned} L_\varepsilon^{N,M}\left[\Psi^{\pm}\right]_i^{j+1} &= L_\varepsilon^{N,M}\left(\frac{1}{\rho} \max_{1\leq i\leq N-1} \left|L_\varepsilon^{N,M}\Psi_i^{j+1}\right| \pm \Psi_i^{j+1}\right) \\ &= \frac{d(x_i)}{\rho} \max_{0\leq i\leq N} \left|L_\varepsilon^{N,M}\Psi_i^{j+1}\right| \pm L_\varepsilon^{N,M}\Psi_i^{j+1} \\ &\geq \max_{0\leq i\leq N} \left|L_\varepsilon^{N,M}\Psi_i^{j+1}\right| \pm L_\varepsilon^{N,M}\Psi_i^{j+1} \geq 0, \end{aligned}$$

where the inequality holds because $d(x_i) \geq \rho$. Therefore, $[\Psi^{\pm}]_i^{j+1}$ satisfy the conditions of the Full-Discrete Maximum Principle (Lemma 7.3.1), which implies that $[\Psi^{\pm}]_i^{j+1} \geq 0$ for $0 \leq i \leq N$. Consequently, we have:
$\left|\Psi_i^{j+1}\right| \leq \frac{1}{\rho} \max_{1\leq i\leq N-1} \left|L_\varepsilon^{N,M}\Psi_i^{j+1}\right|, \quad 0 \leq i \leq N.$ ■

Theorem 7.3.1 (**Error estimate**). Assume $U^{j+1}(x)$ represents the solution of the semi-discrete problem (7.33), and U_i^{j+1} denotes the solution of the fully-discrete problem (7.36). If N represents the number of grid points and C denotes a suitably large constant, the following error bound is fulfilled.

$$\left|L_{\varepsilon,\mu}^{N,M}\left(U^{j+1}(x_i) - U_i^{j+1}\right)\right| \leq CN^{-1}. \tag{7.38}$$

Proof. We define the truncation error using the differential and difference equation as

$$\begin{aligned}
L_{\varepsilon,\mu}^{N,M}\left(U(x_i,t_{j+1})-U_i^{j+1}\right) =& L_{\varepsilon,\mu}^{N,M}\left(U(x_i,t_{j+1})\right)-L_{\varepsilon,\mu}^{N,M}\left(U_i^{j+1}\right)\\
=& -\varepsilon\frac{d^2U^{j+1}(x_i)}{dx^2}+\mu c^{j+1}(x_i)\frac{dU^{j+1}(x_i)}{dx}-d^{j+1}(x_i)-\left[\varepsilon\delta_x^2+\mu c^{j+1}(x_i)D_x^+-d^{j+1}(x_i)\right]\\
=& -\varepsilon\frac{d^2U^{j+1}(x_i)}{dx^2}+\mu c^{j+1}(x_i)\frac{dU^{j+1}(x_i)}{dx}-d^{j+1}(x_i)\\
&-\left[-\frac{\varepsilon}{\phi_i^2}\left(U_{i+1}^{j+1}-2U_i^{j+1}+u_{i-1}^{j+1}\right)+\frac{\mu c^{j+1}(x_i)}{h}\left(U_{i+1}^{j+1}-U_i^{j+1}\right)-d^{j+1}(x_i)\right]
\end{aligned} \tag{7.39}$$

By utilizing the Taylor series expansion for the terms U_{i+1}^{j+1}, U_{i-1}^{j+1}, and $\frac{1}{\phi_i^2}$, we get

$$U_{i+1}^{j+1}=U_i^{j+1}+h\frac{dU^{j+1}(x_i)}{dx}+\frac{h^2}{2!}\frac{d^2U^{j+1}(x_i)}{dx^2}+\frac{h^3}{3!}\frac{d^3U^{j+1}(x_i)}{dx^3}+\frac{h^4}{4!}\frac{d^4U^{j+1}(\xi_i)}{dx^4},\xi\in(x_{i-1},x_{i+1})$$

$$\begin{aligned}
U_{i-1}^{j+1} =& U_i^{j+1}-h\frac{dU^{j+1}(x_i)}{dx}+\frac{h^2}{2!}\frac{d^2U^{j+1}(x_i)}{dx^2}-\frac{h^3}{3!}\frac{d^3U^{j+1}(x_i)}{dx^3}+\frac{h^4}{4!}\frac{d^4U^{j+1}(\xi_i)}{dx^4},\xi\in(x_{i-1},x_{i+1})\\
\frac{1}{\phi_i^2} =& \frac{1}{\frac{h\varepsilon}{\mu c(x_i)}\left(\exp\left(\frac{\mu c(x_i)h}{\varepsilon}\right)-1\right)}=\frac{1}{h^2}-\frac{\mu c^{j+1}(x_i)}{2\varepsilon h}+\frac{(\mu c^{j+1}(x_i))^2}{12\varepsilon^2}
\end{aligned}$$

Applying the above substitutions in (7.39) and performing some simplification, we obtain

$$\begin{aligned}
&-\varepsilon\frac{d^2U^{j+1}}{dx^2}(x_i)+\left(\mu c^{j+1}(x_i)\frac{d^2U^{j+1}(x_i)}{dx^2}-\frac{\mu c^{j+1}(x_i)}{2}\frac{d^2U^{j+1}(x_i)}{dx^2}\right)h+\\
&\left(\frac{(\mu c^{j+1}(x_i))^2}{12\varepsilon^2}\frac{d^2U^{j+1}(x_i)}{dx^2}-\frac{\mu c^{j+1}(x_i)}{6}\frac{d^3U^{j+1}(x_i)}{dx^3}\right)h^2+O(h^3)
\end{aligned} \tag{7.40}$$

By employing Lemma 7.2.4, the bound of the spatial error estimate can be described as

$$\begin{aligned}
\left|L_{\varepsilon,\mu}^{N,M}\left(U(x_i,t_{j+1})-U_i^{j+1}\right)\right| &= \left|L_{\varepsilon,\mu}^{N,M}\left(U(x_i,t_{j+1})\right)-L_{\varepsilon,\mu}^{N,M}\left(U_i^{j+1}\right)\right|\\
&\leq C_1h+C_2h^2+\ldots\\
&\leq Ch=CN^{-1}\text{where } N^{-1}=1/N=h
\end{aligned} \tag{7.41}$$

■

By combining Lemma 7.27 and Theorem 7.3.1, we arrive at Theorem 7.3.2 below.

Theorem 7.3.2. ***(The main result)*** If $u(x,t)$ represents the exact solution of problem (6.1), and U_i^j denotes the solution of the numerical scheme (4.16), the error estimate for the full

discrete scheme can be expressed as:

$$\left|u(x_i,t_j)-U_i^j\right| \le C\,(\Delta t+h)\,,\ \ 0\le i\le N,\ \ 0\le j\le M. \tag{7.42}$$

The aforementioned analysis demonstrates that the proposed method exhibits first-order parameter-uniform convergence in both space and time.

7.4 Numerical examples and discussions

The following examples are implemented to demonstrate the applicability of the proposed scheme in (7.37). Here, maximum absolute errors $Err_{\varepsilon,\mu}^{N,M}$ and numerical rate of convergence, $Roc_{\varepsilon,\mu}^{N,M}$ are calculated on the considered meshes using the double mesh principle given in Doolan et al. (1980) as follows.

$$Err_{\varepsilon,\mu}^{N,M} = \max_{0\le i,j\le N,M}\left|U^{N,M}(x_i,\,t_j)-U^{2N,2M}(x_{2i},\,t_{2j})\right| \quad \text{(maximum absolute errors)}$$

$$Roc_{\varepsilon,\mu}^{N,M} = \log_2\left(\frac{Err_{\varepsilon,\mu}^{N,M}}{Err_{\varepsilon,\mu}^{2N,2M}}\right) \quad \text{(rate of convergence)}$$

Example 7.1. *Consider the following nonlinear (nonlinearity in both convection and reaction terms) singularly perturbed problem*

$$\begin{cases} \varepsilon u_{xx}(x,t)+\mu(1+x)u(x,t)u_x(x,t)-(u(x,t))^2-u_t(x,t)=16x^2(1-x)^2,(x,t)\in(0,1)\times(0,1] \\ u(x,0)=0, \quad x\in(0,1) \\ u(0,t)=0, \quad u(1,t)=0, \quad t\in[0,1] \end{cases}$$

Example 7.2. *Consider the following nonlinear singularly perturbed problem*

$$\begin{cases} \varepsilon u_{xx}(x,t)+\mu(1+xt)u(x,t)u_x(x,t)-(u(x,t))^2-u_t(x,t)=|xt|x^2t^2(1-xt)^2,(x,t)\in(0,1)\times(0,1] \\ u(x,0)=x(1-x^2)\sin x, \quad x\in(0,1) \\ u(0,t)=0, \quad u(1,t)=0, \quad t\in[0,1] \end{cases}$$

For the given examples, their analytical solutions do not exist in explicit form. Consequently, we have applied scheme (7.37) to attain the numerical solution and compute maximum absolute errors, $Err_{\varepsilon,\mu}^{N,M}$, as well as the convergence rates, $Roc_{\varepsilon,\mu}^{N,M}$, and we employed Python software packages for carrying out numerical computations. Table 7.1 presents the numerical results of the nonlinear problem described in Example 7.1 using scheme (7.37) with $\mu=10^{-5}$ and varying values of ε to obtain the numerical solution and compute the corresponding $Err_{\varepsilon,\mu}^{N,M}$, and $Roc_{\varepsilon,\mu}^{N,M}$. In Table 7.2, the values of $Err_{\varepsilon,\mu}^{N,M}$ and $Roc_{\varepsilon,\mu}^{N,M}$ are displayed for various combinations of N and M. The simulations were performed for $\mu=10^{-10}$ and various values of ε, allowing us to examine the impact on $Err_{\varepsilon,\mu}^{N,M}$ and $Roc^{N,M}$. The results obtained from the two tables indicate that the presented method exhibits uniform convergence with a first-order rate in both variables. In Tables 7.3 and 7.4, we explore the effect

of varying the values of ε on the computationn of $Err_{\varepsilon,\mu}^{N,M}$ and $Roc_{\varepsilon,\mu}^{N,M}$. For Tables 7.3, we set $\mu = 10^{-5}$, while for Tables 7.3, we use $\mu = 10^{-10}$. In both cases, the tables demonstrate first-order uniform convergence results. In The graphical results from Figure 7.1 provide an examination of the boundary region behavior of the PDE in Example 7.1. Furthermore, Figure 7.3 shows cases of the Log-Log plots representing the numerical solutions of the problems presented in Example 7.1 and Example 7.2. These plots provide empirical evidence that aligns with the theoretical assumptions made during the analysis.

.

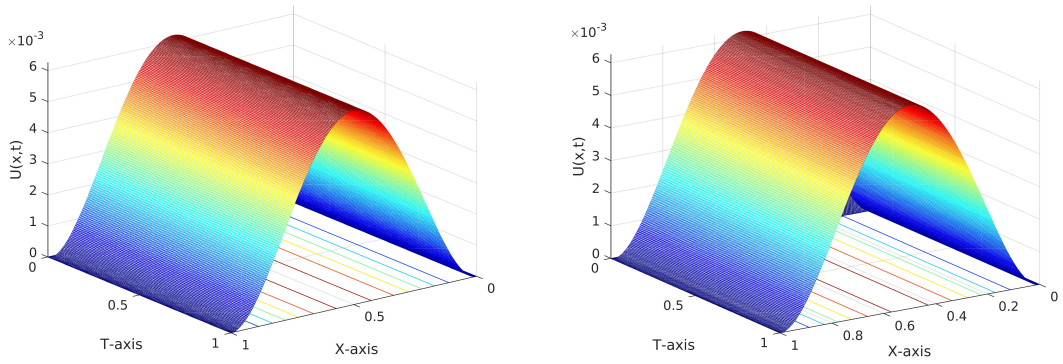

(a) (b)

Figure 7.1: Numerical results of Example 4.1 using scheme (7.37) (a) for $N = 320, M = 160$, $\varepsilon = 10^{-12}$, $\mu = 10^{-2}$ and (b) for $N = 320, M = 160, \varepsilon = 10^{-2}, \mu = 10^{-12}$

.

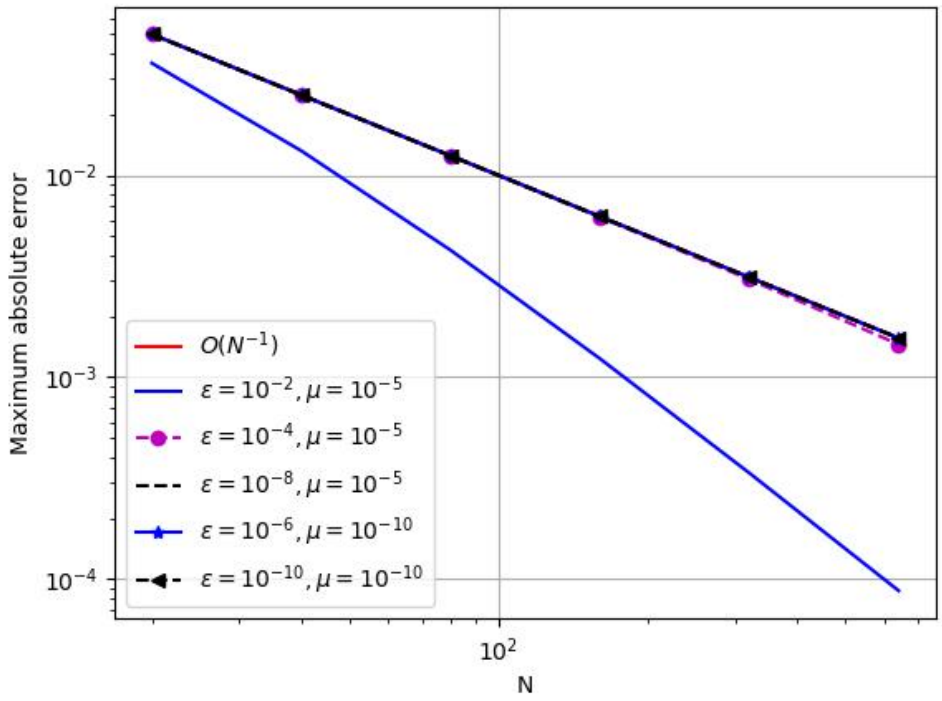

Figure 7.2: Log-Log plots for Example 7.1 using scheme (7.37)

.

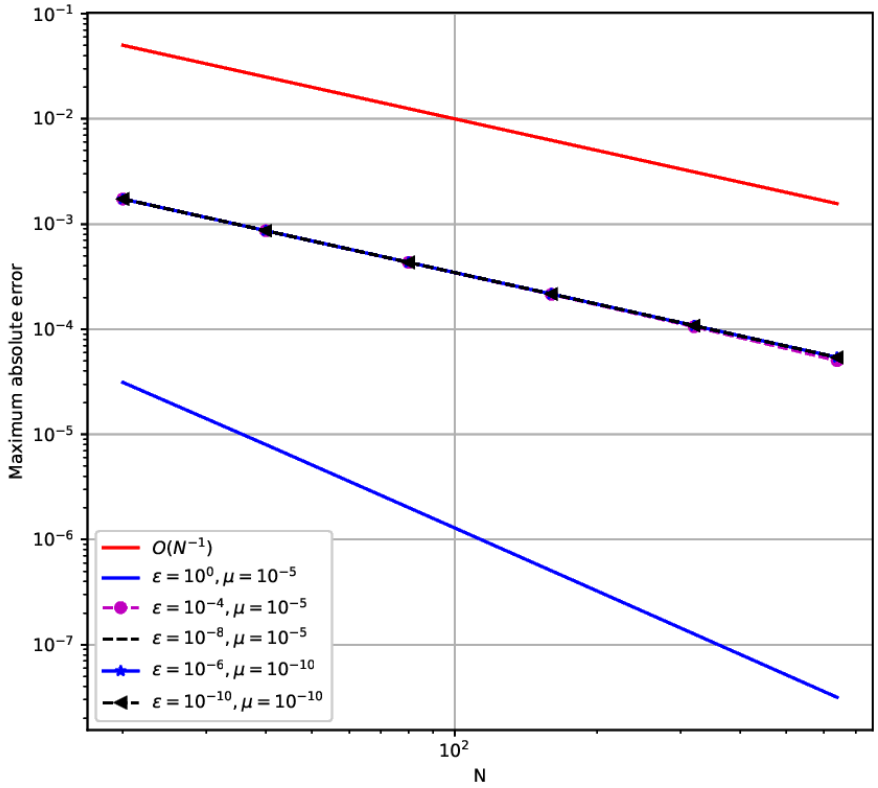

Figure 7.3: Log-Log plots for Example 7.2 using scheme (7.37)

.

Table 7.1: $Err_{\varepsilon,\mu}^{N,M}$ and $Roc_{\varepsilon,\mu}^{N,M}$ using scheme (7.37) for Example 7.1 with $\mu = 10^{-5}$ and different values of ε.

N	20	40	80	160	320	640
$\varepsilon \downarrow$ M	10	20	40	80	160	320
10^{0}	9.0297e-04	2.3126e-04	5.8291e-05	1.4616e-05	3.6584e-06	9.1509e-07
	1.9652	1.9882	1.9957	1.9983	1.9992	-
10^{-2}	3.5951e-02	1.3233e-02	4.2589e-03	1.2359e-03	3.3539e-04	8.7546e-05
	1.4419	1.6356	1.7849	1.8817	1.9377	-
10^{-4}	4.9995e-02	2.4988e-02	1.2477e-02	6.2075e-03	3.0528e-03	1.4547e-03
	1.0005	1.0020	1.0072	1.0239	1.0694	-
10^{-6}	5.0001e-02	2.5001e-02	1.2500e-02	6.2502e-03	3.1251e-03	1.5625e-03
	1.0000	1.0001	1.0000	1.0000	1.0000	-
10^{-8}	5.0000e-02	2.5000e-02	1.2500e-02	6.2500e-03	3.1250e-03	1.5625e-03
	1.0000	1.0001	1.0000	1.0000	1.0000	-
10^{-10}	5.0000e-02	2.5000e-02	1.2500e-02	6.2500e-03	3.1250e-03	1.5625e-03
	1.0000	1.0001	1.0000	1.0000	1.0000	-
10^{-12}	5.0000e-02	2.5000e-02	1.2500e-02	6.2500e-03	3.1250e-03	1.5625e-03
	1.0000	1.0001	1.0000	1.0000	1.0000	-
10^{-14}	5.0000e-02	2.5000e-02	1.2500e-02	6.2500e-03	3.1250e-03	1.5625e-03
	1.0000	1.0001	1.0000	1.0000	1.0000	-
10^{-16}	5.0000e-02	2.5000e-02	1.2500e-02	6.2500e-03	3.1250e-03	1.5625e-03
	1.0000	1.0001	1.0000	1.0000	1.0000	-
$\vdots$	$\vdots$	$\vdots$	$\vdots$	$\vdots$	$\vdots$	$\vdots$
10^{-40}	5.0000e-02	2.5000e-02	1.2500e-02	6.2500e-03	3.1250e-03	1.5625e-03
	1.0000	1.0001	1.0000	1.0000	1.0000	-
$Err_{\varepsilon,\mu}^{N,M}$	5.0000e-02	2.5000e-02	1.2500e-02	6.2500e-03	3.1250e-03	1.5625e-03
$Roc_{\varepsilon,\mu}^{N,M}$	1.0000	1.0001	1.0000	1.0000	1.0000	-

Table 7.2: $Err_{\varepsilon,\mu}^{N,M}$ and $Roc_{\varepsilon,\mu}^{N,M}$ using scheme (7.37) for Example 7.1 with $\mu = 10^{-10}$ and different values of ε.

N	20	40	80	160	320	640
$\varepsilon \downarrow$ M	10	20	40	80	160	320
10^{0}	9.0296e-04	2.3126e-04	5.8292e-05	1.4616e-05	3.6581e-06	9.1526e-07
	1.9651	1.9881	1.9957	1.9984	1.9988	-
10^{-2}	3.5950e-02	1.3233e-02	4.2589e-03	1.2359e-03	3.3539e-04	8.7546e-05
	1.4419	1.6356	1.7849	1.8817	1.9377	-
10^{-4}	4.9994e-02	2.4988e-02	1.2477e-02	6.2073e-03	3.0527e-03	1.4547e-03
	1.0005	1.0020	1.0072	1.0239	1.0694	-
10^{-6}	5.0000e-02	2.5000e-02	1.2500e-02	6.2500e-03	3.1250e-03	1.5625e-03
	1.0000	1.0001	1.0000	1.0000	1.0000	-
10^{-8}	5.0000e-02	2.5000e-02	1.2500e-02	6.2500e-03	3.1250e-03	1.5625e-03
	1.0000	1.0001	1.0000	1.0000	1.0000	-
10^{-10}	5.0000e-02	2.5000e-02	1.2500e-02	6.2500e-03	3.1250e-03	1.5625e-03
	1.0000	1.0001	1.0000	1.0000	1.0000	-
10^{-12}	5.0000e-02	2.5000e-02	1.2500e-02	6.2500e-03	3.1250e-03	1.5625e-03
	1.0000	1.0001	1.0000	1.0000	1.0000	-
10^{-14}	5.0000e-02	2.5000e-02	1.2500e-02	6.2500e-03	3.1250e-03	1.5625e-03
	1.0000	1.0001	1.0000	1.0000	1.0000	-
10^{-16}	5.0000e-02	2.5000e-02	1.2500e-02	6.2500e-03	3.1250e-03	1.5625e-03
	1.0000	1.0001	1.0000	1.0000	1.0000	-
$\vdots$	$\vdots$	$\vdots$	$\vdots$	$\vdots$	$\vdots$	$\vdots$
10^{-40}	5.0000e-02	2.5000e-02	1.2500e-02	6.2500e-03	3.1250e-03	1.5625e-03
	1.0000	1.0001	1.0000	1.0000	1.0000	-
$Err_{\varepsilon,\mu}^{N,M}$	5.0000e-02	2.5000e-02	1.2500e-02	6.2500e-03	3.1250e-03	1.5625e-03
$Roc_{\varepsilon,\mu}^{N,M}$	1.0000	1.0001	1.0000	1.0000	1.0000	-

Table 7.3: $Err_{\varepsilon,\mu}^{N,M}$ and $Roc_{\varepsilon,\mu}^{N,M}$ using scheme (7.37) for Example 7.2 with $\mu = 10^{-5}$ and different values of ε.

N	20	40	80	160	320	640
$\varepsilon \downarrow$ M	10	20	40	80	160	320
10^{0}	3.1193e-05	8.0016e-06	2.0154e-06	5.0521e-07	1.2644e-07	3.1626e-08
	1.9629	1.9892	1.9961	1.9984	1.9993	-
10^{-2}	1.2479e-03	4.5771e-04	1.4724e-04	4.2719e-05	1.1592e-05	3.0256e-06
	1.4470	1.6363	1.7852	1.8817	1.9378	-
10^{-4}	1.7278e-03	8.6360e-04	4.3121e-04	2.1453e-04	1.0551e-04	5.0275e-05
	1.0005	1.0020	1.0072	1.0238	1.0695	-
10^{-6}	1.7280e-03	8.6403e-04	4.3201e-04	2.1601e-04	1.0800e-04	5.4001e-05
	0.9999	1.0000	1.0000	1.0001	1.0000	-
10^{-8}	1.7280e-03	8.6400e-04	4.3200e-04	2.1600e-04	1.0800e-04	5.4001e-05
	1.0000	1.0000	1.0000	1.0000	1.0000	-
10^{-10}	1.7280e-03	8.6400e-04	4.3200e-04	2.1600e-04	1.0800e-04	5.4001e-05
	1.0000	1.0000	1.0000	1.0000	1.0000	-
10^{-12}	1.7280e-03	8.6400e-04	4.3200e-04	2.1600e-04	1.0800e-04	5.4001e-05
	1.0000	1.0000	1.0000	1.0000	1.0000	-
10^{-14}	1.7280e-03	8.6400e-04	4.3200e-04	2.1600e-04	1.0800e-04	5.4001e-05
	1.0000	1.0000	1.0000	1.0000	1.0000	-
10^{-16}	1.7280e-03	8.6400e-04	4.3200e-04	2.1600e-04	1.0800e-04	5.4001e-05
	1.0000	1.0000	1.0000	1.0000	1.0000	-
$\vdots$	$\vdots$	$\vdots$	$\vdots$	$\vdots$	$\vdots$	$\vdots$
10^{-40}	1.7280e-03	8.6400e-04	4.3200e-04	2.1600e-04	1.0800e-04	5.4001e-05
	1.0000	1.0000	1.0000	1.0000	1.0000	-
$Err_{\varepsilon,\mu}^{N,M}$	1.7280e-03	8.6400e-04	4.3200e-04	2.1600e-04	1.0800e-04	5.4001e-05
$Roc_{\varepsilon,\mu}^{N,M}$	1.0000	1.0000	1.0000	1.0000	1.0000	-

Table 7.4: $Err_{\varepsilon,\mu}^{N,M}$ and $Roc_{\varepsilon,\mu}^{N,M}$ using scheme (7.37) for Example 7.2 with $\mu = 10^{-10}$ and different values of ε.

N	20	40	80	160	320	640
$\varepsilon \downarrow$M	10	20	40	80	160	320
10^{0}	3.1192e-05	8.0016e-06	2.0153e-06	5.0523e-07	1.2644e-07	3.1636e-08
	1.9628	1.9893	1.9960	1.9985	1.9988	-
10^{-2}	1.2479e-03	4.5771e-04	1.4724e-04	4.2719e-05	1.1591e-05	3.0256e-06
	1.4470	1.6363	1.7852	1.8819	1.9377	-
10^{-4}	1.7278e-03	8.6358e-04	4.3119e-04	2.1453e-04	1.0550e-04	5.0273e-05
	1.0005	1.0020	1.0071	1.0239	1.0694	-
10^{-6}	1.7280e-03	8.6400e-04	4.3200e-04	2.1600e-04	1.0800e-04	5.3999e-05
	1.0000	1.0001	1.0000	1.0000	1.0000	-
10^{-8}	1.7280e-03	8.6400e-04	4.3200e-04	2.1600e-04	1.0800e-04	5.4001e-05
	1.0000	1.0001	1.0000	1.0000	1.0000	-
10^{-10}	1.7280e-03	8.6400e-04	4.3200e-04	2.1600e-04	1.0800e-04	5.4001e-05
	1.0000	1.0001	1.0000	1.0000	1.0000	-
10^{-12}	1.7280e-03	8.6400e-04	4.3200e-04	2.1600e-04	1.0800e-04	5.4001e-05
	1.0000	1.0001	1.0000	1.0000	1.0000	-
10^{-14}	1.7280e-03	8.6400e-04	4.3200e-04	2.1600e-04	1.0800e-04	5.4001e-05
	1.0000	1.0001	1.0000	1.0000	1.0000	-
10^{-16}	1.7280e-03	8.6400e-04	4.3200e-04	2.1600e-04	1.0800e-04	5.4001e-05
	1.0000	1.0001	1.0000	1.0000	1.0000	-
$\vdots$	$\vdots$	$\vdots$	$\vdots$	$\vdots$	$\vdots$	$\vdots$
10^{-40}	1.7280e-03	8.6400e-04	4.3200e-04	2.1600e-04	1.0800e-04	5.4001e-05
	1.0000	1.0001	1.0000	1.0000	1.0000	-
$Err_{\varepsilon,\mu}^{N,M}$	1.7280e-03	8.6400e-04	4.3200e-04	2.1600e-04	1.0800e-04	5.4001e-05
$Roc_{\varepsilon,\mu}^{N,M}$	1.0000	1.0001	1.0000	1.0000	1.0000	-

7.5 Summary

In this work, a fitted operator scheme has been developed for two-parameter nonlinear singularly perturbed initial boundary value problems. The scheme has been constructed using Euler's implicit discretization on a uniform mesh in the temporal direction and a fitted operator discretization on a uniform spatial mesh. Newton's quasilinearization has been applied to handle the non-linearity. The investigation reveals that the proposed technique was proved to be stable and uniformly convergent of order one in both variables. However, temporal mesh refinement was employed to enhance the convergence rate to the second order. To ensure accuracy and confirm the theoretical results of the suggested method, we have provided two examples and presented them in tables and graphs.

CONCLUSIONS AND RECOMMENDATIONS

Conclusions

The dissertation contributes to the formulation of fitted numerical schemes for a class of two-parameter singularly perturbed problems with time delay in both linear and nonlinear cases. Due to the presence of perturbation parameters attached to the higher-order terms, the solutions of these problems exhibit boundary layers at the endpoints of the domain. Additionally, if these problems contain nonsmooth terms such as coefficient terms and source terms, they can exhibit an interior layer in the region of the point of discontinuity in the solution. The contributions of this dissertation are summarized as follows:

A nonstandard finite difference method called the fitted operator finite difference method was developed for two-parameter singularly perturbed problems with time delay. This method utilized the Crank-Nicolson technique for the time variable and the fitted operator method for the spatial variable on a uniform mesh. The stability estimate and convergence analysis of the formulated scheme were investigated. The analysis revealed that the scheme is accurate and uniformly convergent of order one.

A fitted mesh finite difference method was formulated for time-delay two-parameter singularly perturbed problems, considering both smooth and non-smooth data. The scheme was developed by employing the Crank-Nicolson discretization for the temporal variable and utilizing a hybrid scheme that incorporates central, upwind, and midpoint difference operators for the spatial variable. Convergence analysis was conducted, and it was proven that the method is uniformly convergent for second-order time variables and nearly second-order space variables. This analysis demonstrates the accuracy and reliability of the proposed scheme in approximating solutions for such problems.

A fitted numerical method is developed on a uniform mesh for nonlinear two-parameter singularly perturbed problems. The method incorporates the quasilinearization technique to handle the nonlinearity in the problem. Additionally, a fitted operator finite difference method is applied on a uniform mesh, utilizing Euler's implicit discretization for the time variable and a nonstandard finite difference technique for the spatial variable. The convergence analysis demonstrates that the developed scheme is uniformly convergent with first-order accuracy. This highlights the effectiveness and accuracy of the proposed method in approximating the solutions of the considered nonlinear two-parameter singularly perturbed problems.

Recommendations

The developed numerical methods have wide applicability in numerous applications of mathematics, physics, and engineering, with particular relevance to fields such as fluid dynamics, elasticity, quantum mechanics, reaction-diffusion processes, chemical reactor theory, plasma dynamics, meteorology, diffraction theory, aerodynamics, semiconductor modeling, and hydrodynamics, among the areas where these problems arise. To further enhance the applicability of these numerical schemes and guide future research, the following recommendations are made:

- The methods developed can be expanded to address singularly perturbed differential equations in two dimensions.
- Further modifications can be made to the methods by applying them on non-uniform or graded meshes, such as Bakhvalov's meshes or Volanovic meshes.
- The methods developed can be expanded to address singularly perturbed nonlinear problems with turning points.
- The methods developed can be expanded to address singularly perturbed nonlinear problems with turning points in two dimensions.

REFERENCES

Adomian, G. and Rach, R. (1983). Nonlinear stochastic differential delay equations. *Journal of Mathematical Analysis and Applications*, 91(1):94–101.

Ansari, A., Bakr, S., and Shishkin, G. (2007). A parameter-robust finite difference method for singularly perturbed delay parabolic partial differential equations. *Journal of computational and Applied Mathematics*, 205(1):552–566.

Appadu, A. R., Inan, B., and Tijani, Y. O. (2019). Comparative study of some numerical methods for the burgers–huxley equation. *Symmetry*, 11(11):1333.

Appadu, A. R., Tijani, Y. O., and Munyakazi, J. (2020). Computational study of some numerical methods for the generalized burgers-huxley equation. In *International Conference on Computational Sciences-Modelling, Computing and Soft*, pages 56–67. Springer.

Baranowski, J. (2010). Legendre polynomial approximations of time delay systems. In *Proceeding of 12th International PhD Workshop*, volume 1, pages 15–20.

Bashier, E. B. and Patidar, K. C. (2011). A novel fitted operator finite difference method for a singularly perturbed delay parabolic partial differential equation. *Applied Mathematics and Computation*, 217(9):4728–4739.

Batiha, B., Noorani, M., and Hashim, I. (2008). Application of variational iteration method to the generalized burgers–huxley equation. *Chaos, Solitons & Fractals*, 36(3):660–663.

Bellman, R. E. and Kalaba, R. E. (1965). Quasilinearization and nonlinear boundary-value problems.

Berger, A. E., Han, H. D., and Kellogg, R. B. (1984). A priori estimates and analysis of a numerical method for a turning point problem. *Mathematics of computation*, 42(166):465–492.

Bullo, T. A., Duressa, G. F., and Degla, G. (2021a). Accelerated fitted operator finite difference method for singularly perturbed parabolic reaction-diffusion problems. *Computational Methods for Differential Equations*, 9(3):886–898.

Bullo, T. A., Duressa, G. F., and Degla, G. A. (2021b). Robust finite difference method for singularly perturbed two-parameter parabolic convection-diffusion problems. *International Journal of Computational Methods*, 18(02):2050034.

Cengizci, S., Natesan, S., and ATAY, M. T. (2019). An asymptotic-numerical hybrid method for singularly perturbed system of two-point reaction-diffusion boundary-value problems. *Turkish Journal of Mathematics*, 43(1):460–472.

Chandru, M., Das, P., and Ramos, H. (2018). Numerical treatment of two-parameter singularly perturbed parabolic convection diffusion problems with non-smooth data. *Mathematical Methods in the Applied Sciences*, 41(14):5359–5387.

Chandru, M., Prabha, T., and Shanthi, V. (2017). A parameter robust higher order numerical method for singularly perturbed two parameter problems with non-smooth data. *Journal of Computational and Applied Mathematics*, 309:11–27.

Chen, J. and O'Malley, Jr, R. (1974). On the asymptotic solution of a two-parameter boundary value problem of chemical reactor theory. *SIAM Journal on Applied Mathematics*, 26(4):717–729.

Das, P. (2015). Comparison of a priori and a posteriori meshes for singularly perturbed nonlinear parameterized problems. *Journal of Computational and Applied Mathematics*, 290:16–25.

Das, P. and Mehrmann, V. (2016). Numerical solution of singularly perturbed convection-diffusion-reaction problems with two small parameters. *BIT Numerical Mathematics*, 56(1):51–76.

Das, P. and Natesan, S. (2012). Higher-order parameter uniform convergent schemes for robin type reaction-diffusion problems using adaptively generated grid. *International Journal of Computational Methods*, 9(04):1250052.

Das, P. and Natesan, S. (2013a). Numerical solution of a system of singularly perturbed convection diffusion boundary value problems using mesh equidistribution technique. *Aust. J. Math. Anal. Appl*, 10(1):1–17.

Das, P. and Natesan, S. (2013b). Richardson extrapolation method for singularly perturbed convection-diffusion problems on adaptively generated mesh. *CMES Comput. Model. Eng. Sci*, 90(6):463–485.

Das, P. and Natesan, S. (2015). Adaptive mesh generation for singularly perturbed fourth-order ordinary differential equations. *International Journal of Computer Mathematics*, 92(3):562–578.

Dehghan, M. (2004). Numerical solution of the three-dimensional advection–diffusion equation. *Applied Mathematics and Computation*, 150(1):5–19.

Derzie, E. B., Munyakazi, J. B., and Dinka, T. G. (2022). Parameter-uniform fitted operator method for singularly perturbed burgers-huxley equation. *Journal of Mathematical Modeling*, 10(4):515–534.

Derzie, E. B., Munyakazi, J. B., and Dinka, T. G. (2023). A nsfd method for the singularly perturbed burgers-huxley equation. *Frontiers in Applied Mathematics and Statistics*, 9:1068890.

Doolan, E. P., Miller, J. J., and Schilders, W. H. (1980). *Uniform numerical methods for problems with initial and boundary layers*. Boole Press.

Duressa, G. F. (2021). Novel approach to solve singularly perturbed boundary value problems with negative shift parameter. *Heliyon*, 7(7):e07497.

Duressa, G. F., Daba, I. T., and Deressa, C. T. (2023). A systematic review on the solution methodology of singularly perturbed differential difference equations. *Mathematics*, 11(5):1108.

Ewing, R. E. (1983). Problems arising in the modeling of processes for hydrocarbon recovery. In *The mathematics of reservoir simulation*, pages 3–34. SIAM.

Farrell, P., Hegarty, A., Miller, J. M., O'Riordan, E., and Shishkin, G. I. (2000). *Robust computational techniques for boundary layers*. CRC Press.

Friedrichs, K. and Wasow, W. (1946). Singular perturbations of non-linear oscillations. *Duke Math. J.*, 13(1):367–381.

Govindarao, L., Sahu, S. R., and Mohapatra, J. (2019). Uniformly convergent numerical method for singularly perturbed time delay parabolic problem with two small parameters. *Iranian Journal of Science and Technology, Transactions A: Science*, 43:2373–2383.

Gracia, J., O'Riordan, E., and Pickett, M. (2006). A parameter robust second order numerical method for a singularly perturbed two-parameter problem. *Applied Numerical Mathematics*, 56(7):962–980.

Gupta, V., Kadalbajoo, M. K., and Dubey, R. K. (2019). A parameter-uniform higher order finite difference scheme for singularly perturbed time-dependent parabolic problem with two small parameters. *International Journal of Computer Mathematics*, 96(3):474–499.

Holmes, M. H. (2007). *Introduction to numerical methods in differential equations*. Springer.

İnan, B. (2017). Finite difference methods for the generalized huxley and burgers-huxley equations. *Kuwait Journal of Science*, 44(3).

Ismail, H. N., Raslan, K., and Abd Rabboh, A. A. (2004). Adomian decomposition method for burger's–huxley and burger's–fisher equations. *Applied mathematics and computation*, 159(1):291–301.

Kadalbajoo, M. and Yadaw, A. S. (2012). Parameter-uniform finite element method for two-parameter singularly perturbed parabolic reaction-diffusion problems. *International journal of computational methods*, 9(04):1250047.

Kadalbajoo, M. K. and Gupta, V. (2010). A brief survey on numerical methods for solving singularly perturbed problems. *Applied mathematics and computation*, 217(8):3641–3716.

Kadalbajoo, M. K. and Jha, A. (2012). Exponentially fitted cubic spline for two-parameter singularly perturbed boundary value problems. *International Journal of Computer Mathematics*, 89(6):836–850.

Kadalbajoo, M. K. and Reddy, Y. (1989). Asymptotic and numerical analysis of singular perturbation problems: a survey. *Applied Mathematics and computation*, 30(3):223–259.

Kadalbajoo, M. K., Sharma, K. K., and Awasthi, A. (2005). A parameter-uniform implicit difference scheme for solving time-dependent burgers' equations. *Applied mathematics and computation*, 170(2):1365–1393.

Kaushik, A. (2008). Singular perturbation analysis of bistable differential equation arising in the nerve pulse propagation. *Nonlinear Analysis: Real World Applications*, 9(5):2106–2127.

Kellogg, R. B. and Tsan, A. (1978). Analysis of some difference approximations for a singular perturbation problem without turning points. *Mathematics of Computation*, 32(144):1025–1039.

Kevorkian, J. and Cole, J. (1981). Perturbation methods in applied mathematics.

Kumar, M., Singh, P., and Mishra, H. K. (2007). A recent survey on computational techniques for solving singularly perturbed boundary value problems. *International Journal of Computer Mathematics*, 84(10):1439–1463.

Kumar, S., Kumar, M., et al. (2020). A robust numerical method for a two-parameter singularly perturbed time delay parabolic problem. *Computational and Applied Mathematics*, 39(3):1–25.

Kumar, S., Stecher, G., Li, M., Knyaz, C., and Tamura, K. (2018). Mega x: molecular evolutionary genetics analysis across computing platforms. *Molecular biology and evolution*, 35(6):1547.

Ladyzhenskaya, O., Solonnikov, V., and Ural'tseva, N. (1968). Linear and quasilinear equations of parabolic type, transl. math. *Monographs, Amer. Math. Soc*, 23.

Li-Bin, L., Ying, L., Jian, Z., and Xiaobing, B. (2020). A robust adaptive grid method for singularly perturbed burger-huxley equations. *Electronic Research Archive*, 28(4):1439–1457.

Linß, T. (2009). *Layer-adapted meshes for reaction-convection-diffusion problems*. Springer.

Linss, T. (2010). A posteriori error estimation for a singularly perturbed problem with two small parameters. *International Journal of Numerical Analysis & Modeling*, 7(3).

Mickens, R. (2005). Reduction of computational errors using nonstandard finite difference models. *Journal of Difference Equations and Applications*, 11(1):83–91.

Mickens, R. E. (1994). *Nonstandard finite difference models of differential equations*. world scientific.

Miller, J., O'Riordan, E., and Shishkin, G. (2012). Fitted numerical methods for singular perturbation problems: Error estimates in the maximum norm for linear problems in one and two dimensions. In *Fitted Numerical Methods for Singular Perturbation Problems: Error Estimates in the Maximum Norm for Linear Problems in One and Two Dimensions*, pages 1–176.

Miller, J. J., O'riordan, E., and Shishkin, G. I. (1996). *Fitted numerical methods for singular perturbation problems: error estimates in the maximum norm for linear problems in one and two dimensions*. World scientific.

Munyakazi, J. B. (2015). A robust finite difference method for two-parameter parabolic convection-diffusion problems. *Applied Mathematics & Information Sciences*, 9(6):2877.

Munyakazi, J. B. and Patidar, K. C. (2014). Performance of richardson extrapolation on some numerical methods for a singularly perturbed turning point problem whose solution has boundary layers.

Murray, J. D. (2002). *Mathematical biology: I. An introduction*. Springer.

Nayfeh, A. (2000). Perturbation methods (wiley-vch, weinheim.

Nayfeh, A. H. and Balachandran, B. (2008). *Applied nonlinear dynamics: analytical, computational, and experimental methods*. John Wiley & Sons.

Negero, N. T., Duressa, G. F., Rathour, L., and Mishra, V. N. (2023). A novel fitted numerical scheme for singularly perturbed delay parabolic problems with two small parameters. *Partial Differential Equations in Applied Mathematics*, 8:100546.

O'Malley, R. (1967). Two-parameter singular perturbation problems for second-order equations. *Journal of Mathematics and Mechanics*, 16(10):1143–1164.

O'malley, R. E. et al. (1991). *Singular perturbation methods for ordinary differential equations*, volume 89. Springer.

O'Riordan, E., Pickett, M. L., and Shishkin, G. I. (2003). Singularly perturbed problems modeling reaction-convection-diffusion processes. *Computational Methods in Applied Mathematics*, 3(3):424–442.

O'Malley, Jr, R. (1979). A singular singularly-perturbed linear boundary value problem. *SIAM Journal on Mathematical Analysis*, 10(4):695–708.

O'Riordan, E., Pickett, M., and Shishkin, G. (2006). Parameter-uniform finite difference schemes for singularly perturbed parabolic diffusion-convection-reaction problems. *Mathematics of Computation*, 75(255):1135–1154.

Patidar, K. C. (2008). A robust fitted operator finite difference method for a two-parameter singular perturbation problem1. *Journal of Difference Equations and Applications*, 14(12):1197–1214.

Polak, S., Den Heijer, C., Schilders, W., and Markowich, P. (1987). Semiconductor device modelling from the numerical point of view. *International Journal for Numerical Methods in Engineering*, 24(4):763–838.

Prajapati, V. J. and Meher, R. (2022). A robust analytical approach to the generalized burgers–fisher equation with fractional derivatives including singular and non-singular kernels. *Journal of Ocean Engineering and Science*.

Prandtl, L. (1904). Über flussigkeitsbewegung bei sehr kleiner reibung. *Verhandl. III, Internat. Math.-Kong., Heidelberg, Teubner, Leipzig, 1904*, pages 484–491.

Roos, H., Stynes, M., and Tobiska, L. (1996). Numerical methods for singularly perturbed differential equations springer. *New York*.

Roos, H.-G. (2008). *Robust numerical methods for singularly perturbed differential equations*. Springer.

Roos, H.-G. (2012). Robust numerical methods for singularly perturbed differential equations: a survey covering 2008–2012. *International Scholarly Research Notices*, 2012.

Roos, H. G. and Uzelac, Z. (2003). The sdfem for a convection-diffusion problem with two small parameters. *Computational Methods in Applied Mathematics*, 3(3):443–458.

Roy, N. and Jha, A. (2022). A parameter uniform method for two-parameter singularly perturbed boundary value problems with discontinuous data. *arXiv preprint arXiv:2208.04375*.

Salama, A. and Al-Amery, D. (2015). Asymptotic-numerical method for singularly perturbed differential difference equations of mixed-type. *Journal of applied mathematics & informatics*, 33(5_6):485–502.

Sawangtong, W., Ikot, A. N., and Sawangtong, P. (2023). An approximate analytic solution for the multidimensional fractional-order time and space burger equation based on caputo-katugampola derivative. *International Journal of Theoretical Physics*, 62(12):269.

Schlichting, H. and Kestin, J. (1961). *Boundary layer theory*, volume 121. Springer.

Shanthi, V., Ramanujam, N., and Natesan, S. (2006). Fitted mesh method for singularly perturbed reaction-convection-diffusion problems with boundary and interior layers. *Journal of Applied Mathematics and Computing*, 22:49–65.

Shishkin, G. I. and Shishkina, L. P. (2008). *Difference methods for singular perturbation problems*. CRC Press.

Singh, J., Kumar, S., and Kumar, M. (2018). A domain decomposition method for solving singularly perturbed parabolic reaction-diffusion problems with time delay. *Numerical Methods for Partial Differential Equations*, 34(5):1849–1866.

Sumit, S., Kumar, S., Kuldeep, and Kumar, M. (2020). A robust numerical method for a two-parameter singularly perturbed time delay parabolic problem. *Computational and Applied Mathematics*, 39:1–25.

Van Dyke, M. (1975). Perturbation methods in fluid mechanics/annotated edition. *NASA STI/Recon Technical Report A*, 75:46926.

Van Harten, A. and Schumacher, J. (1978). On a class of partial functional differential equations arising in feed-back control theory. In *North-Holland Mathematics Studies*, volume 31, pages 161–179. Elsevier.

Verhulst, F. (2005). *Methods and applications of singular perturbations: boundary layers and multiple timescale dynamics*, volume 50. Springer Science & Business Media.

Vulanović, R. (2001). A higher-order scheme for quasilinear boundary value problems with two small parameters. *Computing*, 67(4).

Wang, P. K. C. (1963). Asymptotic stability of a time-delayed diffusion system.

Wineman, A. (2007). Nonlinear viscoelastic membranes. *Computers & Mathematics with Applications*, 53(2):168–181.

Woldaregay, M. M., Hunde, T. W., and Mishra, V. N. (2023). Fitted exact difference method for solutions of a singularly perturbed time delay parabolic pde. *Partial Differential Equations in Applied Mathematics*, 8:100556.

Zahra, W. K. and Mhlawy, A. M. (2013). Numerical solution of two-parameter singularly perturbed boundary value problems via exponential spline. *Journal of King Saud University-Science*, 25(3):201–208.

Zak, S. H. et al. (2003). *Systems and control*, volume 198. Oxford University Press New York.

Zibaei, S., Zeinadini, M., and Namjoo, M. (2016). Numerical solutions of burgers–huxley equation by exact finite difference and nsfd schemes. *Journal of Difference Equations and Applications*, 22(8):1098–1113.

APPENDIX A

LIST OF PUBLISHED AND SUBMITTED PAPERS

1. Mekashaw Ali Mohye, Justin B Munyakazi, and Tekle Gemechu Dinka. A non-standard fitted operator finite difference method for two-parameter singularly perturbed time-delay parabolic problems. Frontiers in Applied Mathematics and Statistics. https://doi.org/10.3389/fams.2023.1222162.

2. Mekashaw Ali Mohye, Justin B Munyakazi, and Tekle Gemechu Dinka. A second-order numerical method for two-parameter singularly perturbed time-delay parabolic problems. Journal of Mathematical Modeling, 2023. https://doi.org/10.22124/jmm.2023.24353.2182.

3. Mekashaw Ali Mohye, Justin B Munyakazi, and Tekle Gemechu Dinka. Parameters convergent fitted finite difference scheme for two-parameter singularly perturbed parabolic differential equations, (**Accepted for publication** DOI:10.5556/j.tkjm.56.2025.5244).

4. Mekashaw Ali Mohye, Justin B Munyakazi, and Tekle Gemechu Dinka. A stable numerical technique for solving nonlinear two-parameter singularly perturbed PDEs, (**Under review**).

5. Mekashaw Ali Mohye, Justin B Munyakazi, and Tekle Gemechu Dinka. A new parameter-convergent nonstandard finite difference method for two-parameter singularly perturbed problems, (**Under review**).

APPENDIX B

MATLAB AND PYTHON PROGRAMS

The Matlab and Python programs used to solve the examples can be found on Google Drive as shared below.

1. Matlab program for Example 4.1 of Chapter 4
   https://drive.google.com/file/d/1qJAry1UPRTyfokjT1uwFNNGfULGTTD8_/view?usp=drive_link

2. Matlab program for Example 5.1-5.4 of Chapter 5

   - https://drive.google.com/file/d/1S71Q8WEGHdgN1HyaNPby7kW_FNOF6OWt/view?usp=drive_link
   - https://drive.google.com/file/d/1z-Kw_-nl375p1lFpnUyLELRQISHSfcUN/view?usp=drive_link
   - https://drive.google.com/file/d/1in3Y4_DLf972SCJMBa8LEHvPpeVwiifg/view?usp=drive_link
   - https://drive.google.com/file/d/1BqadFwSLiD2P6qqEc2xD5L1zNIrpu_lo/view?usp=drive_link

3. Matlab program for Example 6.1-6.2 of Chapter 6
   https://drive.google.com/file/d/1V4dv-OtOiOXlnl5UOkPBuGWwmmPRnQ5t/view?usp=drive_link

4. Matlab program for Example 7.1-7.2 of Chapter 7

   - https://drive.google.com/file/d/1vh6dO5xEPM8t-rYonAIVrbLDvcHyEkCO/view?usp=drive_link
   - https://drive.google.com/file/d/1r2hWoXo7vt1ojJ6S4bWQrEkL_Qk5CBVM/view?usp=drive_link